Investigation of Carbamathione Pharmacokinetics and Pharmacodynamics

by *In Vivo* Microdialysis and Capillary Electrophoresis

by

Swetha Kaul
B.A., University of Missouri-Kansas City, Kansas City, MO, 2003
M.S., University of Kansas, Lawrence, KS, 2005

Submitted to the Department of Chemistry and the Graduate Faculty of the University of Kansas in partial fulfillment of the requirements for the degree of Doctor of Philosophy

_____
Dr. Craig E. Lunte

_____
Dr. Morris D. Faiman

_____
Dr. Susan M. Lunte

_____
Dr. Michael Johnson

_____
Dr. Paul R. Hanson

_____
Dr. Todd D. Williams

Date Defended: November 9th, 2010

The Dissertation Committee for Swetha Kaul certifies that this is the approved version of the following dissertation:

Investigation of Carbamathione Pharmacokinetics and Pharmacodynamics

by *In Vivo* Microdialysis and Capillary Electrophoresis

_____

Dr. Craig E. Lunte

Chairperson

Date Approved: November 9th, 2010

ACKNOWLEDGEMENTS

This dissertation would not have been possible without the support and contributions of many people to whom I will always be indebted. I would like to begin by expressing my gratitude to my research advisor, Dr. Craig Lunte. I will always appreciate the freedom he allowed me in my research and the guidance he provided me in my graduate life. Dr. Lunte taught me to how to question thoughts critically and express my ideas coherently.

I would like to thank the University of Kansas, Department of Chemistry and the R. N. Adams Institute for Bioanalytical Chemistry. I would also like to acknowledge my committee members: Dr. Morris Faiman, Dr. Todd Williams, Dr. Susan Lunte, Dr. Michael Johnson, and Dr. Paul Hanson for their input. This project started off as the brainchild of Dr. Faiman and I am grateful for his support and advice ever since I started off as a very green graduate student in his laboratory. I am grateful for the many meetings and constructive criticisms at different stages of my research. I would also like to thank Dr. Williams for his valuable contributions to the mass spectrometry portion of this project and several useful discussions on my project.

The work in Chapter 5 would not have been possible without the input of Anton Heemskerk and Dr. Stobaugh's laboratory. I would like to acknowledge their work in synthesizing an internal standard for carbamathione as well as developing a UPLC-MS/MS method for the detection of carbamathione and DETC-NAC.

I would like to acknowledge the University of Kansas Animal Care Unit for their advice and input with animal housing, care and surgeries. In addition, Dr. Mike Thompson and the pathology lab at Lawrence Memorial Hospital helped this project tremendously by processing the histology slides.

I am thankful to the many members of the Lunte lab with whom I have interacted during the course of my graduate studies. I would like to acknowledge Dr. Kristin Price and Dr. Kristin Aillon for valuable discussions that helped me understand my research area specifically and my graduate life in general. I am grateful to Sara Thomas, Dr. Gillian Whitaker and Stacy-Ann Collins for lending me their ear when I needed to vent and always giving great advice. In particular, I would like to thank Dr. Gillian Whitaker for her contributions to this project. She helped run innumerable samples on the mass spectrometer as well as develop a method for extracting carbamathione from plasma samples. I had also enjoyed getting to know Carl Cooley, Megan Dorris, Andrew Mayer and Sean Willis. I would like to wish them all the best of luck in their graduate careers.

Finally, none of this would have been possible without the love and support of my family and friends. I would like to thank my husband, Agul Kaul for his patience and encouragement particularly in the last few months when we were apart. His love and good humor helped me stay sane and focused through the many set-backs of graduate life. I would like to express my heart-felt gratitude to my parents, Amarnath and Sarada Maganti, and my sister, Shilpa Maganti for being a constant source of strength through the years. I gained a great new family in my in-laws when I got married and I am grateful to Vijay, Nisha and Vinur Kaul for always being there with a kind word and a hot meal.

ABSTRACT

The pharmacological basis for the use of the drug disulfiram for alcoholism is its inhibition of liver aldehyde dehydrogenase ($ALDH_2$). Recent studies have reported that disulfiram exhibited an anti-craving effect with both alcohol addiction and cocaine dependence. Inhibition of $ALDH_2$ cannot explain disulfiram's efficacy in cocaine dependence. The disulfiram metabolite *S*-(*N*, *N*-diethylcarbamoyl) glutathione (carbamathione) is formed from disulfiram and appears in the brain after the administration of disulfiram. Carbamathione has no effect on liver $ALDH_2$ and is a partial non-competitive inhibitor of the *N*-methyl-*D*-aspartic acid (NMDA) glutamate receptor. The effect of carbamathione on the neurotransmitter systems involved in craving and addiction is unknown. The aim of this research project was to develop analytical methods to determine carbamathione and relevant neurotransmitters in rat brain microdialysis samples in order to elucidate the pharmacokinetics and pharmacodynamics of carbamathione. The effect of disulfiram on the brain neurotransmitters was evaluated. The significance of this research is that carbamathione may be involved in the anti-craving effect observed with disulfiram, and thus may be used as a pharmacological tool to improve the effectiveness of disulfiram therapy in cocaine and alcohol addiction.

TABLE OF CONTENTS

1 INTRODUCTION 1

1.1 Alcoholism 2

1.1.1 Epidemiology 2

1.1.2 Pharmacology 2

1.1.3 Neurochemistry 3

1.1.3.1 Dopaminergic System 5

1.1.3.2 GABAergic System 6

1.1.3.3 Glutamatergic System 7

1.1.4 Pharmacotherapeutics 10

1.2 Cocaine Addiction 12

1.2.1 Epidemiology 12

1.2.2 Pharmacology 13

1.2.3 Neurochemistry 14

1.2.3.1 Dopaminergic System 14

1.2.3.2 GABAergic System 17

1.2.3.3 Glutamatergic System 17

1.2.4 Pharmacotherapeutics 18

1.3 Disulfiram 19

1.3.1 History of Disulfiram 19

1.3.2 Bioactivation of Disulfiram 20
1.3.3 Clinical Trials with Disulfiram 20
1.4 Microdialysis 23
1.4.1 Principles of Microdialysis 23
1.4.2 Microdialysis Calibration Methods 27
1.4.3 Tissue Response to Probe Implantation 31
1.4.4 Pharmacokinetic and Pharmacodynamic Studies with Microdialysis 32
1.5 Analytical Methods for Neurotransmitters in Microdialysis Samples ... 33
1.6 References 39

2 *IN VIVO* MICRODIALYSIS AND CE-LIF FOR MONITORING GABA, GLUTAMATE, AND CARBAMATHIONE 59
2.1 Introduction 59
2.1.1 Effect of Carbamathione on GABA and Glutamate 59
2.1.2 CE-LIF for Neurotransmitters in Biological Samples 60
2.1.3 Specific Aims of Research 62
2.2 Experimental 64
2.2.1 Chemicals and Reagents 64
2.2.2 Derivatization 67
2.2.3 CE-LIF Instrumentation 68

2.2.4 Method Development 69
2.2.5 Method Validation Experiments 74
2.2.6 Microdialysis 74
2.2.6.1 Brain Probes 74
2.2.6.2 Animals and Surgery 75
2.2.6.3 Microdialysis Sample Collection 77
2.2.6.4 In Vivo Experiments 77
2.3 Results and Discussion 79
2.3.1 Method Validation Results 79
2.3.2 Microdialysis Probe Calibration 81
2.3.3 Histological Confirmation of Brain Probe Position 81
2.3.4 *In Vivo* Studies 83
2.3.4.1 Experiments on Anesthetized Rats 83
2.3.4.2 Experiments on Awake Rats 88
2.4 Discussion 94
2.5 Conclusions 95
2.6 References 97

3 *IN VIVO* MICRODIALYSIS AND MEKC-LIF FOR MONITORING GABA, GLUTAMATE, DOPAMINE, AND CARBAMATHIONE 104
3.1 Introduction 104

3.1.1 Background and Significance 104
3.1.2 Specific Aims of Research 105
3.2 Experimental 107
3.2.1 Chemicals and Reagents 107
3.2.2 MEKC-LIF Instrumentation 108
3.2.3 MEKC-LIF Method Development 109
3.2.4 MEKC-LIF Method Validation Experiments 114
3.2.5 LC-MS/MS Instrumentation 114
3.2.6 LC-MS/MS Method Development 115
3.2.7 LC-MS/MS Method Validation Experiments 118
3.2.8 Microdialysis 118
3.2.8.1 Brain and Vascular Probes 118
3.2.8.2 Animals and Surgery 121
3.2.8.3 Microdialysis Sample Collection 123
3.2.8.4 In Vivo Experiments 123
3.3 Results and Discussion 125
3.3.1 MEKC-LIF Method Validation Results 125
3.3.2 LC-MS/MS Method Validation Results 125
3.3.3 Microdialysis Probe Calibration 128
3.3.4 Histological Confirmation of Brain Probe Position 130
3.3.5 *In Vivo* Studies 132

3.3.5.1 Administration of 200 mg/kg Carbamathione and 5 min Sampling Interval 132
3.3.5.2 Increased Temporal Resolution for Carbamathione Dose-Response 140
3.4 Discussion 150
3.5 Conclusions 158
3.6 References 160

4 INHIBITION OF DISULFIRAM METABOLISM AND ITS EFFECT ON BRAIN NEUROTRANSMITTERS 167
4.1 Introduction 167
4.1.1 Background and Significance 167
4.1.2 Specific Aims of Research 168
4.2 Experimental 169
4.2.1 Chemicals and Reagents 169
4.2.2 Laboratory–Built MEKC-LIF Instrumentation 170
4.2.3 Method Development 173
4.2.4 Method Validation Experiments 179
4.2.5 Microdialysis 181
4.2.5.1 Brain and Vascular Probes 181
4.2.5.2 Animals and Surgery 182

4.2.5.3 Microdialysis Sample Collection 183
4.2.5.4 In Vivo Experiments 183
4.3 Results and Discussion 184
4.3.1 Method Validation Results 184
4.3.2 *In Vivo* Studies 186
4.3.2.1 Pharmacokinetic Studies 186
4.3.2.2 Pharmacodynamic Studies 193
4.4 Discussion 201
4.5 Conclusions 203
4.6 References 204

5 *IN VIVO* MICRODIALYSIS AND UPLC-MS/MS FOR MONITORING A METABOLITE OF CARBMATHIONE 207
5.1 Introduction 207
5.1.1 Specific Aims of Research 208
5.2 Experimental 210
5.2.1 Chemicals and Reagents 210
5.2.2 UPLC-MS/MS Instrumentation 210
5.2.3 UPLC-MS/MS Method Development 211
5.2.4 Preparation of Standards and Calibration Curves 214
5.2.5 Sample Preparation 215

5.2.6 Microdialysis 215
5.2.6.1 Brain and Vascular Probes 215
5.2.6.2 Animals and Surgery 216
5.2.6.3 Microdialysis Sample Collection 216
5.2.6.4 In Vivo Experiments 217
5.3 Results and Discussion 218
5.3.1 UPLC-MS/MS Calibration Results 218
5.3.2 Microdialysis Probe Calibration 218
5.3.3 *In Vivo* Studies 220
5.4 Discussion 225
5.5 Conclusions 226
5.6 References 227

6 CONCLUSIONS AND FUTURE DIRECTIONS 228
6.1 Summary of Dissertation 228
6.1.1 CE-LIF Method for GABA, Glu, and Carbamathione in Microdialysis Samples 228
6.1.2 MEKC-LIF Method for GABA, Glu, DA, and Carbamathione in Microdialysis Samples 230
6.1.3 Laboratory-Built MEKC-LIF Method for GABA, Glu, DA, and Carbamathione in Microdialysis Samples 233

6.1.4 UPLC-MS/MS Method for Carbamathione and a Metabolite of Carbamathione in Microdialysis Samples 234
6.2 Future Directions 235
6.3 References 239

TABLE OF FIGURES & TABLES

Figure 1.1 Metabolism of ethanol. 4

Figure 1.2 Effect of alcohol on brain neurotransmitters. 9

Figure 1.3 Effect of cocaine on dopamine neurotransmission. 15

Figure 1.4 Bioactivation of disulfiram.[65] 21

Figure 1.5 Principle of microdialysis. 24

Figure 1.6 Commonly used probe designs[78] 25

Figure 1.7 Principle of micellar electrokinetic chromatography.[123] 38

Figure 2.1 NDA derivatization scheme. 61

Figure 2.2 Structure of carbamathione. 63

Table 2.3 Stability of carbamathione under various conditions using LC-MS/MS. 66

Figure 2.4 Effect of varying the concentration of BGE on separation. 70

Figure 2.5 Effect of varying pH of BGE on separation. 71

Figure 2.6 Typical CE-LIF electropherograms. 72

Figure 2.7 Swivel-based awake animal system 78

Table 2.8 Quantitative parameters for the analysis GABA, Glu, and carbamathione in aCSF and microdialysis samples. 80

Figure 2.9 Representative location of microdialysis probe in nucleus accumbens shell.[26] 82

Figure 2.10 Simultaneous monitoring of GABA and Glu in microdialysis samples from the nucleus accumbens of anesthetized rat. 84

Figure 2.11 Carbamathione concentration versus time profile in anesthetized rats. 86

Table 2.12 Pharmacokinetic paramaters of carbamathione in anesthetized rats... 87

Figure 2.13 Simultaneous monitoring of GABA and Glu in microdialysis samples from the nucleus accumbens of awake rat. 90

Figure 2.14 Carbamathione concentration versus time profile in awake rats. ... 91

Table 2.15 Pharmacokinetic paramaters of carbamathione in awake rats. 93

Figure 3.1 Effect of varying temperature on separation by MEKC-LIF. 110

Figure 3.2 Generation of absorbance at 442 nm as a function of time for GABA, Glu, DA, and carbamathione. 112

Figure 3.3 Typical MEKC-LIF electropherograms. 113

Figure 3.4 Tandem mass spectrum of carbamathione after activation of $[M+H]^+$ at 25 eV CE. 117

Figure 3.5 Typical LC-MS/MS chromatograms. 119

Table 3.6 Quantitative parameters for the analysis GABA, Glu, DA, and carbamathione in aCSF and microdialysis samples by MEKC-LIF. 126

Figure 3.7 Representative calibration curves for LC-MS/MS method. 127

Table 3.8 Quantitative parameters for the analysis of carbamathione in Ringer's solution by LC-MS/MS 129

Figure 3.9 Representative locations of microdialysis probes in nucleus accumbens shell and prefrontal cortex. 131

Figure 3.10 GABA, Glu, and DA in nucleus accumbens after a 200 mg/kg dose of carbamathione and 5 min sampling interval. 133

Figure 3.11 GABA, Glu, and DA in prefrontal cortex after a 200 mg/kg dose of carbamathione and 5 min sampling interval. 136

Figure 3.12 Carbamathione concentration versus time profile after 200 mg/kg dose of carbamathione and 5 min sampling interval. 138

Table 3.13 Pharmacokinetic paramaters of carbamathione with 5 min sampling interval. 139

Figure 3.14 GABA levels in the nucleus accumbens after carbamathione administration and 3 min sampling interval..... 141

Figure 3.15 Glu levels in the nucleus accumbens after carbamathione administration and 3 min sampling interval..... 143

Figure 3.16 DA levels in the nucleus accumbens after carbamathione administration and 3 min sampling interval..... 144

Figure 3.17 GABA levels in the prefrontal cortex after carbamathione administration and 3 min sampling interval..... 146

Figure 3.18 Glu levels in the prefrontal cortex after carbamathione administration and 3 min sampling interval..... 147

Figure 3.19 DA levels in the prefrontal cortex after carbamathione administration and 3 min sampling interval..... 149

Figure 3.20 Carbamathione concentration versus time profile after three doses carbamathione and 3 min sampling interval. 151

Table 3.21 Pharmacokinetic paramaters of carbamathione with 3 min sampling interval. 152

Figure 4.1 Schematic diagram of laboratory-built MEKC-LIF system.[7] 171

Figure 4.2 Effect of varying the concentration of the surfactant on separation. 175

Figure 4.3 Effect of adding MEOH to BGE on separation. 176

Figure 4.4 Effect of varying the concentration of the surfactant on separation. 177

Figure 4.5 Typical MEKC-LIF electropherograms..... 180

Table 4.6 Quantitative parameters for the analysis GABA, Glu, DA, and carbamathione in aCSF and microdialysis samples..... 185

Figure 4.7 Carbamathione concentration versus time profile after a 200 mg/kg dose of disulfiram. 187

Figure 4.8 Carbamathione concentration versus time profile after a 200 mg/kg dose of carbamathione. 191

Table 4.9 Pharmacokinetic paramaters of carbamathione with 5 min sampling interval. 192

Figure 4.10 GABA, Glu, and DA in rat brain nucleus accumbens after a 200 mg/kg dose of disulfiram. 194

Figure 4.11 GABA, Glu, and DA in rat brain nucleus accumbens after after a 200 mg/kg dose of disulfiram and a 20 mg/kg dose of NBI. 197

Figure 4.12 GABA, Glu, and DA in rat brain nucleus accumbens after after a 200 mg/kg dose of carbamathione and a 20 mg/kg dose of NBI.. 199

Figure 5.1 Structures of carbamathione, DETC-NAC and diisopropyl carbamathione. 209

Table 5.2 UPLC-MS/MS Gradient. 212

Table 5.3 SRM parameters for the UPLC-MS/MS method. 213

Figure 5.4 Representative calibration curves for UPLC-MS/MS method. 219

Figure 5.5 Carbamathione and DETC-NAC concentration versus time profile after 200 mg/kg dose of disulfiram and 15 min sampling interval in plasma dialysate. 221

Figure 5.6 Carbamathione and DETC-NAC concentration versus time profile after 200 mg/kg dose of disulfiram and 15 min sampling interval in brain dialysate. 222

Figure 5.7 Carbamathione and DETC-NAC concentration versus time profile after 200 mg/kg dose of disulfiram and 15 min sampling interval in brain dialysate. 223

1 INTRODUCTION

Alcohol and cocaine abuse are significant public health issues. Several effective pharmacotherapies for alcohol dependence have been identified, but the search for an effective therapeutic agent for cocaine dependence has proved difficult. It has been suggested that disulfiram offers a promising treatment option since it has shown efficacy in both alcohol and cocaine addiction. In this chapter, the epidemiology, pharmacology, and known pharmacotherapeutic agents for alcohol and cocaine addiction are discussed. In addition, some of the relevant clinical studies linking disulfiram with alcohol and cocaine addiction are also covered. Carbamathione, a metabolite of disulfiram, may play a role in disulfiram's efficacy in alcohol and cocaine addiction since it appears to cross the blood-brain barrier (BBB) and may have an effect on various neurotransmitter systems in the brain. Microdialysis, a powerful *in vivo* tool that can be used to determine various substrates in discrete areas, was used to measure brain neurotransmitters. The principles of microdialysis and the analytical methods used to detect neurotransmitters in microdialysis samples are also discussed.

1.1 Alcoholism

1.1.1 Epidemiology

Alcoholism is one of the most common neuropsychiatric diseases with a worldwide prevalence of 8.5%.[1] Alcohol abuse is not only associated with deleterious effects on the physical and psychological health of individuals, but also has serious socioeconomic outcomes in the form of criminality, decreased productivity, and increased healthcare costs. In fact, it has been estimated that on a worldwide scale, over 6% of an industrialized nation's gross domestic product is spent on costs related to alcohol and alcoholism.[2] In addition, the percentage of total disability-adjusted life years (calculated by adding the years of life lost due to premature mortality and living with disability) of the world population caused by chronic alcohol use is as high as 4% (compared with 2.2% for AIDS).[3] In an estimate of the factors responsible for the global burden of disease, alcohol contributes to 3.2% of all deaths worldwide.[2]

1.1.2 Pharmacology

Alcohol, or more specifically ethanol, is the most commonly used drug of abuse in the world. This is because it is so widely available, can be purchased easily and is not associated with the kind of social stigma related to other drugs of abuse. Ethanol is a relatively simple compound with the chemical formula C_2H_5OH. It is

a clear liquid that is extremely soluble in water and fat tissue. When ingested, alcohol is completely and rapidly absorbed from the duodenum and to a small extent from the stomach into the blood and is distributed into the total body water. The metabolism of alcohol occurs primarily in the liver in a two step process as shown in figure 1.1. In the first step, alcohol is oxidized by the enzyme alcohol dehydrogenase to form acetaldehyde, which is metabolized very rapidly and usually does not accumulate. However, when large amounts of alcohol are consumed, accumulation of acetaldehyde may cause symptoms like headache, nausea and dizziness. In the second step of alcohol metabolism, acetaldehyde is metabolized by the mitochondrial low K_m aldehyde dehydrogenase enzyme ($ALDH_2$) to acetic acid and eventually to carbon dioxide and water.[4]

1.1.3 Neurochemistry

For many years, it was believed that the effects of alcohol were mediated through the non-specific disruption of neuronal lipid bi-layers. However, it is now accepted that alcohol acts by binding with and altering the function of specific receptor proteins, particularly membrane-bound ligand-gated ion channels and voltage-dependent ion channels.[5]

Figure 1.1 **Metabolism of ethanol.**

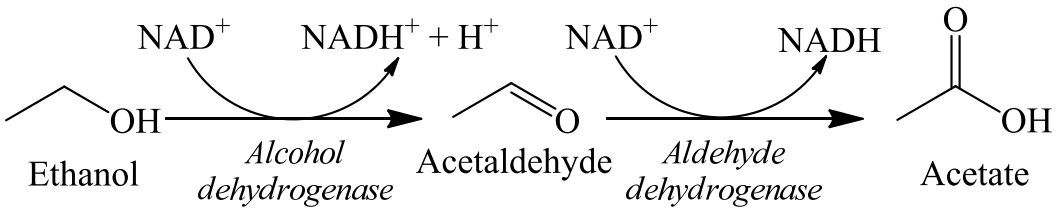

1.1.3.1 Dopaminergic System

It is widely accepted that dopamine neurotransmission within the mesocorticolimbic system plays a critical role in addiction. Dopamine neurons have cell bodies located in the ventral tegmental area (VTA) that send axonal projections to the prefrontal cortex (mesocortical) and the nucleus accumbens (mesolimbic). The dopaminergic brain reward system appears to play a fundamental role in the mechanisms of alcohol intake and craving. Alcohol consumption results in an increase in dopamine levels in the nucleus accumbens, which has been defined as the "reward center" of the brain.[6,7] Earlier studies with self-administration of alcohol in alcohol-dependent rats showed that alcohol increased extracellular dopamine in the nucleus accumbens in a dose-dependent manner, and dopamine antagonists blocked alcohol self-administration in rats.[8-10] Also, the systemic administration of alcohol increased the release of dopamine as well as the rate of dopamine cell firing in brain regions involved in the reinforcing effects of alcohol.[11] Furthermore, in animal studies, dopaminergic drugs affected alcohol self-administration.[12] Neuroimaging studies in humans also revealed an alcohol-induced release of dopamine in the nucleus accumbens area of the central nervous system (CNS), and it was suggested that individuals who are vulnerable to developing alcohol dependence may have a lower central dopaminergic tone.[13-15] Even though many animal studies have suggested a strong relationship between dysfunction of the dopaminergic system and alcohol dependence, clinical studies

with drugs that affected the dopaminergic system have been inconsistent. For example, olanzapine, an antipsychotic, reduced the urge to drink after a drinking cue, but it had no effect on the rewarding effects of alcohol in social drinkers.[16] Earlier studies by Shaw et al. showed that the dopamine D_2 receptor blocking agent tiapride reduced the severity of ethanol withdrawal, improved drinking outcomes, and reduced craving.[17] However, amisulpride, a dopamine D_2 receptor antagonist, had no effect on preventing relapse in alcoholics exhibiting ethanol dependence.[18] Even though these clinical studies were inconclusive, evidence remains that the dopaminergic system may play an important role in the development of novel pharmacotherapeutics for alcohol addiction.

1.1.3.2 GABAergic System

Gamma-amino butyric acid (GABA) is the primary inhibitory neurotransmitter in the mammalian CNS, and activation of $GABA_A$ receptors by GABA tends to decrease neuronal excitability. $GABA_A$ receptors play a central role in both the short and long-term effects of alcohol in the CNS. When $GABA_A$ receptors are acutely exposed to alcohol, there is an increase in receptor activity and potentiating GABA-gated current, which is one of the reasons that alcohol is often thought of as a depressant. Chronic alcohol exposure results in a down-regulation of $GABA_A$ receptor function and may represent a mechanism for tolerance to

alcohol. This decrease in GABAergic function is thought to result in seizure susceptibility observed when chronic alcohol consumption ceases. Low levels of GABA may contribute to symptoms of alcohol withdrawal and associated neurotoxicity. In addition, the $GABA_A$ receptors play a role in mediating dopamine levels in the mesolimbic system. Long-term alcohol exposure decreases $GABA_A$ receptors, which in turn results in an increase in dopamine release in the VTA.[5] During the withdrawal/negative affect stage of addiction, enhanced alcohol self-administration during acute withdrawal was reduced in a dose-dependent manner by the direct administration of a $GABA_A$ agonist into the central nucleus of the amygdala suggesting the involvement of the GABAergic system during acute alcohol withdrawal.[19] The implication of the GABA system in the acute reinforcing effects of alcohol has led to the investigation and clinical trials of several GABAergic agents. Gabapentin, which has structural similarities to GABA, decreased alcohol withdrawal hyper-excitability in hippocampus slices, as well as convulsions in alcohol-withdrawn mice.[20,21]

1.1.3.3 Glutamatergic System

Glutamic acid (glutamate) is the major excitatory amino acid neurotransmitter in the CNS. Its excitatory effect on neurons is mediated by activating receptors, which are gated to ion channels or to a protein that mediates a second messenger.

One of the most powerful effects of alcohol is to reduce the pace of brain activity, in part by decreasing the excitatory actions of the neurotransmitter glutamate at the *N*-methyl-*D*-aspartic acid (NMDA) subtype of glutamate receptor. In several neurochemical studies, pharmacologically relevant concentrations (50 ± 10 mmol/L) of alcohol were shown to inhibit or antagonize the action of agonists at the NMDA receptor. Although acute alcohol administration disrupts glutamatergic neurotransmission by inhibiting the response of the NMDA receptors, chronic alcohol consumption results in the development of glutamate hypersensitivity by up-regulating NMDA receptor number and function. The up-regulation of the NMDA receptor is thought to be a result of the physiological response to prolonged NMDA inhibition. Cessation of prolonged and chronic alcohol consumption causes a marked increase in glutamate activity at postsynaptic neurons and in extreme cases, glutamate-induced excitotoxicity.[22,23] Recent advances in the neurobiology of addiction and the developing knowledge base suggest that the dopaminergic and glutamatergic systems are inter-related (figure 1.2).[24] Considering this circuit, the glutamatergic projection appears to be the final common pathway for the initiation of drug seeking behavior by a drug-associated cue or the drug itself which increases dopamine release in the prefrontal cortex. In addition, the GABAergic and glutamatergic systems also appear to be inter-related (see figure 1.2).

Figure 1.2 Effect of alcohol on brain neurotransmitters.

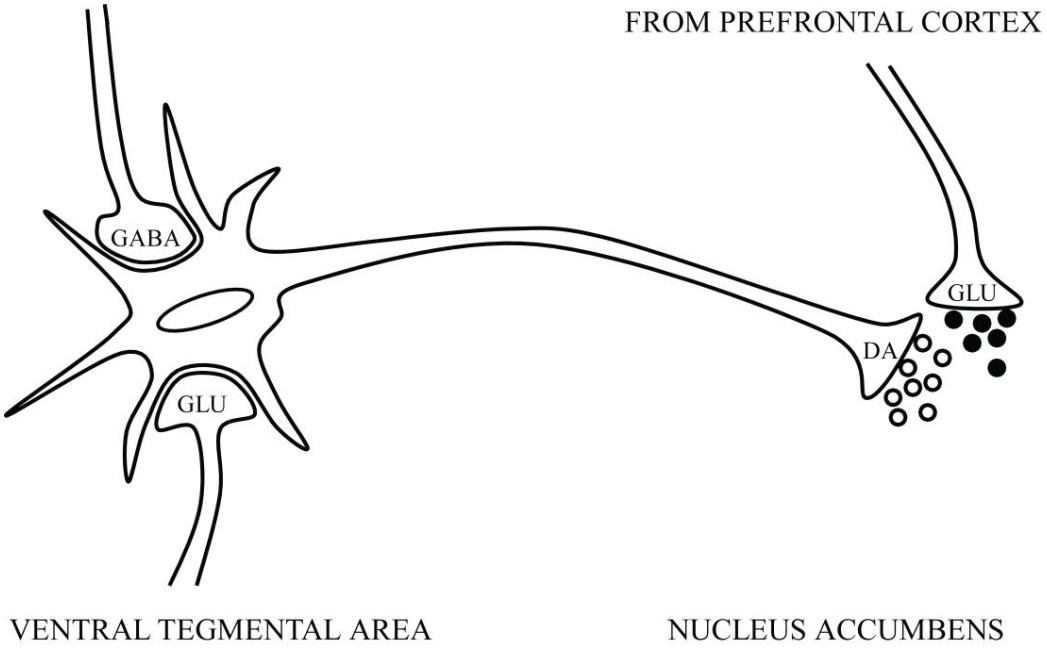

Alcohol consumption facilitates GABAergic transmission by interaction with the $GABA_A$ receptor and inhibits glutamatergic function at the NMDA receptor.

1.1.4 Pharmacotherapeutics

No medication has been found to be effective in treating alcohol abuse and dependence. The only three medications used for the treatment of alcohol abuse that have been approved by the U.S. Food and Drug Administration (FDA) are disulfiram, naltrexone, and acamprosate. Disulfiram has been used since 1948 when its action as a deterrent was first recognized by Hald and Jacobsen.[25] Naltrexone, previously used for opioid dependence was investigated, and in seminal studies, Volpicelli et al. and O'Malley et al. reported that naltrexone offered improvement in alcohol dependence. This led to its subsequent approval by the FDA.[26,27] Acamprosate, which has been used in Europe since the 1990s, was approved by the FDA for ethanol dependence in 2004. The mechanism of action for acamprosate is still not fully understood. The degree of efficacy for each of these agents remains controversial.

Drug discovery and development of new agents specific for ethanol abuse is almost non-existent. There are several reasons for this. One is that ethanol addiction is considered to be a chronic brain disease, progressing from social

drinking to withdrawal and dependence. It is a complex process and is not completely understood. Therefore, from a pharmacotherapeutic standpoint, it is not totally clear which stage of the addiction process should be targeted, which makes drug development difficult. Another and perhaps more important reason is that drug discovery and development and subsequent FDA approval is a time-consuming and costly process. From bench to bedside, drug development takes at least 12 years and often longer, and developmental costs are in excess of $1 billion. Drug discovery by the pharmaceutical industry has therefore focused on disease states that are perceived to have a better opportunity for return on investment: cancer pharmacotherapy; cardiovascular, gastrointestinal, neurological, and behavioral disorders; infectious diseases; and sexually related disorders. Thus the development of new chemical entities by the pharmaceutical industry that are specific for the treatment of ethanol abuse and substance abuse in general has a low priority. Because of the high cost of drug discovery, the discovery approach currently used to identify agents for ethanol abuse is to study agents that have already received FDA approval for other disorders and evaluate their potential as drug candidates. These include topiramate and gabapentin (which affect the GABA and glutamatergic pathways), ondansetron (a serotonin antagonist), baclofen (a $GABA_B$ agonist), aripiprazole (a dopamine partial agonist), rimonabant (a cannabinoid antagonist), and memantine (an NMDA antagonist). Nalmefene, a drug similar to naltrexone, is a non-selective opiate

antagonist, but has advantages over naltrexone such as a longer half-life and lower prevalence of side effects, particularly hepatotoxicity.[28] Because of the different mechanisms of action for many of these agents, studies that combined some of these agents in order to improve therapeutic outcomes have also been initiated Considerable emphasis, however, appears to be on the evaluation of drugs that affect the dopaminergic, GABAergic and glutamatergic systems. [18,26,27,29-33]

1.2 Cocaine Addiction

1.2.1 Epidemiology

The current percentage of cocaine users is not as high as users of other illicit drugs such as methamphetamine and marijuana, yet the considerable health and financial losses that result from cocaine addiction exceed other illicit drugs. The National Survey on Drug Use and Health (NSDUH) estimated that in 2007, there were 2.1 million current (past-month) cocaine users, of whom approximately 610,000 were current crack users. Adults aged 18 to 25 years had a higher rate of current cocaine use than any other age group, with 1.7 percent of young adults reporting past month cocaine use. Repeated cocaine use can produce addiction and other adverse health consequences. In 2007, according to the NSDUH, nearly 1.6 million Americans met the *Diagnostic and Statistical Manual of Mental*

Disorders, 4th Edition (DSM-IV) criteria for dependence on or abuse of cocaine (in any form) in the past 12 months. Since there is no accepted treatment for cocaine addiction, it has become even more important to develop possible pharmacological treatments.[34-36]

1.2.2 Pharmacology

There are basically two forms of cocaine: the hydrochloride salt and the "freebase." The hydrochloride salt is the powdered form and is soluble in water. *Freebase* refers to the compound in a form that has not been protonated by an acid to make the hydrochloride salt. The principal routes of cocaine administration are oral, intranasal, and intravenous. Cocaine use ranges from occasional to compulsive use; there is no safe way to use it. Any route of administration can lead to absorption of toxic amounts of cocaine, leading to cardiovascular and cerebrovascular emergencies that result in death.[37] The short term physiological effects of cocaine include constricted blood vessels, dilated pupils, increased temperature, increased heart rate, and increased blood pressure. Large amounts of cocaine intensify the feeling of euphoria, but may also lead to violent behavior and even death. Cocaine-related deaths often result from cardiac or respiratory arrest. The long-term use of cocaine leads to increased tolerance to the euphoric effects of the drug and paradoxically, increased sensitivity to the

drug's anesthetic and convulsant effects. This may explain why some deaths occur among long-term users after relatively low doses of cocaine. The long term use of cocaine also leads to a state of increased irritability, restlessness and paranoia. This eventually leads to paranoid psychosis, in which the individual loses touch with reality and experiences hallucinations.[37-39] As with alcohol, continued cocaine use results in development of tolerance. This means that higher doses and more frequent use of cocaine are required for the brain to register the same level of pleasure experienced by the initial use. Even after long periods of abstinence, the memory of euphoria associated with cocaine use or even cues associated with the drug, can trigger tremendous craving and relapse for the drug user. [37]

1.2.3 Neurochemistry

1.2.3.1 Dopaminergic System

The dopaminergic system in the brain plays an important role in the reward pathway in addiction. Cocaine acts on the dopaminergic system by binding to the dopamine transporter and preventing dopamine reuptake at the pre-synaptic terminal, which subsequently leads to an increase in brain dopamine.[7,40-42] This effect of cocaine is illustrated in figure 1.3. Thus cocaine acts like an indirect agonist on the dopamine receptor.

Figure 1.3 Effect of cocaine on dopamine neurotransmission.

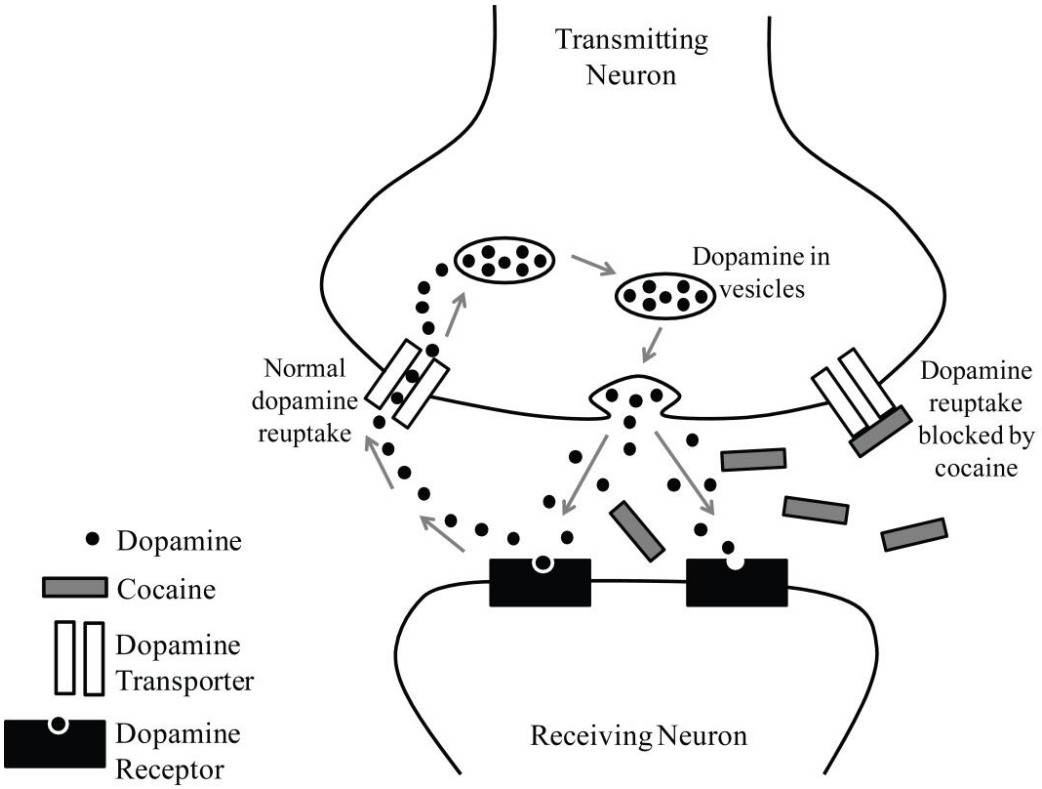

There is considerable evidence that cocaine's addictive ability is linked to reuptake blockade in CNS reward or reinforcement pathways, especially in the mesocorticolimbic system and particularly the nucleus accumbens.[24] For instance, cocaine-induced increases in extracellular dopamine have been linked to its rewarding and craving effects in rodents.[43] In humans, the pharmacokinetic binding profile of [^{11}C]-cocaine indicated that the uptake of labeled cocaine was directly correlated with the self-reported ''high.''[14,15] In light of the implication of dopamine in the mesolimbic and mesocortical systems in cocaine addiction, drugs that affect the dopaminergic pathway have been investigated for the treatment of cocaine abuse. While the dopamine hypothesis as it relates to cocaine addiction may explain some of the addicting processes, studies with drugs that affect the dopaminergic system have been inconsistent. For example, in positron emission tomography studies, methylphenidate, an inhibitor of dopamine reuptake, inhibited 50% of the dopamine transporter and enhanced extracellular dopamine.[14] Yet in a 10-week study, methylphenidate was found to be ineffective in reducing cocaine use in patients.[44] Bromocriptine is a D_2 receptor agonist, and except for one positive outcome, other clinical studies did not support it as a useful agent for the treatment of cocaine abuse.[45-47]

1.2.3.2 GABAergic System

The brain areas that contain dopaminergic neurons (nucleus accumbens) also contain GABAergic synapses.[48] Several studies have shown that the GABAergic system can modulate dopamine levels in the nucleus accumbens. Vigabatrin, a drug that inhibits GABA-transaminase, blocked a cocaine-induced increase in extracellular dopamine in the nucleus accumbens.[49,50] Another study showed that gamma-vinyl-GABA, which increases GABA levels in the brain, blocked cocaine-induced locomotor activity and dopamine release.[51] Topiramate has been shown to potentiate GABAergic transmission. In a 14-week clinical study, topiramate decreased cocaine use compared with the control group.[52] Tiagabine, a selective inhibitor of the GABA transporter, increases GABA in the synapse and in a study with opioid-dependent subjects, tiagabine blocked cocaine use compared with the control group.[53] Gabapentin, a GABA analog, also reduced cocaine use in cocaine smokers.[54]

1.2.3.3 Glutamatergic System

The glutamatergic system has also received increased interest for its role in cocaine addiction. There is both anatomical and physiological evidence that glutamate neurotransmission modulates the function of the nucleus accumbens by interacting with dopamine. Glutamate releasing neurons originating in the

cerebral cortex, hippocampus, and amygdala projected onto neurons in the nucleus accumbens. Both non-competitive and competitive glutamate NMDA antagonists blocked cocaine-induced behavior.[55,56] Considerable evidence exists that the antagonism of glutamate receptors affected cocaine self-administration.[57] Several studies have shown that the glutamatergic system can modulate the dopamine levels in the nucleus accumbens.[58,59] The interactions between the glutamatergic and dopaminergic pathways are believed to play an important role in the relapse of cocaine seeking behavior and cocaine addiction.[60,61]

1.2.4 Pharmacotherapeutics

There are currently no approved treatments for cocaine addiction. Rather than develop new chemical entities for cocaine addiction, most of the treatment options have focused on CNS agents approved for other uses. Using this approach, several CNS drugs have been studied for the treatment of cocaine abuse. GABA agents (topiramate, tiagabine, baclofen and vigabatrin) and agonist replacement agents (modafinil, disulfiram and methylphenidate) appear to be the most effective in treatment of cocaine dependence. Aripiprazole, a partial dopaminergic agonist that may modulate the serotoniergic system, showed some efficacy against cocaine abuse. Preliminary results of human studies with anti-cocaine vaccines, *N*-acetyl cysteine and ondansetron are also promising. Vaccine pharmacotherapy

used anti-cocaine antibodies to sequester cocaine molecules in the peripheral circulation and prevented it from crossing the BBB. *N*-acetyl cysteine reduced cocaine-induced reinstatement of cocaine self-administration in rats. Ondansetron is a serotonin 5-HT_3 receptor antagonist that increased dopamine activity in the nucleus accumbens of rats. These studies suggest that targets of interest in developing new treatments for cocaine dependence should include the dopaminergic, GABAergic and glutamatergic systems.[28,31,40,62]

1.3 Disulfiram

1.3.1 History of Disulfiram

Disulfiram has been used as an alcohol deterrent since 1948, when it was first introduced by Hald and Jacobsen.[63] Disulfiram is an inhibitor of mitochondrial low K_m $ALDH_2$, which catalyzes the oxidation of acetaldehyde to acetate. Ingestion of disulfiram followed by alcohol intake results in a build-up of acetaldehyde. This increase of acetaldehyde in the blood leads to the disulfiram-alcohol reaction, which is characterized by nausea, vomiting, headache, hypotension, and tachycardia. The pharmacological basis of disulfiram is to use it to deter alcoholics from consuming alcohol rather than to produce this adverse reaction.[64]

1.3.2 Bioactivation of Disulfiram

The pathways of disulfiram metabolism are shown in figure 1.4. Disulfiram is bioactivated through a series of intermediates, ultimately forming *S*- methyl *N, N*-diethylthiocarbamate sulfoxide (DETC-MeSO), which has been proposed to be responsible for the $ALDH_2$ inhibition.[66-68] The metabolism of disulfiram is carried out by various cytochrome P450 enzymes in the liver. DETC-MeSO is a very reactive species and is oxidized to *S*- methyl *N, N*-diethylthiocarbamate sulfone (DETC-$MeSO_2$), which carbamoylates glutathione to form carbamathione during phase II metabolism.[69-73]

1.3.3 Clinical Trials with Disulfiram

Acamprosate is a drug that is used in the treatment of alcoholism. Acamprosate is a structural analog of GABA and may have an effect on both GABAergic and NMDA receptors. These neurotransmitters act by sending inhibitory messages to the brain and acamprosate is thought to act by enhancing their inhibitory effects. Acamprosate is also thought to decrease the activity in excitatory glutamate receptors in the brain, which is believed to reduce the desire or craving to consume alcohol; hence its use in alcohol dependence.[74]

Figure 1.4 Bioactivation of disulfiram.[65]

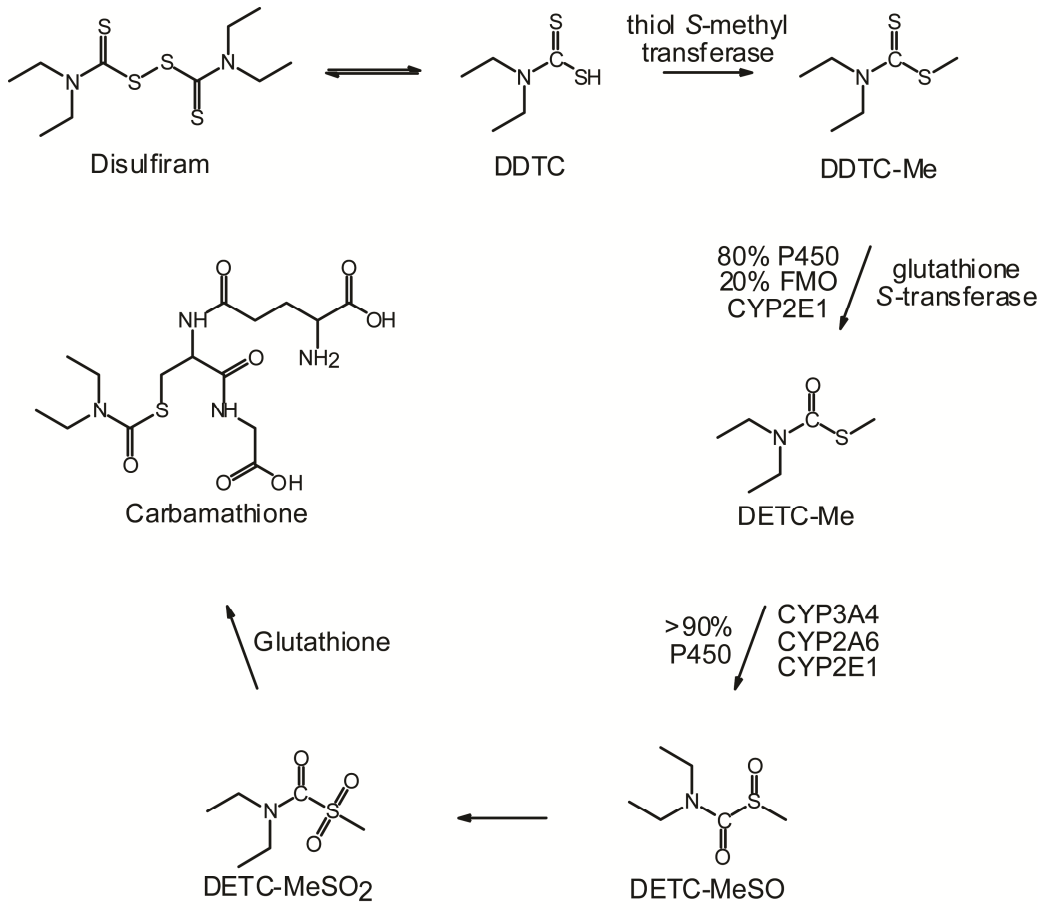

DDTC: diethyldithiocarbamate

DDTC-Me: diethyldithiocarbamate methyl ester

DETC-Me: *S*-methyl *N* ,*N*-diethylthiocarbamate

DETC-MeSO: *S*- methyl *N, N*-diethylthiocarbamate sulfoxide

DETC-MeSO$_2$: *S*- methyl *N, N*-diethylthiocarbamate sulfone

In one placebo-controlled alcohol trial, acamprosate and disulfiram were prescribed to patients.[75] The patients on the disulfiram-acamprosate combination had significantly more abstinent days than the patients that received acamprosate alone. In addition, there were no adverse interactions between acamprosate and disulfiram in 24 patients treated for 12 months.

Another clinical trial in 2005 that investigated the effectiveness of acamprosate and disulfiram in alcohol treatment found disulfiram to be much more effective. Compared with acamprosate, disulfiram was associated with a significantly greater reduction in relapse and significantly more abstinent days.[76]

Disulfiram has also been tested in clinical trials to determine its efficacy in cocaine treatment. Carroll et al. treated 121 outpatients for 12 weeks. The 32 women and 89 men met the criteria for cocaine dependence as specified in the DSM-IV, and these volunteers reported abusing cocaine 13 days during the month and 2.5 days during the week before treatment on average. During the study, each patient received either 250 mg/day of disulfiram or a placebo. The trial showed that disulfiram helped cocaine addicts reduce abuse of the drug from 2.5 days a week to 0.5 days a week on average. The finding built on previous studies in which other investigators demonstrated disulfiram's promise in two subgroups of cocaine abusers—alcoholics and those with co-occurring opioid addiction. The

results suggested that disulfiram was effective in treating the general population of cocaine-addicted patients, including those that were not alcoholic. The medication's effectiveness in non-alcoholic patients provided evidence that disulfiram reduced cocaine abuse directly rather than by reducing the concurrent alcohol abuse.[77]

1.4 Microdialysis

1.4.1 Principles of Microdialysis

Microdialysis is an *in vivo* sampling method by which chemical substances can be removed and introduced without removing or injecting fluids. The principle of microdialysis is based on the passive diffusion of a compound along its concentration gradient across a semi-permeable membrane (figure 1.5). Microdialysis involves the implantation of a microdialysis probe into a specific region of a tissue or fluid-filled space. A variety of probe designs have been employed in the study of biological tissues including concentric, flexible, linear, and shunt or by-pass (figure 1.6). The semi-permeable membranes used to make microdialysis probes range from low- to high-molecular weight cutoffs.

Figure 1.5 Principle of microdialysis.

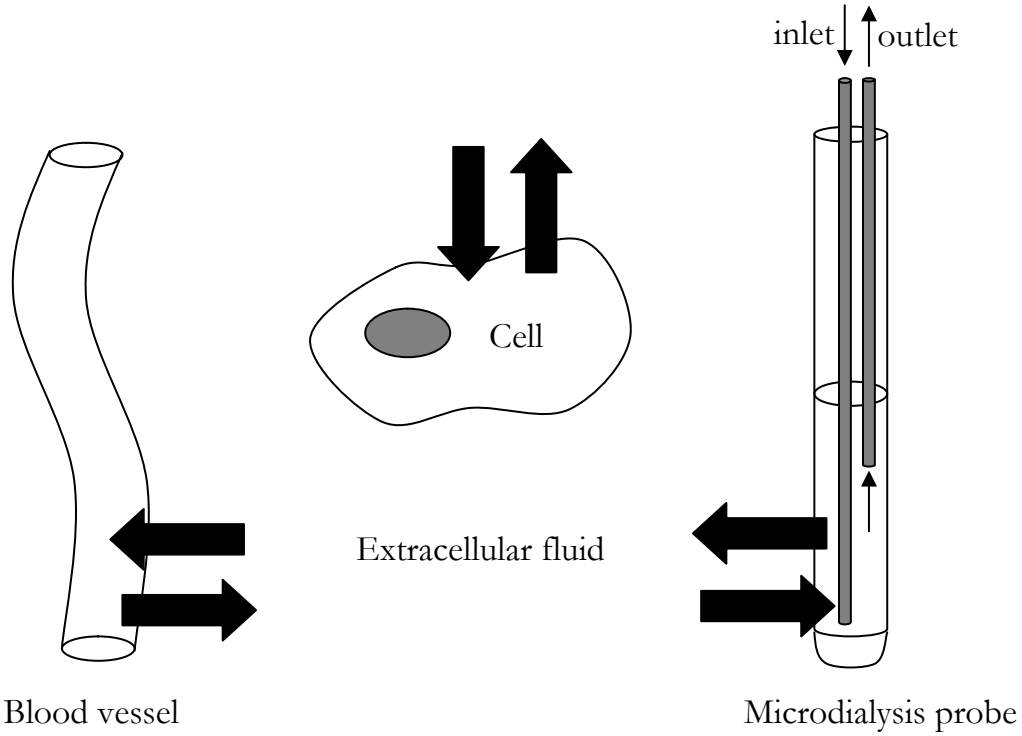

Figure 1.6 Commonly used probe designs[78]

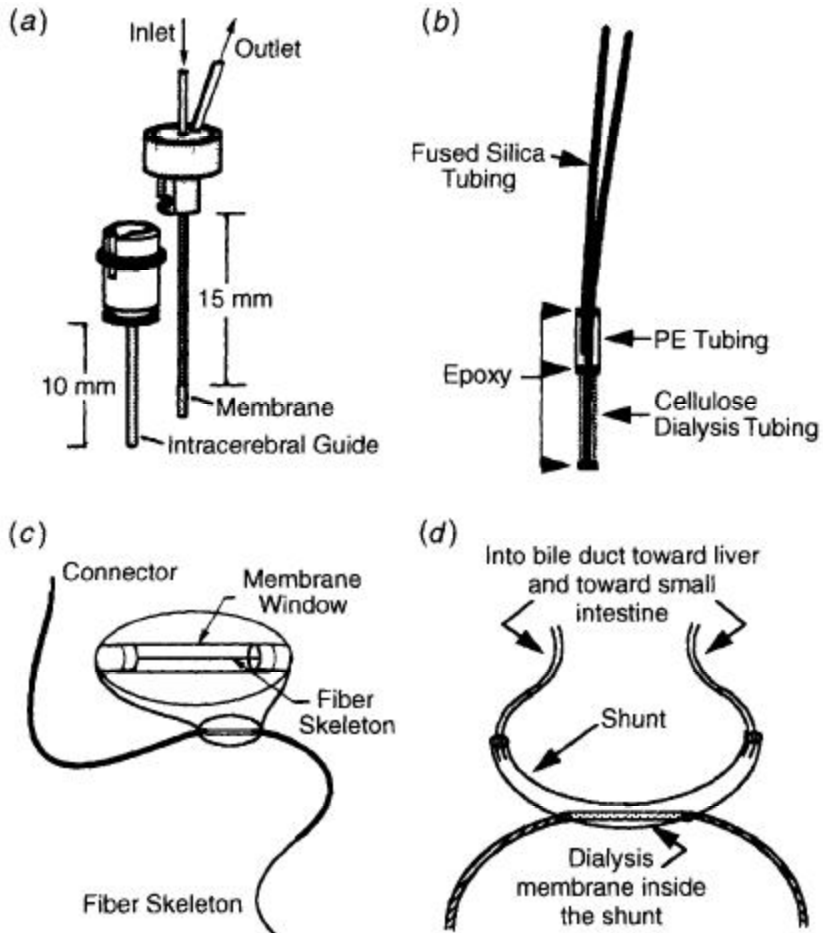

a. Rigid concentric probe typically used for brain microdialysis

b. Flexible cannula probe typically used for implantation into a blood vessel

c. Linear probe typically used to sample peripheral tissue such as skin or muscle

d. Shunt or by-pass probe is usually used for sampling the bile duct

During microdialysis, a physiologically compatible perfusion fluid (perfusate such as Ringer's solution) is pumped through the probe at a low and constant flow rate (typically 0.1-5.0 L/min). Exchange of solutes occurs in both directions across the semi-permeable membrane of the probe, depending on the solute concentration gradients. Thus the probe can be used in delivery of compounds as well as in the sampling experiments.[79,80] For a perfusate that lacks the compound of interest; the microdialysis sample concentration is usually a fraction of the extracellular unbound concentration of that compound in the tissue. This fraction is referred to as the extraction efficiency (EE). In investigations that examine changes in the levels of endogenous compounds from their baseline values, it may not be necessary to determine the EE, assuming the EE remains relatively constant throughout the experiment. However, in pharmacokinetic (PK) investigations without baseline values for exogenous substances, knowledge of the EE becomes crucial for the determination of true extracellular tissue concentrations.[78,81-83] Many experimental conditions affect probe calibration, including perfusion rate, temperature, probe membrane composition, surface area, nature of the tissue, and properties of the analyte of interest. In general, higher perfusion flow rates lead to the lower EE whereas higher temperatures and greater probe membrane areas usually result in increased EE.[83]

Development and refinement of the microdialysis methodology over the past 20 years has led to its increased acceptance in studies of drug distribution, metabolism, and pharmacodynamics (PD). However, one of the most important applications of microdialysis is in the measurement of compounds in the brain. These studies have examined not only neurotransmitters but also, in the past several years, the drug distribution to specific regions of the CNS. Microdialysis has permitted the investigation of the distribution kinetics and delivery of drugs to a wide variety of target tissues, allowing for the measurement of unbound, pharmacologically active drug levels over time in the relevant species and tissue.[84,85]

1.4.2 Microdialysis Calibration Methods

Calibration methods are important in microdialysis experiments when quantitative information on extracellular fluid concentrations is desired. Although EE may approach 100% for long probes and slow flow rates, the commonly used perfusate flow rate (1-2 μL/min) and membrane length (2-10 mm) usually result in EE that are much less than 100% in animal experiments. In addition, microdialysis sampling is usually carried out under non-equilibrium conditions since the perfusate is continuously pumped through the probe. The general equation to

determine microdialysis probe EE by the ratio of concentration (C) of analyte in the dialysate and the sample is as follows[86-88]:

$$EE = \frac{C_{perfusate} - C_{dialysate}}{C_{perfusate} - C_{tissue}} \quad (1)$$

In vivo the C_{tissue} cannot be determined directly, so the use of microdialysis sampling as a quantitative tool relies on the determination of the EE. A number of methods have been used to calculate the EE of microdialysis probes. The most frequently used calibration methods are the low-flow-rate method, the no-net-flux (or zero-net-flux) method, the dynamic (or extended) no-net-flux method, retrodialysis and calibration by delivery of analyte.[86-90] The general requirement of these methods is that the extraction fraction is the same whether the solute exchange across the membrane occurs by either loss or gain as predicted by the linear models. The low-flow-rate method is based on the assumption that EE is close to 100% and is generally applied in clinical microdialysis with longer probes and low flow rates (≤0.3 μL/min). The no-net-flux method requires steady-state concentration in the tissue, whereas perfusate concentrations are changed in several discrete steps within one experiment. The dynamic no-net-flux method allows for time-varying *in vivo* concentrations, but this approach requires that

probes be perfused with a different constant concentration in at least three different groups.[83,86,88,90]

The most common calibration method is retrodialysis by marker compound, which is performed before or after analyte administration without the analyte being present in the tissue. The advantage is that the solute of interest is measured; however, a drawback is that possible changes in EE over time are not measured. This method is not applicable to endogenous compounds because the requirement of no concentration in the tissue during the calibration interval cannot be met. Changes in EE during the experiment can be partially taken into account via retrodialysis by a marker compound. A good marker should have similar diffusion, transport, and if necessary similar metabolism properties as the analyte of interest. The ideal standard is thus a deuterated or radioactive form of the analyte; however, labeling an analyte can be expensive. In addition, the marker must be analytically distinguishable from the analyte in order to monitor both compounds. Finding a compound with analogous properties of transport through the probe makes retrodialysis a difficult method for probe calibration.[80,82,91]

An alternate calibration method to retrodialysis is to determine the EE of the microdialysis probe by delivery of analyte of interest through the probe. A low concentration of the analyte is perfused through the probe and microdialysis samples are analyzed once a steady state of delivery is achieved.[83] The extraction efficiency by delivery (EE_d) is derived from equation 1. For delivery studies, there is no initial concentration of analyte in the tissue so the equation becomes:

$$EE_d = \frac{C_{perfusate} - C_{dialysate}}{C_{dialysate}} \quad (2)$$

For recovery studies, there is no analyte in the perfusate so the EE, derived from equation 1 becomes:

$$EE_r = \frac{C_{dialysate}}{C_{tissue}} \quad (3)$$

Transport across the probe should be independent of direction, therefore, equal for both the delivery and recovery. By this assumption, the EE_d value equals the EE_r. Therefore, the analyte concentration in the tissue of interest (C_{tissue}), can be calculated by determining the concentration in the dialysate ($C_{dialysate}$) and substituting the EE_d for the extraction efficiency by recovery (EE_r) in equation 3.[83,89]

1.4.3 Tissue Response to Probe Implantation

Microdialysis probe implantation in tissues inevitably leads to immune reactions, particularly when the probe is implanted for extended periods. These reactions have been well-characterized in the literature and tend to be consistent. After implantation, a small amount of hemorrhaging occurs around the implantation sit, but contact between the tissue and membrane is still maintained. Inflammation is the initial acute immune response of the tissue and it lasts 3 to 4 hours after implantation. Blood flow increases to the implantation site and neutrophils begin to infiltrate, surrounding the probe. Eight hours after implantation, neutrophil infiltration continues to increase and some necrosis is evident. 1-3 days after probe implantations, macrophages infiltrate and begin to remove the necrotic tissue and any bacteria present. For extended implants (1 week or more), the tissue eventually begins to generate a capsule of connective tissue around the probe to isolate it from the rest of the tissue. Angiogenesis also occurs with the fibrous capsule.[92,93]

To allow "tissue equilibration" (i.e., to provide time for the initial trauma to subside), probe perfusion for more than half an hour has shown to be sufficient before starting probe calibration, although longer recovery times (12-24 hours) may be required. This is based on the finding that several markers of tissue trauma (e.g., thromboxane B2, adenosine triphosphate, adenosine, K^+, glucose,

lactate, lactate/pyruvate ratio) are elevated after probe insertion and reach baseline or become undetectable within this time range.[94,95]

One of the controversial questions addressed in CNS microdialysis research is the integrity of the BBB after probe implantation. It was shown that the BBB maintained its chemical selectivity with respect to mannitol and tritiated water.[96] Additional studies indicate a functional BBB in terms of passive and active transport mechanisms when optimal surgical and experimental conditions are employed in implanting microdialysis probes into the brain.[96,97]

1.4.4 Pharmacokinetic and Pharmacodynamic Studies with Microdialysis

In order to measure the relationship between drug concentrations in the blood (PK) and drug response (PD) it is essential to measure the drug in the tissue that represents the specific site of action. Microdialysis allows the sampling of the extracellular fluid of tissue and thus generates more relevant data than serum or plasma concentrations alone. For drugs that affect the CNS, a complex relationship exists between the dose and the response. Factors such disease condition, age, and weight all affect the response to a drug. Microdialysis can be particularly useful in these kinds of mechanism-based PK and PD studies of drugs. Several key mechanisms govern the dose-response relationship of drugs,

including plasma PK, BBB transport, tissue distribution, pathological conditions and drug-target interaction. Microdialysis is well suited to determine passive and active membrane transport mechanisms, such as those of the BBB. Intercellular chemical communication in the brain occurs via the extracellular fluid and an added advantage of microdialysis is that extracellular biomarkers of drug response and disease progression can be sought and monitored.[81,91,98-100]

1.5 Analytical Methods for Neurotransmitters in Microdialysis Samples

In neurochemistry, the *in vivo* monitoring of the extracellular concentrations of neurotransmitters plays a key role in the understanding of the molecular, electrophysiological, or behavioral events. Microdialysis is a frequently used technique to continuously sample the extracellular space of discrete brain regions. The microdialysis technique is a suitable method for this purpose in comparison to biosensors, which can detect only one neurotransmitter at a time.[101,102] Moreover, microdialysis is an ideal tool for the study of *in vivo* extracellular neurotransmitter levels in relationship to pharmacotherapeutic agents. Other sampling methods such as the push-pull technique and homogenization cause more tissue damage than microdialysis. In addition, tissue homogenization destroys neurotransmitter compartmentalization since it cannot be used to differentiate between released or free neurotransmitters and intercellular stores.

The microdialysis technique requires a small-diameter (<300 μm) dialysis tube to be stereotaxically implanted in a defined brain area. The neurotransmitters in the collected microdialysis samples can be identified and measured either online or after storage. As a sampling tool, microdialysis can be coupled to a variety of analytical techniques allowing virtually any neurotransmitter or drug to be measured with high selectivity and sensitivity. In many cases, multiple analytes can be detected in one sample, which facilitates studies of neurotransmitter interactions. Because samples can be collected over time, microdialysis can be used to obtain both basal concentrations and dynamic information on brain chemistry. [103,104]

Analysis of microdialysis samples from the brain has conventionally used classical high-performance liquid chromatography (HPLC) with electrochemical or fluorometric detection, and also enzymatic or radioenzymatic methods.[102,105-108] However, these analytical techniques exhibit poor concentration sensitivity and require large volume samples to determine neurotransmitter contents, leading to lengthy sampling times (15–30 min), although this requirement has been reduced by the breakthrough of microbore HPLC.[78,105,109,110] The temporal resolution is even worse when samples have to be split for the simultaneous determination of different classes of neurotransmitters. As a consequence, most of the previous microdialysis experiments were severely limited by the temporal resolution of

microdialysis (10–30 min) compared with rapid changes occurring in the extracellular concentrations of neurotransmitters.

In contrast, microdialysis coupled to capillary electrophoresis (CE), a more recent technique, can allow the monitoring of rapid changes in the extracellular concentration of neurotransmitters. CE is able to analyze nanoliter volume samples with low limits of detection and appears to be suitable for microdialysis at high sampling rates. Recent studies show significant progress in high temporal resolution monitoring of neurotransmitters with sampling times of 10-30 s being utilized.[111-114]

For the last few years, CE mainly coupled to laser-induced fluorescence (LIF) detection has been explored as an alternative to conventional analytical techniques for the determination of various compounds in biological fluids.[115-117] In brain microdialysis samples, excitatory amino acids (i.e. glutamate and aspartate) and GABA were often analyzed, and to a lesser extent catecholamines, dopamine, and noradrenaline.[112,115,118-120] Since none of these compounds have native fluorescence, a number of reagents have been utilized in derivatization reaction to employ LIF detection. Some of these reagents include *o*-phthalaldehyde (325 nm), naphthalene-2, 3-dicarboxaldehyde (442 nm), fluorescein isothiocyante (488 nm), and imidazole naphthalene-2, 3-dicarboxaldehyde (488 nm).

Micellar electrokinetic chromatography (MEKC), a modification of CE, has been used recently in combination with LIF for the simultaneous detection of several amino acid neurotransmitters and catecholamines.[119,121,122] MEKC is performed by adding an ionic micelle such as sodium dodecylsulfate (SDS) to the running solution of CE without modifying the instrument. The separation principle of MEKC is based on the differential migration of the ionic micelles and the bulk running buffer under electrophoresis conditions and on the interaction between the analyte and the micelle. Hence MEKC's separation principle is similar to that of chromatography. MEKC is a useful technique particularly for the separation of small molecules, both neutral and charged, and yields high-efficiency separation in a short time with minimum amounts of sample and reagents.

SDS is the most commonly used surfactant in MEKC applications. The anionic character of the sulfate groups of SDS cause the surfactant and micelles to have electrophoretic mobility that is counter to the direction of the strong electroosmotic flow. As a result, the surfactant monomers and micelles migrate quite slowly, although their net movement is still towards the cathode. During a MEKC separation, analytes distribute themselves between the hydrophobic interior of the micelle and hydrophilic buffer solution as shown in figure 1.7. MEKC allows the efficient separation of biogenic amines and amino acids in biological samples. The MEKC-LIF methods that have been used recently

displayed good specificity, sensitivity, reliability, and efficiency of separation and detection for a large number of neurotransmitters.

Figure 1.7 Principle of micellar electrokinetic chromatography.[123]

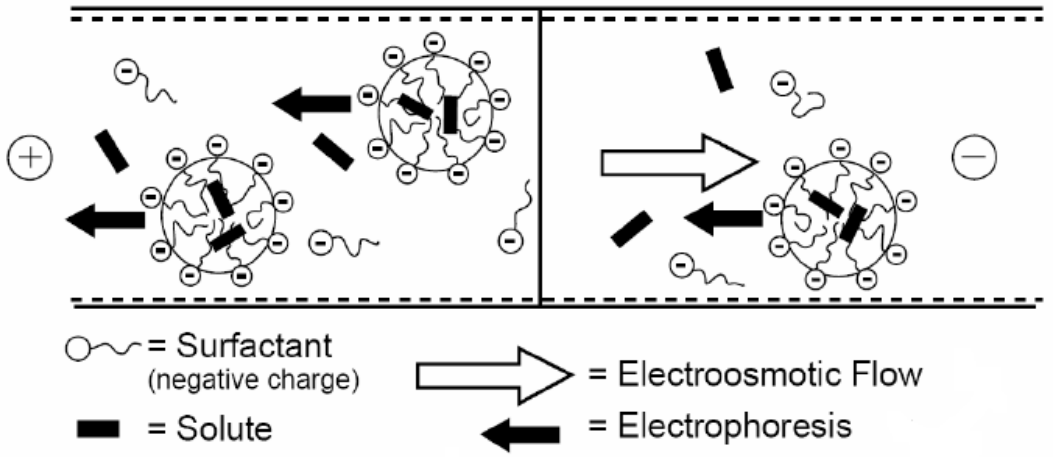

1.6 References

1 Enoch, M. A. The role of GABA(A) receptors in the development of alcoholism. *Pharmacol Biochem Be* **90**, 95-104, (2008).

2 Spanagel, R. Alcoholism: A Systems Approach From Molecular Physiology to Addictive Behavior. *Physiol Rev* **89**, 649-705, (2009).

3 Spanagel, R. & Kiefer, F. Drugs for relapse prevention of alcoholism: ten years of progress. *Trends Pharmacol Sci* **29**, 109-115, (2008).

4 Medical consequences of alcohol abuse. *Alcohol Res Health* **24**, 27-31, (2000).

5 Davies, M. The role of GABAA receptors in mediating the effects of alcohol in the central nervous system. *Journal of psychiatry & neuroscience* **28**, 263-274, (2003).

6 Lapish, C. C., Seamans, J. K. & Chandler, L. J. Glutamate-dopamine cotransmission and reward processing in addiction. *Alcoholism-Clinical and Experimental Research* **30**, 1451-1465, (2006).

7 Di Chiara, G., Bassareo, V., Fenu, S., De Luca, M. A., Spina, L., Cadoni, C., Acquas, E., Carboni, E., Valentini, V. & Lecca, D. Dopamine and drug addiction: the nucleus accumbens shell connection. *Neuropharmacology* **47**, 227-241, (2004).

8 Rassnick, S., Pulvirenti, L. & Koob, G. F. Oral ethanol self-administration in rats is reduced by the administration of dopamine and glutamate

receptor antagonists into the nucleus accumbens. *Psychopharmacology (Berl)* **109**, 92-98, (1992).

9 Weiss, F., Lorang, M. T., Bloom, F. E. & Koob, G. F. Oral alcohol self-administration stimulates dopamine release in the rat nucleus accumbens: genetic and motivational determinants. *J Pharmacol Exp Ther* **267**, 250-258, (1993).

10 Weiss, F., Parsons, L. H., Schulteis, G., Hyytia, P., Lorang, M. T., Bloom, F. E. & Koob, G. F. Ethanol self-administration restores withdrawal-associated deficiencies in accumbal dopamine and 5-hydroxytryptamine release in dependent rats. *J Neurosci* **16**, 3474-3485, (1996).

11 Li, T. K., Spanagel, R., Colombo, G., McBride, W. J., Porrino, L. J., Suzuki, T. & Rodd-Henricks, Z. A. Alcohol reinforcement and voluntary ethanol consumption. *Alcoholism-Clinical and Experimental Research* **25**, 117s-126s, (2001).

12 Hodge, C. W., Chappelle, A. M. & Samson, H. H. Dopamine receptors in the medial prefrontal cortex influence ethanol and sucrose-reinforced responding. *Alcoholism: Clinical and Experimental Research* **20**, 1631-1638, (1996).

13 Boileau, I., Assaad, J.-M., Pihl, R. O., Benkelfat, C., Leyton, M., Diksic, M., Tremblay, R. E. & Dagher, A. Alcohol promotes dopamine release in the human nucleus accumbens. *Synapse* **49**, 226-231, (2003).

14 Volkow, N. D., Fowler, J. S., Wang, G. J. & Goldstein, R. Z. Role of dopamine, the frontal cortex and memory circuits in drug addiction: insight from imaging studies. *Neurobiol Learn Mem* **78**, 610-624, (2002).

15 Volkow, N. D., Fowler, J. S., Wang, G. J., Baler, R. & Telang, F. Imaging dopamine's role in drug abuse and addiction. *Neuropharmacology* **56 Suppl 1**, 3-8, (2009).

16 Hutchison, K. E., Swift, R., Rohsenow, D. J., Monti, P. M., Davidson, D. & Almeida, A. Olanzapine reduces urge to drink after drinking cues and a priming dose of alcohol. *Psychopharmacology* **155**, 27-34, (2001).

17 Shaw, G. K., Majumdar, S. K., Waller, S., MacGarvie, J. & Dunn, G. Tiapride in the long-term management of alcoholics of anxious or depressive temperament. *Br J Psychiatry* **150**, 164-168, (1987).

18 Marra, D., Warot, D., Berlin, I., Hispard, E., Notides, C., Tilikete, S., Payan, C., Lepine, J. P., Dally, S. & Aubin, H. J. Amisulpride does not prevent relapse in primary alcohol dependence: Results of a pilot randomized, placebo-controlled trial. *Alcoholism-Clinical and Experimental Research* **26**, 1545-1552, (2002).

19 Roberts, A. J., Cole, M. & Koob, G. F. Intra-amygdala muscimol decreases operant ethanol self-administration in dependent rats. *Alcoholism, clinical and experimental research* **20**, 1289-1298, (1996).

20 Bailey, C. P., Molleman, A. & Little, H. Comparison of the effects of drugs on hyperexcitability induced in hippocampal slices by withdrawal from chronic ethanol consumption. *Br. J. Pharmacol.* **123**, 215-222, (1998).

21 Watson, W. P., Robinson, E. & Little, H. J. The novel anticonvulsant, gabapentin, protects against both convulsant and anxiogenic aspects of the ethanol withdrawal syndrome. *Neuropharmacology* **36**, 1369-1375, (1997).

22 Dahchour, A. & De Witte, P. Effect of repeated ethanol withdrawal on glutamate microdialysate in the hippocampus. *Alcoholism-Clinical and Experimental Research* **23**, 1698-1703, (1999).

23 Gass, J. T. & Olive, M. F. Glutamatergic substrates of drug addiction and alcoholism. *Biochemical Pharmacology* **75**, 218-265, (2008).

24 Kalivas, P. W. & Volkow, N. D. The neural basis of addiction: a pathology of motivation and choice. *The American journal of psychiatry* **162**, 1403-1415, (2005).

25 Hald, J. & Jacobsen, E. A drug sensitizing the organism to ethyl alcohol. *Lancet* **2**, 1001-1004, (1948).

26 Volpicelli, J. R., Alterman, A. I., Hayashida, M. & O'Brien, C. P. Naltrexone in the treatment of alcohol dependence. *Archives of general psychiatry* **49**, 876-880, (1992).

27 Omalley, S. S., Jaffe, A. J., Chang, G., Schottenfeld, R. S., Meyer, R. E. & Rounsaville, B. Naltrexone and Coping Skills Therapy for Alcohol Dependence - a Controlled-Study. *Archives of general psychiatry* **49**, 881-887, (1992).

28 Ross, S. & Peselow, E. Pharmacotherapy of Addictive Disorders. *Clin Neuropharmacol* **32**, 277-289, (2009).

29 Williams, S. H. Medications for treating alcohol dependence. *American family physician* **72**, 1775-1780, (2005).

30 Johnson, B. A., Ait-Daoud, N., Bowden, C. L., DiClemente, C. C., Roache, J. D., Lawson, K., Javors, M. A. & Ma, J. Z. Oral topiramate for treatment of alcohol dependence: a randomised controlled trial. *Lancet* **361**, 1677-1685, (2003).

31 Kenna, G. A., Nielsen, D. M., Mello, P., Schiesl, A. & Swift, R. M. Pharmacotherapy of dual substance abuse and dependence. *Cns Drugs* **21**, 213-237, (2007).

32 Pettinati, H. M., Volpicelli, J. R., Kranzler, H. R., Luck, G., Rukstalis, M. R. & Cnaan, A. Sertraline treatment for alcohol dependence: interactive effects of medication and alcoholic subtype. *Alcoholism, clinical and experimental research* **24**, 1041-1049, (2000).

33 Salloum, I. M., Cornelius, J. R., Daley, D. C., Kirisci, L., Himmelhoch, J. M. & Thase, M. E. Efficacy of valproate maintenance in patients with

bipolar disorder and alcoholism - A double-blind placebo-controlled study. *Archives of general psychiatry* **62**, 37-45, (2005).

34 Studies, S. O. o. A. *The National Survey on Drug Use and Health*, <http://oas.samhsa.gov/nsduh.htm> (2007).

35 Lipton, D. S. & Johnson, B. D. Smack, crack, and score: two decades of NIDA-funded drugs and crime research at NDRI 1974-1994. *Subst Use Misuse* **33**, 1779-1815, (1998).

36 O'Brien, M. S. & Anthony, J. C. Risk of becoming cocaine dependent: epidemiological estimates for the United States, 2000-2001. *Neuropsychopharmacology* **30**, 1006-1018, (2005).

37 Carrera, M. R., Meijler, M. M. & Janda, K. D. Cocaine pharmacology and current pharmacotherapies for its abuse. *Bioorg Med Chem* **12**, 5019-5030, (2004).

38 Karch, S. B. Cocaine cardiovascular toxicity. *South Med J* **98**, 794-799, (2005).

39 Boghdadi, M. S. & Henning, R. J. Cocaine: pathophysiology and clinical toxicology. *Heart Lung* **26**, 466-483; quiz 484-465, (1997).

40 Karila, L., Gorelick, D., Weinstein, A., Noble, F., Benyamina, A., Coscas, S., Blecha, L., Lowenstein, W., Martinot, J. L., Reynaud, M. & Lepine, J. P. New treatments for cocaine dependence: a focused review. *Int J Neuropsychoph* **11**, 425-438, (2008).

41 Sofuoglu, M. & Kosten, T. R. Novel approaches to the treatment of cocaine addiction. *Cns Drugs* **19**, 13-25, (2005).

42 Kuhar, M. J., Ritz, M. C. & Boja, J. W. The Dopamine Hypothesis of the Reinforcing Properties of Cocaine. *Trends in Neurosciences* **14**, 299-302, (1991).

43 Fontana, D., Post, R. M., Weiss, S. R. & Pert, A. The role of D1 and D2 dopamine receptors in the acquisition and expression of cocaine-induced conditioned increases in locomotor behavior. *Behav Pharmacol* **4**, 375-387, (1993).

44 Schubiner, H., Saules, K. K., Arfken, C. L., Johanson, C. E., Schuster, C. R., Lockhart, N., Edwards, A., Donlin, J. & Pihlgren, E. Double-blind placebo-controlled trial of methylphenidate in the treatment of adult ADHD patients with comorbid cocaine dependence. *Exp Clin Psychopharm* **10**, 286-294, (2002).

45 Moscovitz, H., Brookoff, D. & Nelson, L. A Randomized Trial of Bromocriptine for Cocaine Users Presenting to the Emergency Department. *J Gen Intern Med* **8**, 1-4, (1993).

46 Handelsman, L., Rosenblum, A., Palij, M., Magura, S., Foote, J., Lovejoy, M. & Stimmel, A. Bromocriptine for cocaine dependence - A controlled clinical trial. *Am J Addiction* **6**, 54-64, (1997).

47 Montoya, I. D., Preston, K. L., Rothman, R. & Gorelick, D. A. Open-label pilot study of bupropion plus bromocriptine for treatment of cocaine dependence. *Am J Drug Alcohol Ab* **28**, 189-196, (2002).

48 McFarland, K. & Kalivas, P. W. The circuitry mediating cocaine-induced reinstatement of drug-seeking behavior. *Journal of Neuroscience* **21**, 8655-8663, (2001).

49 Dewey, S. L., Morgan, A. E., Ashby, C. R., Horan, B., Kushner, S. A., Logan, J., Volkow, N. D., Fowler, J. S., Gardner, E. L. & Brodie, J. D. A novel strategy for the treatment of cocaine addiction. *Synapse* **30**, 119-129, (1998).

50 Dewey, S. L., Morgan, A. E., Ashby, C. R., Logan, J., Kushner, S. A., Kornetsky, C., Volkow, N. D., Fowler, J. S. & Brodie, J. D. A new gabaergic strategy for treating cocaine addiction. *J Nucl Med* **39**, 99p-100p, (1998).

51 Gerasimov, M. R., Schiffer, W. K., Gardner, E. L., Marsteller, D. A., Lennon, I. C., Taylor, S. J. C., Brodie, J. D., Ashby, C. R. & Dewey, S. L. GABAergic blockade of cocaine-associated cue-induced increases in nucleus accumbens dopamine. *European Journal of Pharmacology* **414**, 205-209, (2001).

52 Kampman, K. M., Pettinati, H., Lynch, K. G., Dackis, C., Sparkman, T., Weigley, C. & O'Brien, C. P. A pilot trial of topiramate for the treatment

of cocaine dependence. *Drug and Alcohol Dependence* **75**, 233-240, (2004).

53 Gonzalez, G., Sevarino, K., Sofuoglu, M., Poling, J., Oliveto, A., Gonsai, K., George, T. P. & Kosten, T. R. Tiagabine increases cocaine-free urines in cocaine-dependent methadone-treated patients: results of a randomized pilot study. *Addiction (Abingdon, England)* **98**, 1625-1632, (2003).

54 Hart, C. L., Ward, A. S., Collins, E. D., Haney, M. & Foltin, R. W. Gabapentin maintenance decreases smoked cocaine-related subjective effects, but not self-administration by humans. *Drug and Alcohol Dependence* **73**, 279-287, (2004).

55 Karler, R. & Calder, L. D. Excitatory Amino-Acids and the Actions of Cocaine. *Brain Research* **582**, 143-146, (1992).

56 Schenk, S., Valadez, A., Mcnamara, C., House, D. T., Higley, D., Bankson, M. G., Gibbs, S. & Horger, B. A. Development and Expression of Sensitization to Cocaine Reinforcing Properties - Role of Nmda Receptors. *Psychopharmacology* **111**, 332-338, (1993).

57 Pulvirenti, L. & Koob, G. F. Lisuride Reduces Intravenous Cocaine Self-Administration in Rats. *Pharmacol Biochem Be* **47**, 819-822, (1994).

58 Imperato, A., Honore, T. & Jensen, L. H. Dopamine release in the nucleus caudatus and in the nucleus accumbens is under glutamatergic control

through non-NMDA receptors: a study in freely-moving rats. *Brain Res* **530**, 223-228, (1990).

59 Youngren, K. D., Daly, D. A. & Moghaddam, B. Distinct actions of endogenous excitatory amino acids on the outflow of dopamine in the nucleus accumbens. *J Pharmacol Exp Ther* **264**, 289-293, (1993).

60 Cornish, J. L. & Kalivas, P. W. Glutamate transmission in the nucleus accumbens mediates relapse in cocaine addiction. *J Neurosci* **20**, RC89, (2000).

61 Cornish, J. L., Duffy, P. & Kalivas, P. W. A role for nucleus accumbens glutamate transmission in the relapse to cocaine-seeking behavior. *Neuroscience* **93**, 1359-1367, (1999).

62 van den Brink, W. & van Ree, J. M. Pharmacological treatments for heroin and cocaine addiction. *Eur Neuropsychopharmacol* **13**, 476-487, (2003).

63 Hald, J. & Jacobsen, E. A drug sensitizing the organism to ethyl alcohol. *Lancet* **2**, 1001-1005, (1948).

64 O'Shea, B. Disulfiram revisited. *Hosp Med* **61**, 849-851, (2000).

65 Kaul, S., Williams, T. D., Lunte, C. E. & Faiman, M. D. LC-MS/MS determination of carbamathione in microdialysis samples from rat brain and plasma. *J Pharm Biomed Anal* **51**, 186-191, (2010).

66 Nagendra, S. N., Madan, A. & Faiman, M. D. S-Methyl N,N-Diethylthiolcarbamate Sulfone, an in-Vitro and in-Vivo Inhibitor of Rat-Liver Mitochondrial Low K-M Aldehyde Dehydrogenase. *Biochemical Pharmacology* **47**, 1465-1467, (1994).

67 Nagendra, S. N., Faiman, M. D., Davis, K., Wu, J. Y., Newby, X. & Schloss, J. V. Carbamoylation of brain glutamate receptors by a disulfiram metabolite. *The Journal of biological chemistry* **272**, 24247-24251, (1997).

68 Ningaraj, N. S., Schloss, J. V., Williams, T. D. & Faiman, M. D. Glutathione carbamoylation with S-methyl N,N-diethylthiolcarbamate sulfoxide and sulfone. Mitochondrial low Km aldehyde dehydrogenase inhibition and implications for its alcohol-deterrent action. *Biochem Pharmacol* **55**, 749-756, (1998).

69 Madan, A., Parkinson, A. & Faiman, M. D. Identification of the human and rat P450 enzymes responsible for the sulfoxidation of S-methyl N,N-diethylthiolcarbamate (DETC-ME). The terminal step in the bioactivation of disulfiram. *Drug Metab Dispos* **23**, 1153-1162, (1995).

70 Madan, A. & Faiman, M. D. Characterization of diethyldithiocarbamate methyl ester sulfine as an intermediate in the bioactivation of disulfiram. *J Pharmacol Exp Ther* **272**, 775-780, (1995).

71 Hart, B. W. & Faiman, M. D. Bioactivation of S-methyl N,N-diethylthiolcarbamate to S-methyl N,N-diethylthiolcarbamate sulfoxide. Implications for the role of cytochrome P450. *Biochem Pharmacol* **46**, 2285-2290, (1993).

72 Yourick, J. J. & Faiman, M. D. Disulfiram metabolism as a requirement for the inhibition of rat liver mitochondrial low Km aldehyde dehydrogenase. *Biochem Pharmacol* **42**, 1361-1366, (1991).

73 Jin, L., Davis, M. R., Hu, P. & Baillie, T. A. Identification of novel glutathione conjugates of disulfiram and diethyldithiocarbamate in rat bile by liquid chromatography-tandem mass spectrometry. Evidence for metabolic activation of disulfiram in vivo. *Chem Res Toxicol* **7**, 526-533, (1994).

74 Boothby, L. A. & Doering, P. L. Acamprosate for the treatment of alcohol dependence. *Clin Ther* **27**, 695-714, (2005).

75 Besson, J., Aeby, F., Kasas, A., Lehert, P. & Potgieter, A. Combined efficacy of acamprosate and disulfiram in the treatment of alcoholism: a controlled study. *Alcohol Clin Exp Res* **22**, 573-579, (1998).

76 de Sousa, A. & de Sousa, A. An open randomized study comparing disulfiram and acamprosate in the treatment of alcohol dependence. *Alcohol Alcohol* **40**, 545-548, (2005).

77 Carroll, K. M., Fenton, L. R., Ball, S. A., Nich, C., Frankforter, T. L., Shi, J. & Rounsaville, B. J. Efficacy of disulfiram and cognitive behavior therapy in cocaine-dependent outpatients: a randomized placebo-controlled trial. *Arch Gen Psychiatry* **61**, 264-272, (2004).

78 Davies, M. I. A review of microdialysis sampling for pharmacokinetic applications. *Analytica Chimica Acta* **379**, 227-249, (1999).

79 Chaurasia, C. S. In vivo microdialysis sampling: theory and applications. *Biomed Chromatogr* **13**, 317-332, (1999).

80 Davies, M. I., Cooper, J. D., Desmond, S. S., Lunte, C. E. & Lunte, S. M. Analytical considerations for microdialysis sampling. *Adv Drug Deliv Rev* **45**, 169-188, (2000).

81 deLange, E. C. M., Danhof, M., deBoer, A. G. & Breimer, D. D. Methodological considerations of intracerebral microdialysis in pharmacokinetic studies on drug transport across the blood-brain barrier. *Brain Res Rev* **25**, 27-49, (1997).

82 Ungerstedt, U. Microdialysis - Principles and Applications for Studies in Animals and Man. *J Intern Med* **230**, 365-373, (1991).

83 Zhao, Y. P., Liang, X. Z. & Lunte, C. E. Comparison of Recovery and Delivery in-Vitro for Calibration of Microdialysis Probes. *Analytica Chimica Acta* **316**, 403-410, (1995).

84 Joukhadar, C. & Muller, M. Microdialysis: current applications in clinical pharmacokinetic studies and its potential role in the future. *Clin Pharmacokinet* **44**, 895-913, (2005).

85 Lunte, S. M. & Lunte, C. E. Microdialysis sampling for pharmacological studies: HPLC and CE analysis. *Adv Chromatogr* **36**, 383-432, (1996).

86 Larsson, C. I. The Use of an Internal Standard for Control of the Recovery in Microdialysis. *Life Sciences* **49**, Pl73-Pl78, (1991).

87 Lonnroth, P., Jansson, P. A. & Smith, U. A Microdialysis Method Allowing Characterization of Intercellular Water Space in Humans. *American Journal of Physiology* **253**, E228-E231, (1987).

88 Song, Y. & Lunte, C. E. Comparison of calibration by delivery versus no net flux for quantitative in vivo microdialysis sampling. *Analytica Chimica Acta* **379**, 251-262, (1999).

89 Song, Y. & Lunte, C. E. Calibration methods for microdialysis sampling in vivo: muscle and adipose tissue. *Analytica Chimica Acta* **400**, 143-152, (1999).

90 Stahle, L., Segersvard, S. & Ungerstedt, U. A comparison between three methods for estimation of extracellular concentrations of exogenous and endogenous compounds by microdialysis. *J Pharmacol Methods* **25**, 41-52, (1991).

91 Weiss, D. J., Lunte, C. E. & Lunte, S. M. In vivo microdialysis as a tool for monitoring pharmacokinetics. *Trac-Trend Anal Chem* **19**, 606-616, (2000).

92 Clark, H., Barbari, T. A., Stump, K. & Rao, G. Histologic evaluation of the inflammatory response around implanted hollow fiber membranes. *J Biomed Mater Res* **52**, 183-192, (2000).

93 Wisniewski, N., Klitzman, B., Miller, B. & Reichert, W. M. Decreased analyte transport through implanted membranes: Differentiation of biofouling from tissue effects. *J Biomed Mater Res* **57**, 513-521, (2001).

94 Chen, K. C. Effects of tissue trauma on the characteristics of microdialysis zero-net-flux method sampling neurotransmitters. *J Theor Biol* **238**, 863-881, (2006).

95 Dykstra, K. H., Hsiao, J. K., Morrison, P. F., Bungay, P. M., Mefford, I. N., Scully, M. M. & Dedrick, R. L. Quantitative examination of tissue concentration profiles associated with microdialysis. *Journal of neurochemistry* **58**, 931-940, (1992).

96 Hoistad, M., Chen, K. C., Nicholson, C., Fuxe, K. & Kehr, J. Quantitative dual-probe microdialysis: evaluation of [3H]mannitol diffusion in agar and rat striatum. *Journal of neurochemistry* **81**, 80-93, (2002).

97 Bungay, P. M., Newton-Vinson, P., Isele, W., Garris, P. A. & Justice, J. B. Microdialysis of dopamine interpreted with quantitative model

incorporating probe implantation trauma. *Journal of neurochemistry* **86**, 932-946, (2003).

98 Hansen, D. K., Davies, M. I., Lunte, S. M. & Lunte, C. E. Pharmacokinetic and metabolism studies using microdialysis sampling. *Journal of pharmaceutical sciences* **88**, 14-27, (1999).

99 Joukhadar, C. & Muller, M. Microdialysis - Current applications in clinical pharmacokinetic studies and its potential role in the future. *Clin Pharmacokinet* **44**, 895-913, (2005).

100 Chaurasia, C. S., Muller, M., Bashaw, E. D., Benfeldt, E., Bolinder, J., Bullock, R., Bungay, P. M., DeLange, E. C. M., Derendorf, H., Elmquist, W. F., Hammarlund-Udenaes, M., Joukhadar, C., Kellogg, D. L., Lunte, C. E., Nordstrom, C. H., Rollema, H., Sawchuk, R. J., Cheung, B. W. Y., Shah, V. P., Stahle, L., Ungerstedt, U., Welty, D. F. & Yeo, H. AAPS-FDA workshop white paper: Microdialysis principles, application and regulatory perspectives. *Pharmaceutical Research* **24**, 1014-1025, (2007).

101 Georganopoulou, D. G., Carley, R., Jones, D. A. & Boutelle, M. G. Development and comparison of biosensors for in-vivo applications. *Faraday Discuss*, 291-303, (2000).

102 van der Zeyden, M., Oldenziel, W. H., Rea, K., Cremers, T. I. & Westerink, B. H. Microdialysis of GABA and glutamate: analysis,

interpretation and comparison with microsensors. *Pharmacol Biochem Behav* **90**, 135-147, (2008).

103 Torregrossa, M. M. & Kalivas, P. W. Microdialysis and the neurochemistry of addiction. *Pharmacol Biochem Behav* **90**, 261-272, (2008).

104 Lee, G. J., Park, J. H. & Park, H. K. Microdialysis applications in neuroscience. *Neurol Res* **30**, 661-668, (2008).

105 Kehr, J. Determination of gamma-aminobutyric acid in microdialysis samples by microbore column liquid chromatography and fluorescence detection. *J Chromatogr B Biomed Sci Appl* **708**, 49-54, (1998).

106 Kehr, J., Dechent, P., Kato, T. & Ogren, S. O. Simultaneous determination of acetylcholine, choline and physostigmine in microdialysis samples from rat hippocampus by microbore liquid chromatography/electrochemistry on peroxidase redox polymer coated electrodes. *J Neurosci Methods* **83**, 143-150, (1998).

107 Obrenovitch, T. P. & Zilkha, E. Microdialysis coupled to online enzymatic assays. *Methods* **23**, 63-71, (2001).

108 Smolders, I., De Klippel, N., Sarre, S., Ebinger, G. & Michotte, Y. Tonic GABA-ergic modulation of striatal dopamine release studied by in vivo microdialysis in the freely moving rat. *Eur J Pharmacol* **284**, 83-91, (1995).

109 Smolders, I., Sarre, S., Michotte, Y. & Ebinger, G. The Analysis of Excitatory, Inhibitory and Other Amino-Acids in Rat-Brain Microdialysates Using Microbore Liquid-Chromatography. *J Neurosci Meth* **57**, 47-53, (1995).

110 Telting-Diaz, M. & Lunte, C. E. Distribution of tacrine across the blood-brain barrier in awake, freely moving rats using in vivo microdialysis sampling. *Pharm Res* **10**, 44-48, (1993).

111 Lada, M. W., Vickroy, T. W. & Kennedy, R. T. High temporal resolution monitoring of glutamate and aspartate in vivo using microdialysis on-line with capillary electrophoresis with laser-induced fluorescence detection. *Anal Chem* **69**, 4560-4565, (1997).

112 Sauvinet, V., Parrot, S., Benturquia, N., Bravo-Moraton, E., Renaud, B. & Denoroy, L. In vivo simultaneous monitoring of gamma-aminobutyric acid, glutamate, and L-aspartate using brain microdialysis and capillary electrophoresis with laser-induced fluorescence detection: Analytical developments and in vitro/in vivo validations. *Electrophoresis* **24**, 3187-3196, (2003).

113 Wang, M., Roman, G. T., Schultz, K., Jennings, C. & Kennedy, R. T. Improved temporal resolution for in vivo microdialysis by using segmented flow. *Anal Chem* **80**, 5607-5615, (2008).

114 Shou, M., Ferrario, C. R., Schultz, K. N., Robinson, T. E. & Kennedy, R. T. Monitoring dopamine in vivo by microdialysis sampling and on-line CE-laser-induced fluorescence. *Anal Chem* **78**, 6717-6725, (2006).

115 Benturquia, N., Parrot, S., Sauvinet, V., Renaud, B. & Denoroy, L. Simultaneous determination of vigabatrin and amino acid neurotransmitters in brain microdialysates by capillary electrophoresis with laser-induced fluorescence detection. *J Chromatogr B Analyt Technol Biomed Life Sci* **806**, 237-244, (2004).

116 Denoroy, L., Parrot, S., Renaud, L., Renaud, B. & Zimmer, L. In-capillary derivatization and capillary electrophoresis separation of amino acid neurotransmitters from brain microdialysis samples. *J Chromatogr A* **1205**, 144-149, (2008).

117 Bowser, M. T. & Kennedy, R. T. In vivo monitoring of amine neurotransmitters using microdialysis with on-line capillary electrophoresis. *Electrophoresis* **22**, 3668-3676, (2001).

118 Parrot, S., Sauvinet, V., Xavier, J. M., Chavagnac, D., Mouly-Badina, L., Garcia-Larrea, L., Mertens, P. & Renaud, B. Capillary electrophoresis combined with microdialysis in the human spinal cord: a new tool for monitoring rapid peroperative changes in amino acid neurotransmitters within the dorsal horn. *Electrophoresis* **25**, 1511-1517, (2004).

119 Siri, N., Lacroix, M., Garrigues, J. C., Poinsot, V. & Couderc, F. HPLC-fluorescence detection and MEKC-LIF detection for the study of amino acids and catecholamines labelled with naphthalene-2,3-dicarboxyaldehyde. *Electrophoresis* **27**, 4446-4455, (2006).

120 Smith, S. E. & Sharp, T. An investigation of the origin of extracellular GABA in rat nucleus accumbens measured in vivo by microdialysis. *J Neural Transm Gen Sect* **97**, 161-171, (1994).

121 Freed, A. L. & Lunte, S. M. Separation of naphthalene-2,3-dicarboxaldehyde-derivatized-substance P and its metabolites by micellar electrokinetic chromatography. *Electrophoresis* **21**, 1992-1996, (2000).

122 Tseng, H. M., Li, Y. & Barrett, D. A. Profiling of amine metabolites in human biofluids by micellar electrokinetic chromatography with laser-induced fluorescence detection. *Anal Bioanal Chem* **388**, 433-439, (2007).

123 Otsuka, K. & Terabe, S. Micellar electrokinetic chromatography. *Mol Biotechnol* **9**, 253-271, (1998).

2 *IN VIVO* MICRODIALYSIS AND CE-LIF FOR MONITORING GABA, GLUTAMATE, AND CARBAMATHIONE

2.1 Introduction

The first step in determining the pharmacokinetics (PK) and pharmacodynamics (PD) of carbamathione is the development of a method to separate and detect carbamathione and the relevant neurotransmitters simultaneously in a microdialysis samples. The development of this method would allow the monitoring of carbamathione-induced changes in the neurotransmitters. The following chapter describes a capillary electrophoresis in conjunction with laser-induced fluorescence (CE-LIF) method that was developed to achieve this goal.

2.1.1 Effect of Carbamathione on GABA and Glutamate

There has been renewed interest in disulfiram due to recent clinical trials. Disulfiram was effective in reducing cocaine and alcohol consumption and was reported to reduce craving. Disulfiram is a pro-drug that requires bioactivation to *S*- methyl *N, N*-diethylthiocarbamate sulfoxide (DETC-MeSO) for the inhibition of aldehyde dehydrogenase ($ALDH_2$).[1-3] Another disulfiram metabolite, carbamathione is formed after DETC-MeSO and was found in the brain after administration of both disulfiram and DETC-MeSO.[4,5] Carbamathione has no effect on liver $ALDH_2$ when administered to rodents, but studies show

carbamathione is a partial non-competitive inhibitor of the *N*-methyl-*D*-aspartic acid (NMDA) glutamate receptor.[4,6] Evidence in the literature suggests that the glutamatergic and GABAergic systems may play a role in ethanol addiction.[7-11] In light of carbamathione's effect on the NMDA receptors, it was important to study the effect of carbamathione administration on brain glutamate (Glu) and gamma-amino butyric acid (GABA) levels as a step towards providing an explanation for disulfiram's efficacy in clinical trials.

2.1.2 CE-LIF for Neurotransmitters in Biological Samples

CE allows the monitoring of rapid changes in brain neurotransmitters with very small volume requirements. CE-LIF has recently been used to determine various compounds in biological samples.[12-14] In the brain microdialysis samples, excitatory amino acids such as Glu and GABA have been analyzed.[15,16] Since neurotransmitters are not natively fluorescent, derivatization prior to separation is required.[17-19] For this study, napthalene-2,3-dicarboxyaldehyde (NDA) was chosen since it is not fluorescent itself and it reacts rapidly to give stable fluorescent cyanobenzo[*f*]isoindol (CBI) derivatives. The derivatization of the primary amine provided the added advantage of including carbamathione in the analysis of a sample since it is also a primary amine. The derivatization scheme of NDA is shown if figure 2.1.

Figure 2.1 NDA derivatization scheme.

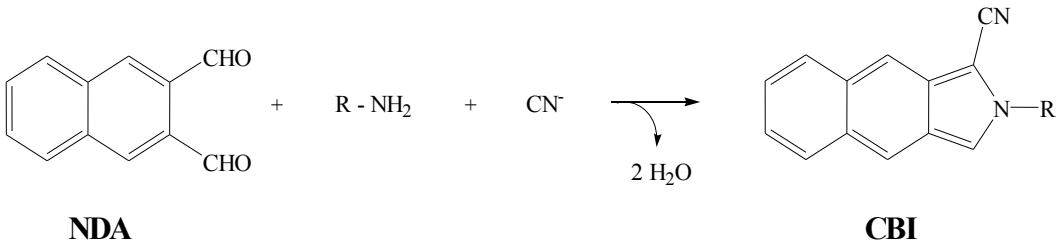

2.1.3 Specific Aims of Research

The goal of this research was to apply CE separation methods to determine the changes (if any) in the amino acid neurotransmitters from the nucleus accumbens of a rat brain as related to the administration of carbamathione. Existing CE separation methods were modified and optimized in order to include carbamathione in the analysis of GABA and Glu. Since carbamathione has a primary amine functional group (figure 2.2), it can be derivatized along with GABA and Glu using the NDA derivatization scheme. The derivatives were detected using LIF detection. The required limits of detection and quantification for the analytical method were based on the known concentrations of GABA, Glu and carbamathione in the nucleus accumbens. The expected concentration range for GABA and Glu in microdialysis samples from rat brain nucleus accumbens are 40-100 nmol/L and 0.7-2.5 μmol/L, respectively.[12,20-22] Previous studies with carbamathione have demonstrated that micromolar concentrations of carbamathione were detected in rat brain dialysate after a 200 mg/kg dose of carbamathione.[23] The temporal resolution achieved for this method was 5 min. The neurotransmitter and carbamathione data were used to establish PK and PD relationships between the administration of the drug and changes in the neurotransmitter systems.

Figure 2.2 Structure of carbamathione.

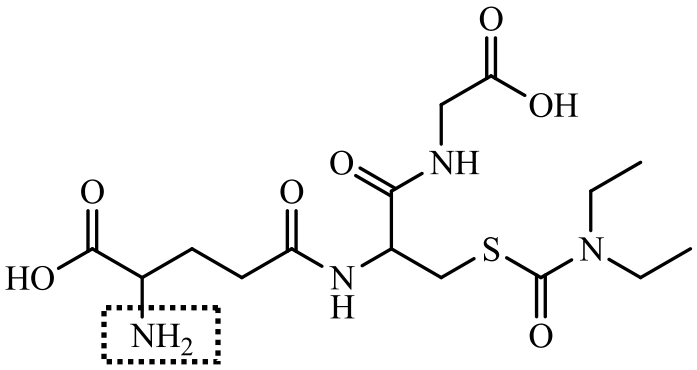

2.2 Experimental

2.2.1 Chemicals and Reagents

Napthalene-2, 3-dicarboxyaldehyde (NDA) was purchased from Invitrogen (Molecular Probes, Eugene, OR, USA). Sodium cyanide (NaCN) was purchased from Fluka (Buchs, Switzerland). Glutamate (Glu), gamma-amino butyric acid (GABA), 2-aminoadipic acid (AAP), sodium tetraborate, boric acid, and perchloric acid were purchased from Sigma (St. Louis, MO, USA). Sodium bicarbonate ($NaHCO_3$), sodium chloride (NaCl), potassium chloride (KCl), magnesium chloride ($MgCl_2$), calcium chloride ($CaCl_2$), monosodium phosphate (NaH_2PO_4), disodium hydrogen phosphate (Na_2HPO_4), sodium hydroxide (NaOH), hydrochloric acid (HCl), ethanol, methanol (MeOH), and acetonitrile (ACN) were purchased from Fisher Scientific (Pittsburgh, PA, USA). Isoflurane and ketamine were purchased from Fort Dodge Animal Health (Fort Dodge, IA, USA). Xylazine was purchased from Lloyd Laboratories (Shenandoah, IA, USA). Acepromazine was purchased from Boehringer Ingelheim Vetmedica, Inc. (St. Joseph, MO, USA). VetBond tissue glue was purchased from 3M (St. Paul, MN, USA). Lactated Ringer's was purchased from B Braun Medical Inc. (Irvine, CA, USA). Ultrapure water was obtained with a Milli-Q system (Millipore, Bedford, MA, USA).

Carbamathione was synthesized using methods previously developed.[6,24] The structure of carbamathione was confirmed by mass spectrometry and nuclear magnetic resonance (NMR ^{1}H, D_2O).[5] Exact mass determination of $[M + H]^+$ $C_{15}H_{27}N_4O_7S$ was 407.1594 ± 0.0014 (n = 4) which was 2.3 ppm from the expected mass. The NMR chemical shifts were δ 1.14 m 6H ($(CH_3CH_2)_2N$-), δ 2.11 m 2H (Glu- β,β'), δ 2.45 m 2H (Glu-γ,γ'), δ 3.15 m 1H (Cys- β), δ 3.37 m, 5H ($(CH_3CH_2)_2N$-, Cys- β), δ 3.81 t 1H (Glu-α), δ 3.85 s 2H (Gly-α,α'), δ 4.55 t, 1H (Cys- α). The purity of the carbamathione synthesized was determined by HPLC with UV detection at 215 nm. A sample of 1000 nmol/L concentration gave a chromatogram with signal-to-noise ratio (S/N) > 100 and there was no other detectable peak. Liquid chromatography coupled with mass spectrometry (LC/MS) injections of the standard revealed no other MS detectable peaks during the LC gradient. LC-MS/MS was also used to evaluate the stability of the synthesized carbamathione under different temperature and storage conditions. Samples of carbamathione were subjected to room temperature (25° C), -20° C, and three freeze-thaw cycles. Stability data are shown in table 2.3. Carbamathione was determined to be stable under different temperature and storage conditions. All the samples evaluated displayed variability of less that 10% relative standard deviation (R.S.D.).

Table 2.3 Stability of carbamathione under various conditions using LC-MS/MS.

All stability studies were conducted at three concentrations of carbamathione (5.0×10^{-9}, 1.0×10^{-7}, 5.0×10^{-6} mol/L) with three determinations each.

Storage Conditions	Concentration (mol/L)		RSD (%)
	Nominal	Mean Measured	
Freeze-thaw stability	5.0×10^{-9}	5.520	8.0%
	1.0×10^{-7}	101.3	3.4%
	5.0×10^{-6}	5167	5.5%
Stability at room temperature (2h)	5.0×10^{-9}	4.979	7.0%
	1.0×10^{-7}	102.5	5.1%
	5.0×10^{-6}	5041	2.7%
Stability at room temperature (4h)	5.0×10^{-9}	4.779	9.0%
	1.0×10^{-7}	95.55	6.9%
	5.0×10^{-6}	5111	6.3%
Stability at -20° C (10 days)	5.0×10^{-9}	4.583	7.4%
	1.0×10^{-7}	103.4	2.8%
	5.0×10^{-6}	5016	6.6%
Stability at -20° C (20 days)	5.0×10^{-9}	5.060	8.2%
	1.0×10^{-7}	105.8	3.9%
	5.0×10^{-6}	5088	8.7%

Artificial cerebrospinal fluid (aCSF) contained 145 mmol/L NaCl, 2.7 mmol/L KCl, 1.0 mmol/L $MgCl_2$, 1.2 mmol/L $CaCl_2$, 0.45 mmol/L NaH_2PO_4, and 2.33 mmol/L Na_2HPO (pH 7.4). The aCSF was filtered through a 0.2-µm pore size cellulose acetate membrane filter and stored at room temperature (25° C). Standard solutions of amino acids (1 mmol/L each) were dissolved in 0.1 mol/L perchloric acid and stored at 4° C. Borate buffer for derivatization was obtained by dissolving 7.73 g of boric acid and 11.92 g of sodium tetraborate, respectively in 250 mL of ultrapure water each. The pH of the sodium tetraborate solution was measured with a pH-meter and adjusted until 8.7 with the boric acid solution. A 3 mmol/L NDA solution was prepared in ACN-water (50:50, v/v) weekly and stored at 4° C. An 87 mmol/L NaCN solution was prepared in ultrapure water and stored at 4° C. The background electrolyte (BGE) consisted of 50 mmol/L boric acid. The pH of the solution was adjusted to 9.6 with a 1 mol/L NaOH solution.

2.2.2 Derivatization

A borate-NaCN solution (100:20, v/v) was prepared by adding 20 µL of 87 mmol/L NaCN to 100 µL of the derivatization borate buffer. On the day of analysis, 5 µL of dialysate sample and 5 µL of standards were derivatized at room temperature (25° C) by adding 1 µL of internal standard (10 µmol/L AAP), 1 µL of the borate-NaCN solution and 1 µL of 3 mmol/L NDA solution.

2.2.3 CE-LIF Instrumentation

The electrophoretic system consisted of an automatic P/ACE MDQ system (Beckman-Coulter, Fullerton, CA, USA) equipped with an external LIF detector (ZETALIF, Picometrics, Toulouse, France). The excitation was performed by a helium-cadmium laser (Omnichrome, Chino, CA, USA) at a wavelength of 442 nm. A 50 μm id fused-silica capillary (Polymicro Technology, Phoenix, AZ, USA) was used (75 cm total length, 60 cm effective), with a separation voltage of 27.5 kV for 12 min. Each day, before the analyses were performed, the capillary was sequentially flushed at 20 psi with MeOH for 5 min, ultrapure water for 2 min, 1 mol/L HCl for 5 min, ultrapure water for 2 min, 1 mol/L NaOH for 10 min, ultrapure water for 2 min and finally with the BGE for 5 min. Between analyses, the capillary was flushed at 20 psi with 1 mol/L NaOH for 3 min, with ultrapure water for 0.5 min and then with the BGE for 1.5 min. All the solutions injected onto the capillary were sterilized using a disposable 0.22 μm polyethersulfone (PES) membrane syringe filter (Millipore, Co. Cork, Ireland). Samples were introduced by hydrodynamic injections for 5 s at 0.5 psi. Electropherograms were acquired on Beckman 32 Karat software.

2.2.4 Method Development

Experiments to optimize the separation buffer were carried out using standards of GABA, Glu, and carbamathione prepared in aCSF and rat brain microdialysis samples. The separation of GABA, Glu, carbamathione and the internal standard (IS) was studied by varying the concentration and pH of the boric acid solution. Increasing the concentration of boric acid (figure 2.4) and increasing the pH (figure 2.5) both resulted in increased resolution and migration times. However, when 75 mmol/L boric acid or a buffer at pH 10 was used, the currents generated at higher separation voltages (> 22.5 kV) resulted in joule heating. When 25 mmol/L boric acid or a pH 9.2 buffer was used, poor peak shapes were observed with a marked increase in the peak widths of GABA and carbamathione (see figures 2.3 and 2.4). The run buffer ultimately chosen for the separation was 50 mmol/L boric acid at pH 9.6 because it represented a good compromise between run time and peak resolution. In addition, the currents produced with this buffer did not result in joule heating when voltages up to 30 kV were applied. The resolution data with this buffer indicated good separation between standards (R > 1.5) for all pairs tested.

Peak identification in microdialysis samples were carried out by comparing migration times with those present in standards (figure 2.6).

Figure 2.4 Effect of varying the concentration of BGE on separation.

Effect of increasing boric acid concentration on separation of NDA-derivatized GABA (1), carbamathione (2), IS (3), and Glu (4). IS was AAP. Electropherograms were obtained using varying concentrations of boric acid buffer (pH 9.6) under a 27.5 kV voltage. NDA-derivatized compounds were detected using LIF detection (ex. 442 nm).

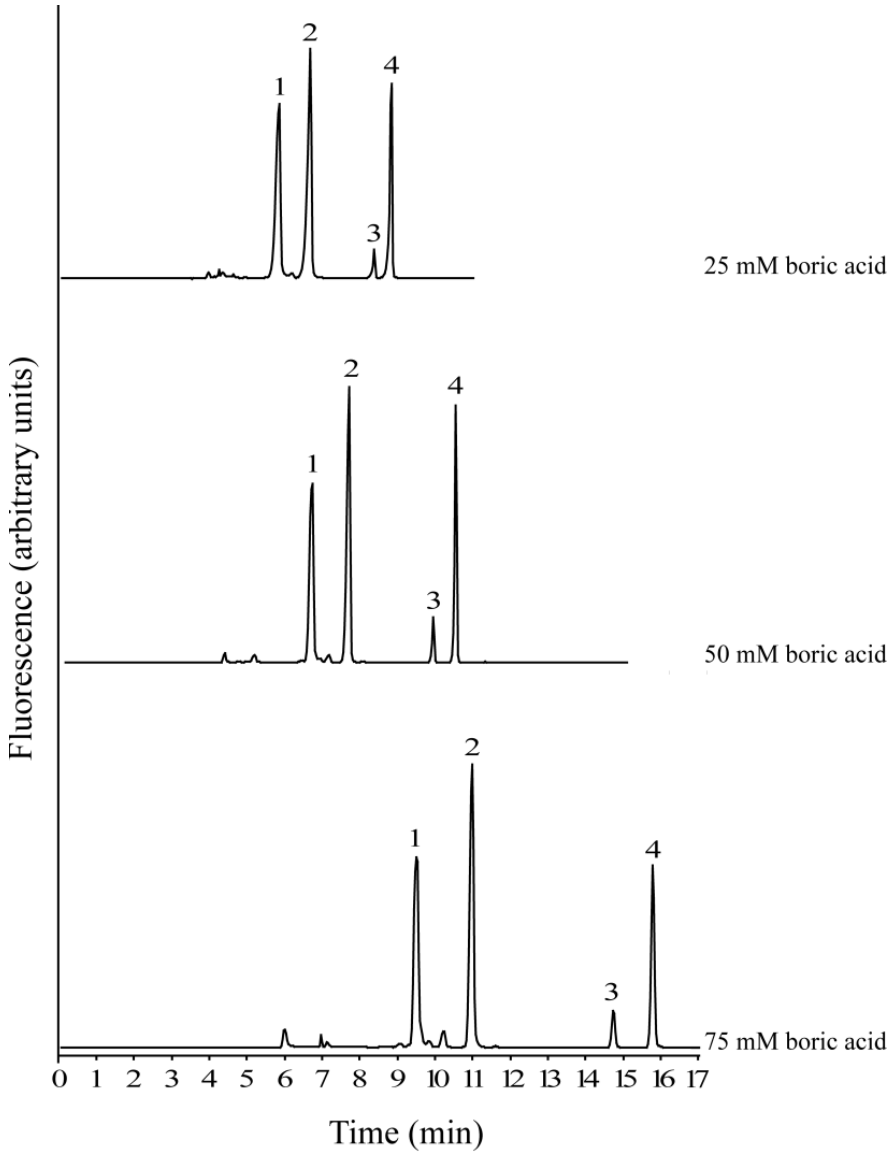

Figure 2.5 Effect of varying pH of BGE on separation.

Effect of pH acid concentration on separation of NDA-derivatized GABA (1), carbamathione (2), IS (3), and Glu (4). IS was AAP. Electropherograms were obtained using 50 mmol/L boric acid buffer at varying pH levels under 27.5 kV voltage. NDA-derivatized compounds were detected using LIF detection (ex. 442 nm).

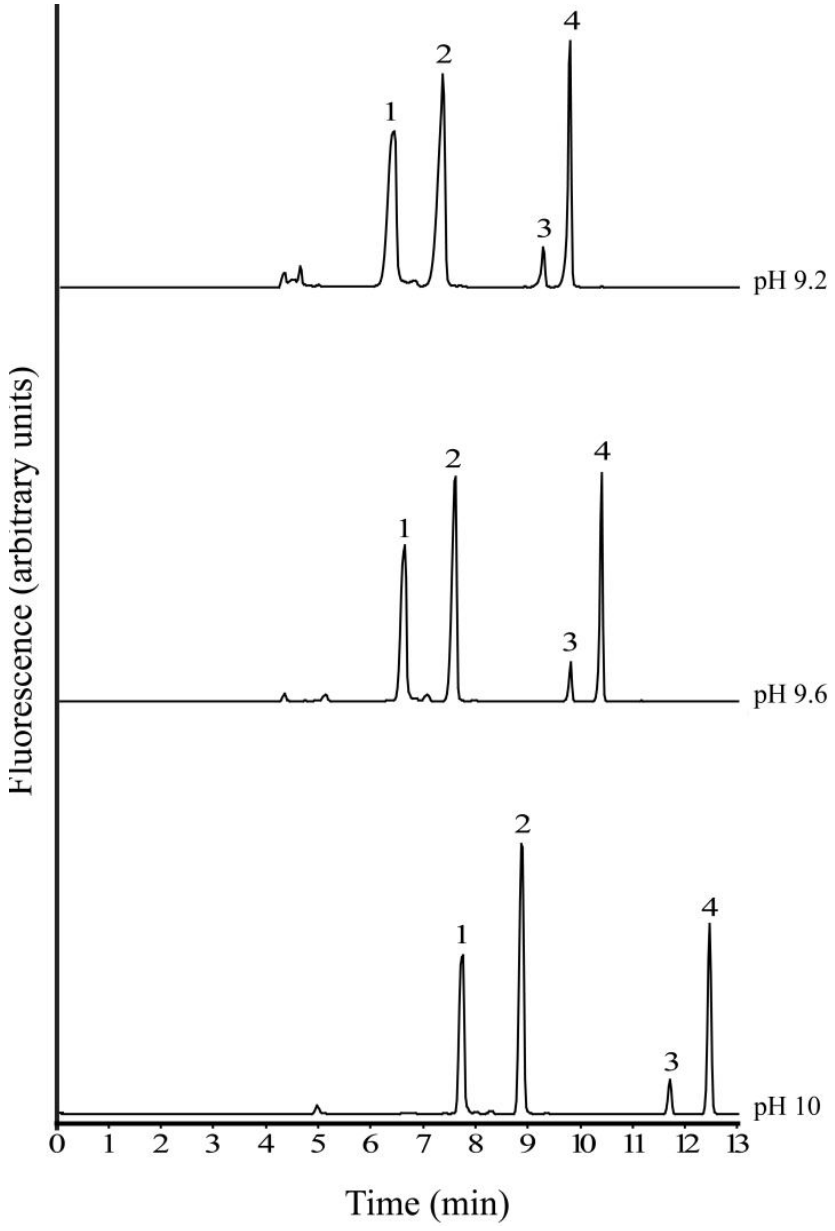

Figure 2.6 Typical CE-LIF electropherograms.

Electropherograms of standard solution (A) containing GABA (1), carbamathione (2), and Glu (4) compared to dialysate obtained from rat brain (B). IS (3) was AAP. Electropherograms were obtained using 50 mmol/L boric acid buffer (pH 9.6) under a 27.5 kV voltage. NDA-derivatized compounds were detected using LIF detection (ex. 442 nm).

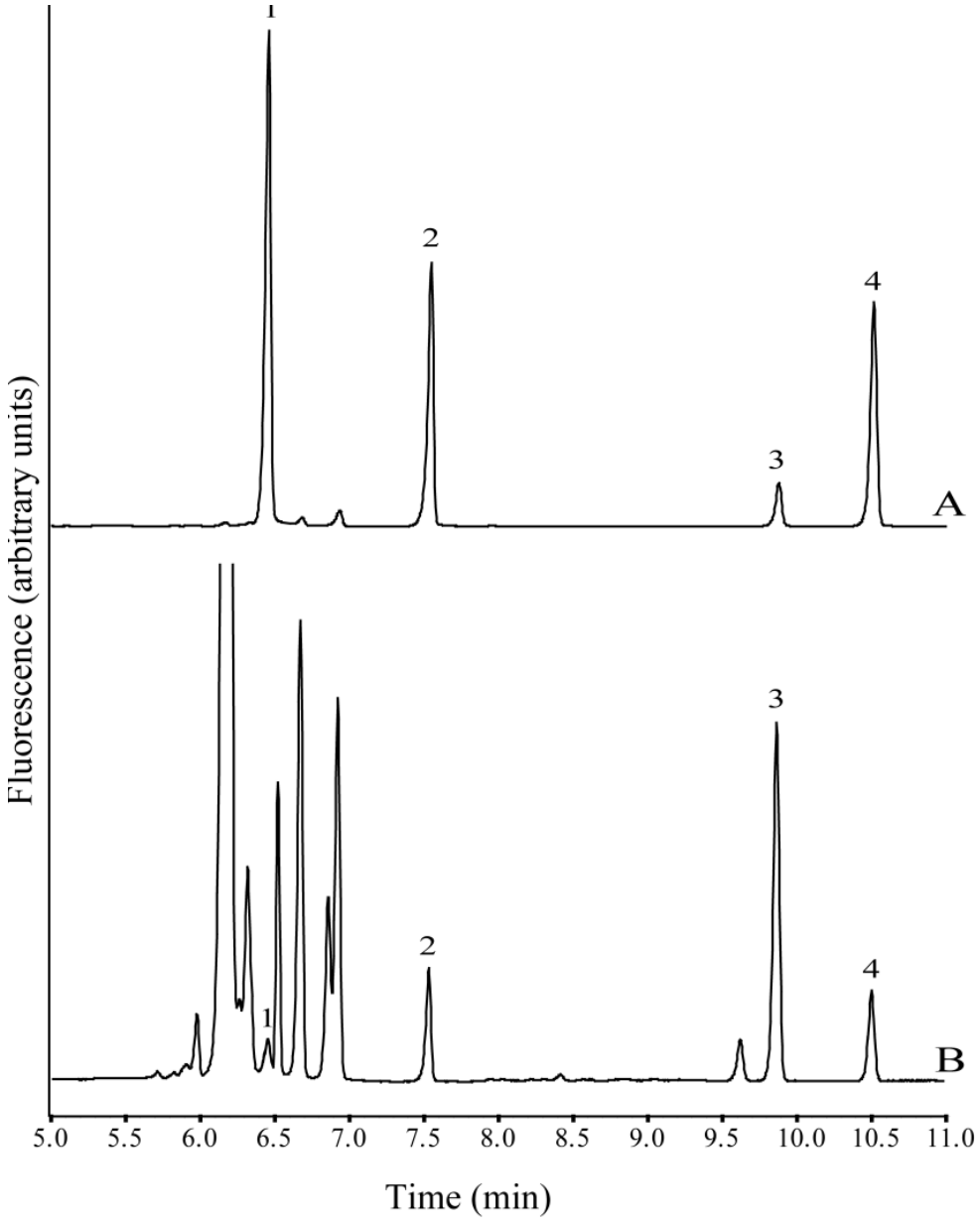

In addition, the observed height of the peaks of interest increased when exogenous Glu and GABA were added to the microdialysis samples. No additional peaks appeared when Glu and GABA were added. Background peaks associated with NDA derivatization did not interfere with any of the analytes of interest.

A 5 s sample hydrodynamic injection at 0.5 psi was chosen because it was a good compromise between separation and sensitivity. It was observed that if time of injection was increased, the width of the peaks increased and analytes were less separated. Voltages between 20-30 kV were tested and the best separation was obtained at 27.5 kV.

In summary, separations were carried out using 50 mmol/L boric acid buffer at pH 9.6 and a running voltage of 27.5 kV in 75 x 50 μm id fused-silica capillary (60 cm effective). Separations were performed at room temperature (25° C). Figure 2.6 shows a typical electropherogram of derivatized microdialysis sample from the rat brain nucleus accumbens spiked with IS.

2.2.5 Method Validation Experiments

Calibration standards for method validation contained GABA prepared in a concentration range of 10^{-9}- 10^{-6} mol/L, Glu in a concentration range of 10^{-9}- 10^{-6} mol/L and carbamathione prepared in a range of 10^{-8}- 10^{-5} mol/L. Calibration plots were plotted as the ratio of the area of compound of interest to area of the internal standard versus concentration (number of concentrations of each analyte, n = 7). The limits of detection and quantification were calculated as the analyte concentration that resulted in peaks with signal-to-noise ratio (S/N) of 3 and 10, respectively. Intra-day and inter-day reproducibility were determined using standards of Glu, GABA, and carbamathione prepared in aCSF and microdialysis samples. The accuracy of the method was calculated from the analysis of standards in aCSF, microdialysis samples and microdialysis samples spiked with known concentrations of standards (in triplicate).

2.2.6 Microdialysis

2.2.6.1 Brain Probes

Microdialysis samples were obtained from the brain utilizing microdialysis probes with 2 mm membranes purchased from CMA Microdialysis (North Chelmsford, MA, USA). The relative recovery of carbamathione through the microdialysis probes were estimated by delivery experiments.[25] Delivery experiments were

carried out by perfusing 1 μmol/L carbamathione through the microdialysis probes *in vivo* at 1 μL/min, and determining the percentage that diffused through the membrane.

2.2.6.2 Animals and Surgery

All experiments were carried out in accordance with Institutional Animal Care and Use Committee (IACUC) animal protocols. Male Sprague Dawley rats weighing 300-400 g were used for all experiments. The rats were housed in temperature controlled rooms with access to food and water *ad libitum* prior to surgery. The rats were initially anesthetized by isofluorane inhalation followed by an subcutaneous (s.c.) injection of a ketamine (67.5 mg/kg), xylazine (3.4 mg/kg) and acepromazine (0.67 mg/kg) mixture. Booster doses of ketamine (1:4 dilution with Ringer's solution) were administered by intramuscular (i.m.) injections in the anesthetized experiments. Incision sites were prepared by shaving away as much hair as possible. For awake animal experiments, sterile surgeries were conducted. The microdialysis probes and surgical instruments were sterilized by ethylene oxide. The incision sites were prepared by shaving and washing with alternating scrubs of Prodine (Phoenix Pharmaceutical, Inc., St. Joseph, MO, USA) and with a 70% (v:v) solution of aqueous ethanol. The rat's body temperature was maintained during the surgical procedure by placing the animal on microwaveable

heating pads. After the surgical procedures, the rats were administered 0.5 to 3 mL/kg of saline s.c. to prevent dehydration.

The femoral vein of the rat was cannulated for intravenous (i.v.) dosing. A small midline skin incision was made on the inside of the leg and the femoral blood vessels were located. The large blue vein was cleared from fine connective tissue by blunt dissection and cotton swab. The femoral vein was externalized by placing a spatula under it perpendicular to the axis of the vein. A 1 cm section of femoral vein was temporarily ligated with silk ligatures. Using a pair of fine spring scissors a nick was made between ligatures and a PE-10 cannula was inserted into the femoral vein to the vena cava lumen. The femoral vein was ligated on either side of the cut. The femoral cannula was then filled with saline solution and stoppered until dosing. The brain probe was implanted as previously described.[5] Briefly, the rat was placed in a stereotaxic apparatus to implant the brain probe. The coordinates of the insertion site, the nucleus accumbens shell, relative to the bregma line were +2.2 mm anterior, +1.5 mm lateral and −6.5 mm ventral, according to the rat stereotaxic atlas.[26] A guide cannula was lowered into the nucleus accumbens using a micromanipulator and fixed in place using skull screws and dental cement. The guide cannula was later replaced with the brain probe. For the awake animal experiments, the femoral cannula was externalized

through a sterile incision in the neck. All incisions were closed with stitches or surgical staples.

2.2.6.3 Microdialysis Sample Collection

Microdialysis samples were collected using a CMA 100 microinfusion pump and a HoneyComb fraction collector (Bioanalytical Systems Inc., West Lafayette, IN, USA). Connection of the microinjection pump and the fraction collector to the microdialysis probes was accomplished with tubing connectors (Bioanalytical Systems Inc., West Lafayette, IN, USA). After implantation, the brain probes were perfused with aCSF at 1 μL/min. For the awake animal experiments, the rats were placed in a rat turn equipped with a swivel arm (Bioanalytical Systems Inc., West Lafayette, IN, USA) as shown in figure 2.7. The dead volume between the dialysis site and the fraction collector was also determined in order to accurately monitor the neurochemical changes. The delay due to the dead volume was estimated to be 685 s and upon the administration of carbamathione, microdialysis samples were collected after this period of time.

2.2.6.4 In Vivo Experiments

The collection of 5 min samples was initiated after a 3 h waiting period for anesthetized experiments and a 24 h waiting period for awake experiments.

Figure 2.7 Swivel-based awake animal system

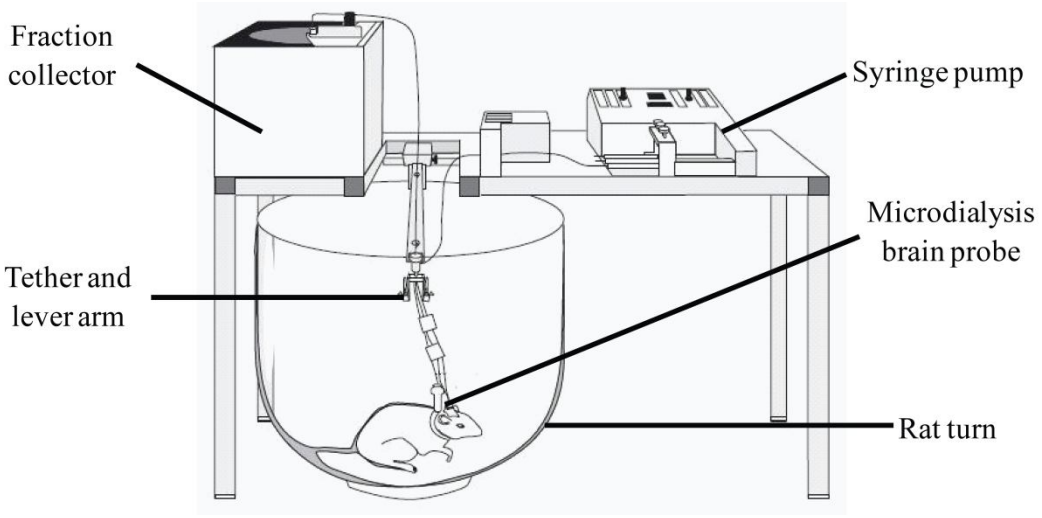

www.microdialysis.se

For dosing purposes, the carbamathione dose (200 mg/kg) was prepared by adding a few drops of 1 mol/L $NaHCO_3$ solution and bringing the volume up to 1 mL with saline solution. After the i.v. administration of carbamathione through the femoral cannula, microdialysis samples were collected for 3 h. At the end of the experiments, the rats were sacrificed by placement in an isofluorane chamber for approximately 30 min. Rat brains were harvested in order to perform a histological confirmation of brain probe position.

2.3 Results and Discussion

2.3.1 Method Validation Results

Validation was carried out in accordance with instructions for good laboratory practice.[27,28] Validation parameters were determined for GABA, Glu, and carbamathione in standards as well as brain microdialysis samples. The final results are shown in table 2.8. The regression coefficient of the calibration obtained with standard solutions and microdialysis samples showed good linearity and led to the routine use of only three points of the calibration curve. Limits of detection and quantification were lower than concentrations measured in microdialysis samples from the nucleus accumbens.

Table 2.8 Quantitative parameters for the analysis GABA, Glu, and carbamathione in aCSF and microdialysis samples.

aCSF	GABA	Glu	Carbamathione
Calibration range (mol/L)	10^{-9}-10^{-6}	10^{-9}-10^{-6}	10^{-8}-10^{-5}
Regression coefficient of calibration (r^2)	0.9969	0.9981	0.9990
Intra-assay repeatability (%RSD)[a]	9.7	8.4	7.5
Intra-day repeatability (%RSD)[a]	6.2	3.9	4.8
Inter-day repeatability (%RSD)[b]	8.0	3.1	5.3
Accuracy (%)[c]	2.2-1.1	1.5-0.9	4.1-1.5
Limits of detection (mol/L)	1.0×10^{-8}	6.0×10^{-9}	1.5×10^{-8}
Limits of quantification (mol/L)	5.0×10^{-8}	3.0×10^{-8}	6.0×10^{-8}

Microdialysis Samples	GABA	Glu	Carbamathione
Calibration range (mol/L)[d]	10^{-9}-10^{-6}	10^{-9}-10^{-6}	10^{-8}-10^{-5}
Regression coefficient of calibration (r^2)	0.9950	0.9978	0.9970
Intra-assay repeatability (%RSD)[a]	11.5	9.4	8.8
Intra-day repeatability (%RSD)[a]	7.5	6.7	6.1
Accuracy (%)[c,d]	7.6-3.6	2.8-1.1	3.0-1.9

a. Ten replicates

b. Ten days, three replicates each

c. Three replicates, tested concentrations of 10^{-7}- 5×10^{-7} mol/L for GABA, Glu and carbamathione

d. Spiked microdialysis samples (the added volume represents 10% of the microdialysis sample volume)

2.3.2 Microdialysis Probe Calibration

The characteristics of the implanted microdialysis probes were evaluated at the end of each experiment. Based on the delivery experiments, the *in vivo* extraction efficiency by delivery (EE_d) (mean ± standard error of mean [SEM], $n = 3$) for carbamathione was determined to be 10.8 ± 1.5% for the brain probes. The concentrations of carbamathione determined in the microdialysis samples were corrected for the EE_d of the probe used. The *in vitro* extraction efficiency by recovery (EE_r) (mean ± SEM, $n = 3$) for GABA and Glu was estimated to be 9.5 ± 0.8% and 12.9 ± 1.1% respectively. The concentrations of GABA and Glu were expressed as percent (mean ± SEM) of baseline concentrations in order to monitor changes from basal levels upon administration of carbamathione.

2.3.3 Histological Confirmation of Brain Probe Position

Microdialysis probe locations were examined histologically after completion of the experiments. After the rats were euthanized by isofluorane inhalation, the brains were removed and fixed in buffered formalin (10%). The tissues from the nucleus accumbens were embedded in paraffin wax and stained with hematoxylin-eosin. Only probes with at least 85% of the active dialysis membrane in the nucleus accumbens were included in the study. The representative location of microdialysis probe in the nucleus accumbens shell is shown in figure 2.9.

Figure 2.9 Representative location of microdialysis probe in nucleus accumbens shell.[26]

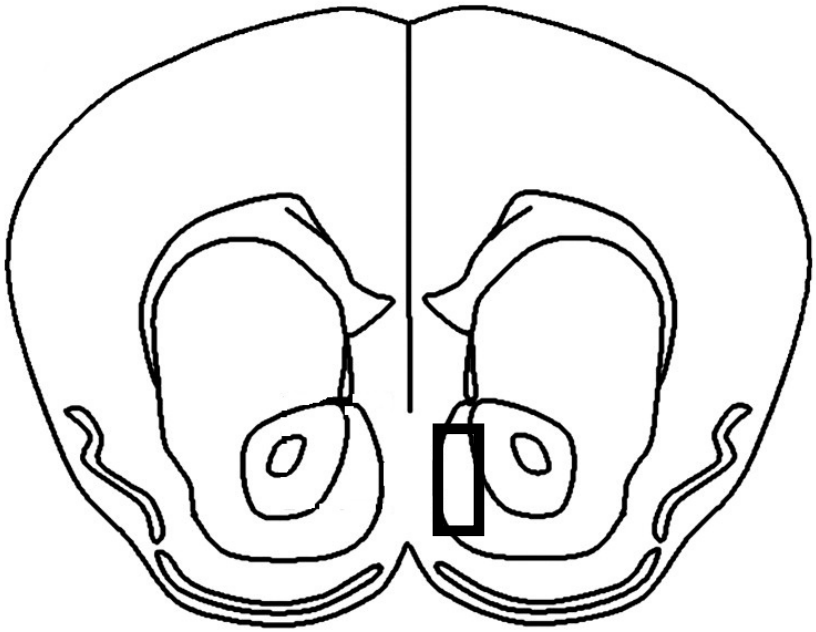

2.3.4 *In Vivo* Studies

Linear regression analysis was performed to test the existence of a statistically significant linearity for the calibration curves. Changes in concentration of Glu and GABA were expressed as percent of the basal concentration, measured before drug or vehicle administration. Data are given as mean ± SEM. Comparison between treated and control rats were achieved on percentage transformed data using analysis of variance (ANOVA) and post-hoc comparison by Tukey-Kramer test. The level of significance was set at $P < 0.05$ for all comparisons.

2.3.4.1 Experiments on Anesthetized Rats

The CE-LIF method developed was initially used for the study of carbamathione-induced changes in GABA and in the brain of anesthetized rats. For this purpose 200 mg/kg carbamathione was administered i.v. as a bolus dose and brain microdialysis samples were collected. The effect of carbamathione administration on basal levels of GABA and Glu in anesthetized rats is shown in figure 2.10. The basal concentrations of GABA and Glu in microdialysis samples from the brain nucleus accumbens were 83.5 ± 12.9 nmol/L and 1.06 ± 0.23 μmol/L, respectively. Basal Glu concentrations were significantly increased by 91% ($P <$ 0.05 Tukey-Kramer test) from the first 5 min fraction after carbamathione administration.

Figure 2.10 Simultaneous monitoring of GABA and Glu in microdialysis samples from the nucleus accumbens of anesthetized rat.

White squares represent experiments with carbamathione administration (n = 5) and black squares represent control experiments (n = 3). Carbamathione (200 mg/kg) was administered i.v. (black arrow). Data shown as percent (mean ± SEM) of baseline preceding administration of drug or vehicle. * represents $P < 0.05$ versus control (ANOVA, Tukey-Kramer test).

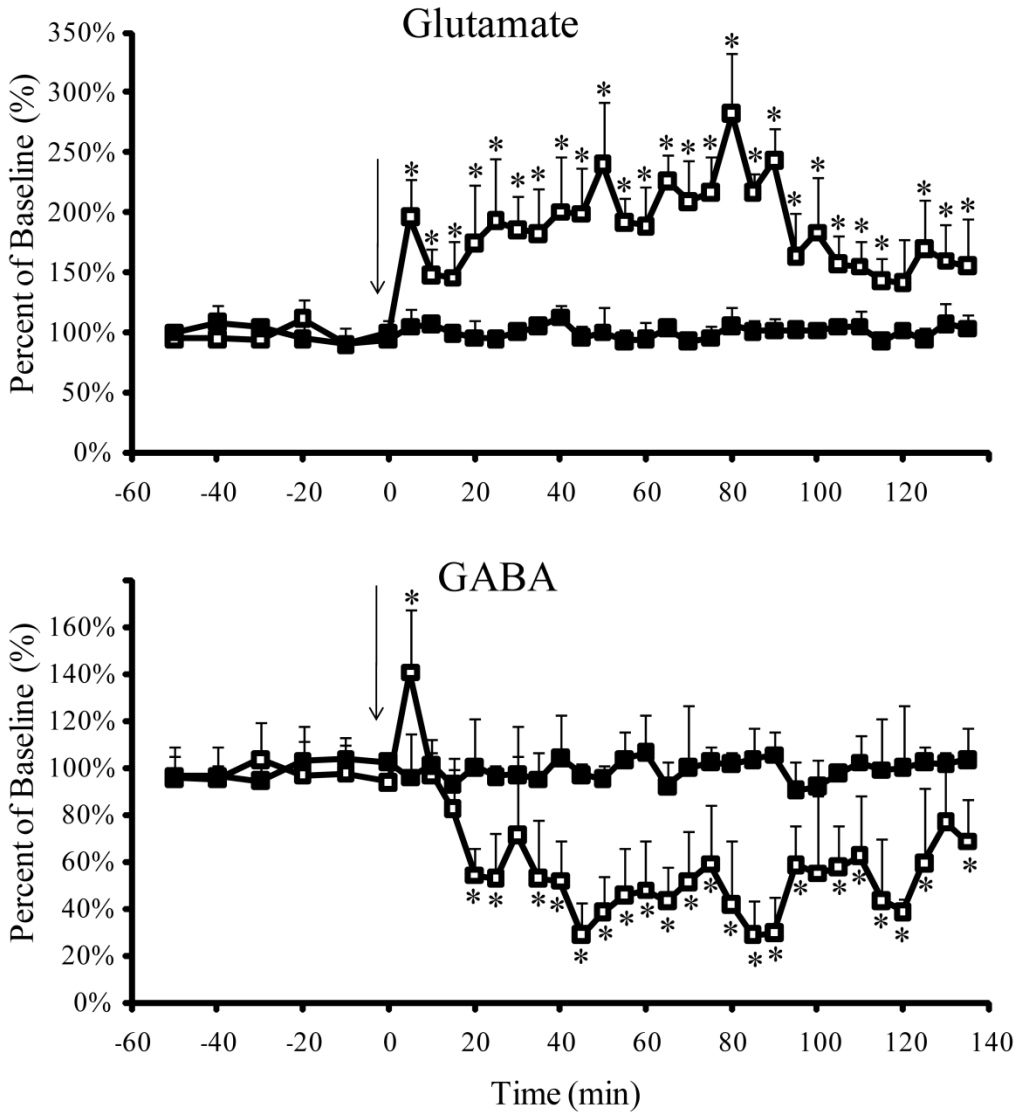

The increase in Glu concentration from basal levels continued over the next 2 h after carbamathione administration with a peak increase of 177% ($P < 0.05$ Tukey-Kramer test) at the sixteenth fraction (i.e. + 80 min). Basal GABA concentrations were significantly increased by 44% ($P < 0.05$ Tukey-Kramer test) from the first fraction following carbamathione administration, but during the next 15 min were reduced by 46% ($P < 0.05$ Tukey-Kramer test). GABA concentrations continued to remain reduced over the next 2 h following carbamathione administration. The lowest concentration of GABA was obtained in the eighteenth fraction (i.e. + 90 min) where basal GABA concentrations were significantly reduced by 76% ($P < 0.05$ Tukey-Kramer test).

Since carbamathione is also a primary amine and can be derivatized by NDA it was included in the CE-LIF analysis of brain samples. This allowed the clearance of carbamathione from the brain nucleus accumbens to be monitored. Figure 2.11 shows concentration in brain microdialysis samples versus time profile for carbamathione after the i.v. administration of carbamathione (200 mg/kg, $n = 5$). Carbamathione concentrations increased to a peak at 10 min after administration and then proceeded to fall exponentially. The PK parameters of carbamathione in the brain nucleus accumbens are given in table 2.12.

Figure 2.11 Carbamathione concentration versus time profile in anesthetized rats.

Concentration of carbamathione in rat brain nucleus accumbens following carbamathione administration (200 mg/kg i.v., n = 5). Microdialysis samples were collected every 5 min. Data shown as concentration (mean ± SEM).

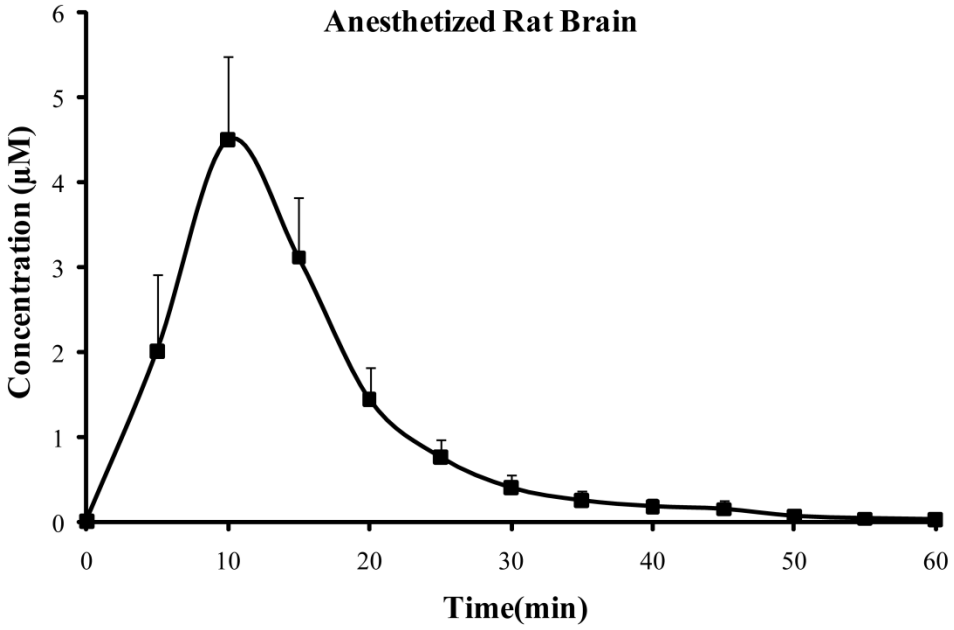

Table 2.12 Pharmacokinetic paramaters of carbamathione in anesthetized rats.

Pharmacokinetic parameters of carbamathione in rat brain nucleus accumbens following carbamathione administration (200 mg/kg i.v., n = 5). Data expressed as mean ± SEM.

Pharmacokinetic Parameters	Carbamathione
C_{max} (µmol/L)	4.5 ± 1.1
t_{max} (min)	7.5± 2.5
$t_{1/2}$ (min)	5.5 ± 0.7
K_{elim} (1/min)	0.13 ± 0.01
AUC (µmol/L min)	166 ± 40

C_{max} = maximum concentration

t_{max} = time to maximum concentration

$t_{1/2}$ = elimination half-life

K_{elim} = elimination constant

AUC = area under the dialysate concentration versus time profile

It is interesting to note that the half-life of carbamathione in the brain is only 5.5 ± 0.7 min and carbamathione was undetectable in microdialysis samples from the brain at 45 min after administration. However, the changes to basal concentrations of GABA and Glu upon carbamathione administration were observed to last for over 2 h (see figure 2.10). This finding suggests that carbamathione may be broken down rapidly to produce more long lived metabolites that cause some of the more sustained changes from basal levels observed in GABA and Glu. Alternatively, carbamathione does not directly impact GABA and Glu, but initiates a process that continues after carbamathione is no longer detectable.

2.3.4.2 Experiments on Awake Rats

Although initial experiments were performed on anesthetized rats, it was important to establish the relationship between carbamathione and the amino acid neurotransmitters in awake animal experiments. It is well established that the anesthetic ketamine has an effect on Glu neurotransmission.[21,29] Awake animal experiments allow the monitoring of brain neurotransmitters without the effects of the anesthesia. The same dose of carbamathione that was administered in the anesthetized animal experiments (200 mg/kg i.v.) was administered to the awake animals as a bolus dose and brain microdialysis samples were collected from the nucleus accumbens. The basal concentrations of GABA and Glu in microdialysis samples from the nucleus accumbens were 97.8 ± 16.4 nmol/L and 1.81 ± 0.19

μmol/L, respectively. The effect of carbamathione administration on basal levels of GABA and Glu in awake rats is shown in figure 2.13. Basal Glu concentrations were significantly increased by 84% ($P < 0.05$ Tukey-Kramer test) from the first fraction following carbamathione administration, but during the next 45 min were reduced by 44% ($P < 0.05$ Tukey-Kramer test). Glu concentrations continued to remain reduced over the next 70 min following carbamathione administration. The lowest concentration of Glu was obtained in the fourteenth fraction (i.e. + 70 min) whereas basal Glu concentrations were significantly reduced by 34% ($P < 0.05$ Tukey-Kramer test). Basal GABA concentrations were significantly increased by 23% ($P < 0.05$ Tukey-Kramer test) from the first fraction following carbamathione administration, but during the next 20 min were reduced by 53% ($P < 0.05$ Tukey-Kramer test). GABA concentrations continued to remain reduced over the next 110 min following carbamathione administration. The lowest concentration of GABA was obtained in the thirteenth fraction (i.e. + 65 min) where basal GABA concentrations were significantly reduced by 22% ($P < 0.05$ Tukey-Kramer test).

Figure 2.14 shows concentration in brain microdialysis samples versus time profile for carbamathione after the i.v. administration of carbamathione (200 mg/kg, $n = 5$). Carbamathione concentrations increased to a peak at 10 min after administration and then proceeded to fall exponentially.

Figure 2.13 Simultaneous monitoring of GABA and Glu in microdialysis samples from the nucleus accumbens of awake rat.

White squares represent experiments with carbamathione administration (n = 5) and black squares represent control experiments (n = 3). Carbamathione (200 mg/kg) was administered i.v. (black arrow). Data shown as percent (mean ± SEM) of baseline preceding administration of drug or vehicle. * represents $P < 0.05$ versus control (ANOVA, Tukey-Kramer test).

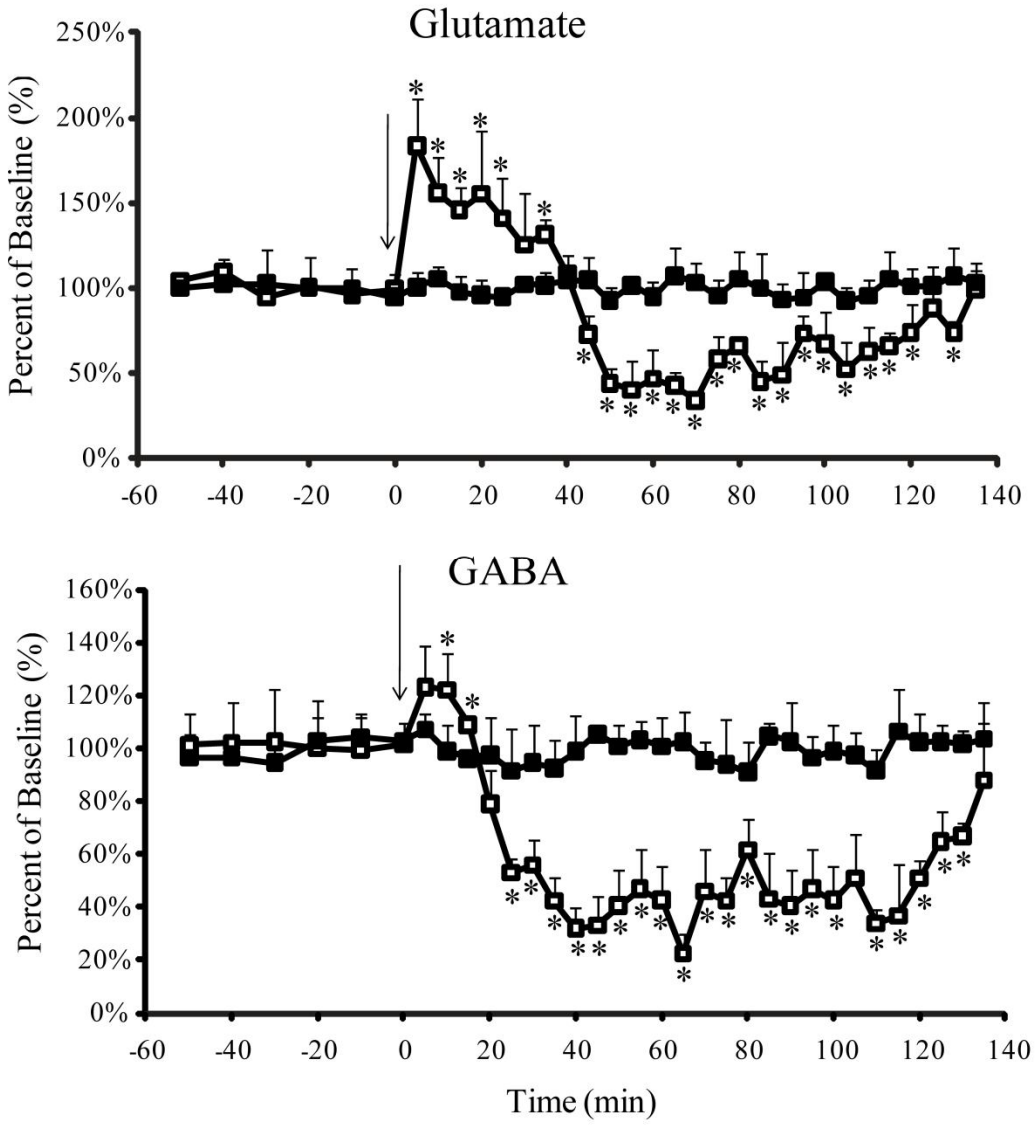

Figure 2.14 Carbamathione concentration versus time profile in awake rats.

Concentration of carbamathione in rat brain nucleus accumbens following carbamathione administration (200 mg/kg i.v., n = 5). Microdialysis samples were collected every 5 min. Data shown as concentration (mean ± SEM).

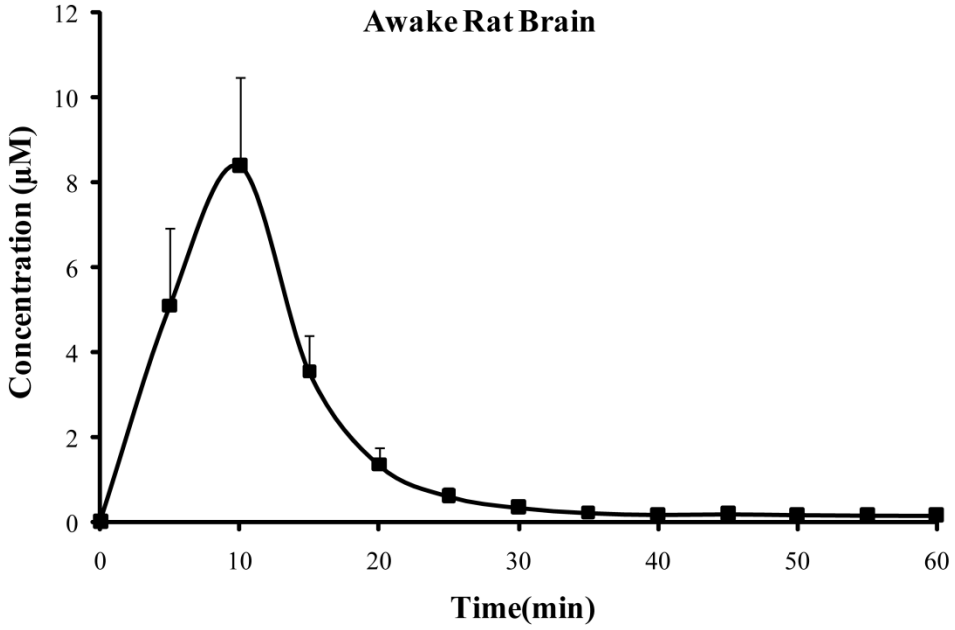

The PK parameters of carbamathione in brain nucleus accumbens are given in table 2.15. Again, it is important to note that the half-life of carbamathione in the brain nucleus accumbens is only 4.4 ± 0.6 min and carbamathione was undetectable in microdialysis samples from the brain nucleus accumbens at 35 min after administration.

The results obtained from administration of carbamathione in awake animals differ from those obtained from anesthetized animals. Some of these results are expected. For instance, the PK of carbamathione clearance is faster in awake animals than in anesthetized animals because the basal metabolic rate is higher in non-anesthetized animals. The clearance was determined from the elimination rate constant, K_{elim}, which was 0.13 ± 0.01 min^{-1} for anesthetized rats and 0.16 ± 0.02 min^{-1} for awake rats. Since carbamathione is eliminated at a faster rate for the awake rats, these rats also displayed a shorter elimination half-life, $t_{1/2}$ (4.4± 0.6 min) than those determined for the anesthetized rats (5.5 ± 0.7 min).

Table 2.15 Pharmacokinetic paramaters of carbamathione in awake rats.

Pharmacokinetic parameters of carbamathione in rat brain nucleus accumbens following carbamathione administration (200 mg/kg i.v., n = 5). Data expressed as mean ± SEM.

Pharmacokinetic Parameters	Carbamathione
C_{max} (µmol/L)	8.4 ± 2.1
t_{max} (min)	7.5 ± 2.5
$t_{1/2}$ (min)	4.4 ± 0.6
K_{elim} (1/min)	0.16 ± 0.02
AUC (µmol/L min)	242 ± 39

C_{max} = maximum concentration

t_{max} = time to maximum concentration

$t_{1/2}$ = elimination half-life

K_{elim} = elimination constant

AUC = area under the dialysate concentration versus time profile

2.4 Discussion

Administration of carbamathione was correlated to changes in GABA and Glu in anesthetized and awake rats. These changes differed slightly in the two cases. Basal GABA levels were significantly reduced after the administration of carbamathione in both awake and anesthetized rats. However, while Glu concentrations were significantly increased after the administration of carbamathione in anesthetized rats, basal Glu levels were only initially increased in awake rats. In awake rats, 20 min after the administration of carbamathione, concentrations of Glu were significantly reduced from basal levels. One explanation for this difference is the anesthesia (ketamine) used in the case of anesthetized rats.

Ketamine is a known non-competitive glutamate NMDA antagonist and previous studies have shown that when a drug-induced glutamate receptor response was being measured, there was significant interference of ketamine with the NMDA glutamate receptor-mediated component of the response in anesthetized rats.[29,30] Another study demonstrated that ketamine produced an increase of Glu transmission between the prefrontal cortex and nucleus accumbens associated with an increase in extracellular Glu levels in the nucleus accumbens of rats.[31] These studies suggest that the presence of ketamine would alter the response

observed in the form of an increase in Glu after the administration of carbamathione in anesthetized rats.

It is interesting to note that carbamathione is also a partial NMDA antagonist and the increase in Glu from basal levels observed in awake animals can be correlated with the clearance of carbamathione in the brain nucleus accumbens.[32] As previously discussed, the majority of carbamathione was eliminated from the brain at 40 min after drug administration. This suggests that the initial increase from basal Glu concentration after carbamathione administration in awake animals may be due to carbamathione and the subsequent decrease from basal Glu levels may be due to other metabolites of the drug or other processes that were triggered by carbamathione administration. The role of carbamathione as a partial NMDA antagonist is important since NMDA antagonists such as memantine have been shown to be effective in treating alcohol dependence.[33] NMDA antagonists have also been shown to block cocaine-induced behavior.[34,35]

2.5 Conclusions

The work in this chapter showed the application of a CE-LIF method for the simultaneous detection of GABA, Glu and carbamathione in rat brain dialysate. The analytical method was validated and it exhibited good linearity, accuracy and

reproducibility with nanomolar detection limits. The inclusion of carbamathione in the analysis provided the added advantage of obtaining PK and PD data. The administration of carbamathione was correlated with changes in the brain neurotransmitter systems in both awake and anesthetized rats. Although this system has been demonstrated specifically for the determination of GABA and Glu, it can potentially be applied to any primary amine analyte in brain dialysate. By changing separation conditions, other amino acids could potentially be added to the analysis. Future studies will focus on the addition of dopamine to the present analysis because dopamine has been shown to be one of the neurotransmitters involved in the pathways associated with addiction.[36,37] In addition, studies to determine the metabolites of carbamathione will also be carried out since the effect on the GABA, Glu and DA systems appears to continue even when carbamathione has been cleared from the brain.

2.6 References

1 Hart, B. W. & Faiman, M. D. In vitro and in vivo inhibition of rat liver aldehyde dehydrogenase by S-methyl N,N-diethylthiolcarbamate sulfoxide, a new metabolite of disulfiram. *Biochemical pharmacology* **43**, 403-406, (1992).

2 Madan, A. & Faiman, M. D. Characterization of diethyldithiocarbamate methyl ester sulfine as an intermediate in the bioactivation of disulfiram. *J Pharmacol Exp Ther* **272**, 775-780, (1995).

3 Madan, A., Parkinson, A. & Faiman, M. D. Identification of the Human and Rat P450 Enzymes Responsible for the Sulfoxidation of S-Methyl N,N-Diethylthiolcarbamate (Detc-Me) - the Terminal Step in the Bioactivation of Disulfiram. *Drug Metabolism and Disposition* **23**, 1153-1162, (1995).

4 Nagendra, S. N., Faiman, M. D., Davis, K., Wu, J. Y., Newby, X. & Schloss, J. V. Carbamoylation of brain glutamate receptors by a disulfiram metabolite. *The Journal of biological chemistry* **272**, 24247-24251, (1997).

5 Kaul, S., Williams, T. D., Lunte, C. E. & Faiman, M. D. LC-MS/MS determination of carbamathione in microdialysis samples from rat brain and plasma. *J Pharm Biomed Anal* **51**, 186-191, (2010).

6 Jin, L., Davis, M. R., Hu, P. & Baillie, T. A. Identification of novel glutathione conjugates of disulfiram and diethyldithiocarbamate in rat bile by liquid chromatography-tandem mass spectrometry. Evidence for metabolic activation of disulfiram in vivo. *Chemical research in toxicology* **7**, 526-533, (1994).

7 Lovinger, D. M. Excitotoxicity and Alcohol-Related Brain-Damage. *Alcoholism-Clinical and Experimental Research* **17**, 19-27, (1993).

8 Smothers, C. T., Mrotek, J. J. & Lovinger, D. M. Chronic ethanol exposure leads to a selective enhancement of N-methyl-D-aspartate receptor function in cultured hippocampal neurons. *Journal of Pharmacology and Experimental Therapeutics* **283**, 1214-1222, (1997).

9 Tsai, G. & Coyle, J. T. The role of glutamatergic neurotransmission in the pathophysiology of alcoholism. *Annu Rev Med* **49**, 173-184, (1998).

10 Wirkner, K., Poelchen, W., Koles, L., Muhlberg, K., Scheibler, P., Allgaier, C. & Illes, P. Ethanol-induced inhibition of NMDA receptor channels. *Neurochem Int* **35**, 153-162, (1999).

11 Hyytia, P. & Koob, G. F. GABAA receptor antagonism in the extended amygdala decreases ethanol self-administration in rats. *European journal of pharmacology* **283**, 151-159, (1995).

12 Benturquia, N., Parrot, S., Sauvinet, V., Renaud, B. & Denoroy, L. Simultaneous determination of vigabatrin and amino acid

neurotransmitters in brain microdialysates by capillary electrophoresis with laser-induced fluorescence detection. *J Chromatogr B Analyt Technol Biomed Life Sci* **806**, 237-244, (2004).

13 Parrot, S., Bert, L., Mouly-Badina, L., Sauvinet, V., Colussi-Mas, J., Lambas-Senas, L., Robert, F., Bouilloux, J. P., Suaud-Chagny, M. F., Denoroy, L. & Renaud, B. Microdialysis monitoring of catecholamines and excitatory amino acids in the rat and mouse brain: recent developments based on capillary electrophoresis with laser-induced fluorescence detection--a mini-review. *Cellular and molecular neurobiology* **23**, 793-804, (2003).

14 Zhou, S. Y., Zuo, H., Stobaugh, J. F., Lunte, C. E. & Lunte, S. M. Continuous in vivo monitoring of amino acid neurotransmitters by microdialysis sampling with on-line derivatization and capillary electrophoresis separation. *Analytical chemistry* **67**, 594-599, (1995).

15 Sauna, Z. E., Shukla, S. & Ambudkar, S. V. Disulfiram, an old drug with new potential therapeutic uses for human cancers and fungal infections. *Mol Biosyst* **1**, 127-134, (2005).

16 Denoroy, L., Parrot, S., Renaud, L., Renaud, B. & Zimmer, L. In-capillary derivatization and capillary electrophoresis separation of amino acid neurotransmitters from brain microdialysis samples. *J Chromatogr A* **1205**, 144-149, (2008).

17 O'Brien, K. B., Esguerra, M., Klug, C. T., Miller, R. F. & Bowser, M. T. A high-throughput on-line microdialysis-capillary assay for D-serine. *Electrophoresis* **24**, 1227-1235, (2003).

18 Siri, N., Lacroix, M., Garrigues, J. C., Poinsot, V. & Couderc, F. HPLC-fluorescence detection and MEKC-LIF detection for the study of amino acids and catecholamines labelled with naphthalene-2,3-dicarboxyaldehyde. *Electrophoresis* **27**, 4446-4455, (2006).

19 Dang, F. Q. & Chen, Y. Capillary electrophoresis of FITC labeled amino acids with laser-induced fluorescence detection. *Sci China Ser B* **42**, 663-669, (1999).

20 Huang, M., Li, Z., Dai, J., Shahid, M., Wong, E. H. & Meltzer, H. Y. Asenapine increases dopamine, norepinephrine, and acetylcholine efflux in the rat medial prefrontal cortex and hippocampus. *Neuropsychopharmacology* **33**, 2934-2945, (2008).

21 Moghaddam, B., Adams, B., Verma, A. & Daly, D. Activation of glutamatergic neurotransmission by ketamine: A novel step in the pathway from NMDA receptor blockade to dopaminergic and cognitive disruptions associated with the prefrontal cortex. *Journal of Neuroscience* **17**, 2921-2927, (1997).

22 Ueda, T., Mitchell, R., Kitamura, F., Metcalf, T., Kuwana, T. & Nakamoto, A. Separation of Naphthalene-2,3-Dicarboxaldehyde-Labeled

Amino-Acids by High-Performance Capillary Electrophoresis with Laser-Induced Fluorescence Detection. *Journal of Chromatography* **593**, 265-274, (1992).

23 Maganti, S. A. *A proposed new mechanism of action for disulfiram in alcohol and cocaine addiction* M.S. thesis, University of Kansas, (2006).

24 Schloss, J. V. Therapeutic Compositions. U.S.A. patent (2007).

25 Zhao, Y. P., Liang, X. Z. & Lunte, C. E. Comparison of Recovery and Delivery in-Vitro for Calibration of Microdialysis Probes. *Analytica Chimica Acta* **316**, 403-410, (1995).

26 Paxinos, G. & Watson, C. *The Rat Brain in Stereotaxic Coordinates*. (Academic Press, 1982).

27 Karnes, H. T., Shiu, G. & Shah, V. P. Validation of bioanalytical methods. *Pharm Res* **8**, 421-426, (1991).

28 O'Shea, T. J., Weber, P. L., Bammel, B. P., Lunte, C. E., Lunte, S. M. & Smyth, M. R. Monitoring excitatory amino acid release in vivo by microdialysis with capillary electrophoresis-electrochemistry. *J Chromatogr* **608**, 189-195, (1992).

29 Lorrain, D. S., Baccei, C. S., Bristow, L. J., Anderson, J. J. & Varney, M. A. Effects of ketamine and N-methyl-D-aspartate on glutamate and dopamine release in the rat prefrontal cortex: Modulation by a group II

selective metabotropic glutamate receptor agonist LY379268. *Neuroscience* **117**, 697-706, (2003).

30 Albrecht, J., Hilgier, W., Zielinska, M., Januszewski, S., Hesselink, M. & Quack, G. Extracellular concentrations of taurine, glutamate, and aspartate in the cerebral cortex of rats at the asymptomatic stage of thioacetamide-induced hepatic failure: modulation by ketamine anesthesia. *Neurochem Res* **25**, 1497-1502, (2000).

31 Razoux, F., Garcia, R. & Lena, I. Ketamine, at a dose that disrupts motor behavior and latent inhibition, enhances prefrontal cortex synaptic efficacy and glutamate release in the nucleus accumbens. *Neuropsychopharmacology* **32**, 719-727, (2007).

32 Ningaraj, N. S., Chen, W. Q., Schloss, J. V., Faiman, M. D. & Wu, J. Y. S-methyl-N,N-diethylthiocarbamate sulfoxide elicits neuroprotective effect against N-methyl-D-aspartate receptor-mediated neurotoxicity. *Journal of biomedical science* **8**, 104-113, (2001).

33 Gass, J. T. & Olive, M. F. Glutamatergic substrates of drug addiction and alcoholism. *Biochemical Pharmacology* **75**, 218-265, (2008).

34 Karila, L., Gorelick, D., Weinstein, A., Noble, F., Benyamina, A., Coscas, S., Blecha, L., Lowenstein, W., Martinot, J. L., Reynaud, M. & Lepine, J. P. New treatments for cocaine dependence: a focused review. *Int J Neuropsychoph* **11**, 425-438, (2008).

35 Uys, J. D. & LaLumiere, R. T. Glutamate: The New Frontier in Pharmacotherapy for Cocaine Addiction. *Cns Neurol Disord-Dr* **7**, 482-491, (2008).

36 Di Chiara, G., Bassareo, V., Fenu, S., De Luca, M. A., Spina, L., Cadoni, C., Acquas, E., Carboni, E., Valentini, V. & Lecca, D. Dopamine and drug addiction: the nucleus accumbens shell connection. *Neuropharmacology* **47**, 227-241, (2004).

37 Koob, G. F. & Le Moal, M. Addiction and the brain antireward system. *Annu Rev Psychol* **59**, 29-53, (2008).

3 *IN VIVO* MICRODIALYSIS AND MEKC-LIF FOR MONITORING GABA, GLUTAMATE, DOPAMINE, AND CARBAMATHIONE

3.1 Introduction

In the previous chapter describes the development of a capillary electrophoresis coupled with laser-induced fluorescence (CE-LIF) method to detect gamma-amino butyric acid (GABA), glutamate (Glu), and carbamathione in microdialysis samples from the brain nucleus accumbens. However, the method in the analysis did not include dopamine (DA), which has been shown to be a key neurotransmitter in alcohol and cocaine addiction. In addition, microdialysis samples were only collected from the brain. In order to determine the pharmacokinetics (PK) and pharmacodynamics (PD) of carbamathione, it was important to obtain microdialysis samples from the plasma, particularly after the intravenous (i.v.) administration of the drug. These samples would then have to be analyzed to detect and quantify carbamathione. The following chapter describes a micellar electrokinetic chromatography coupled with laser-induced fluorescence (MEKC-LIF) method that was developed to achieve these goals.

3.1.1 Background and Significance

One of the first steps in the development of carbamathione as a possible pharmacotherapeutic agent in either alcohol and/or cocaine addiction is

characterizing its effects on various neurotransmitters *in vivo*. Evidence in the literature suggests that the dopaminergic, glutamatergic, and GABAergic systems play an important role in addiction.[1] Therefore, it is of interest to study the effect of carbamathione on these neurotransmitters in a time-dependent and dose-dependent manner. Microdialysis provides an ideal tool for studying the PD of carbamathione in a specific brain region. The use of a fluorescence detection scheme provides the selectivity and sensitivity necessary in such studies. MEKC in combination with LIF provides a highly sensitive method for the measurement of GABA, Glu, and DA in microdialysis samples.[2-5]

3.1.2 Specific Aims of Research

The goal of this research was to apply an MEKC separation method to determine the changes in the GABA, Glu, and DA from the nucleus accumbens and prefrontal cortex of a rat brain as related to the administration of carbamathione. An existing MEKC-LIF separation method was modified and optimized in order to include carbamathione in the analysis of GABA, Glu, and DA in the microdialysis samples.[4] An liquid chromatography-tandem mass spectrometric (LC-MS/MS) method was used to determine the concentration of carbamathione in plasma microdialysis samples.[6] The MEKC-LIF method was not suitable for the analysis of plasma microdialysis samples because the derivatized plasma

dialysate displayed several endogenous peaks. Carbamathione could not be sufficiently resolved from these endogenous peaks. In addition, the LC-MS/MS method was specific for carbamathione, which was the only analyte of interest in the plasma. The determination of the concentration of carbamathione in plasma dialysate was necessary in monitoring carbamathione PK. The limits of detection and quantification for both the MEKC-LIF and LC-MS/MS methods satisfied the analytical requirements of this study based on the expected concentration ranges for the analytes of interest. The expected concentration range for GABA, Glu and dopamine in microdialysis samples from rat brain are 40-100 nmol/L, 0.7-2.5 μmol/L and 1-15 nmol/L, respectively.[4,5,7-9] Previous studies with carbamathione have demonstrated that micromolar concentrations of carbamathione were detected in rat brain dialysate after a 200 mg/kg dose of carbamathione.[10] The temporal resolution achieved for this method was initially 5 min and later reduced to 3 min to obtain additional PK and PD data. The neurotransmitter and carbamathione data was used to establish PK and PD relationships between the administration of various doses of the drug and changes observed in the neurotransmitter systems.

3.2 Experimental

3.2.1 Chemicals and Reagents

In addition to the chemicals listed in Chapter 2 (2.2.1 Chemicals and Reagents), several other chemicals were purchased for these studies. Dopamine (DA), 2-aminobutyric acid (2-ABA), *s*-hexylglutathione (SGSH), lithium tetraborate (LTB), and lithium dodecylsulfate (LDS) were purchased from Sigma (St. Louis, MO, USA). Ammonium formate and formic acid were purchased from Fisher Scientific (Pittsburgh, PA, USA). Ultrapure water was obtained with a Milli-Q system (Millipore, Bedford, MA, USA) and a WaterPro Plus water purification system (18 MΩ/cm) (Labconco, Kansas City, MO, USA). Carbamathione was synthesized using methods previously developed.[11,12]

Ringer's solution, which was used as perfusate for the vascular microdialysis probes, consisted of 145 mmol/L sodium chloride, 2.7 mmol/L potassium chloride, 1.0 mmol/L magnesium chloride, and 1.2 mmol/L calcium chloride. The Ringer's solution was filtered through a 0.2 μm pore size cellulose acetate membrane filter and stored at room temperature (25° C). Artificial cerebrospinal fluid (aCSF) was prepared as described in Chapter 2 (2.2.1 Chemicals and Reagents). SGSH was prepared as a 1 mmol/L stock solution in 1 mol/L of ammonium hydroxide.

Standard solutions of amino acids (1 mmol/L each) were dissolved in 0.1 mol/L perchloric acid and stored at 4° C. A stock solution of 1 mmol/L carbamathione (molecular weight [M.W.] 406 g/mol) was prepared in 10 mmol/L ammonium formate. Carbamathione calibration standards were prepared by serially diluting the carbamathione stock solution with aCSF or Ringer's.

The background electrolyte (BGE) consisted of 22.5 mmol/L LTB (pH 9.2) and 20 mmol/L LDS. The borate buffer for derivatization was prepared as described in Chapter 2 (2.2.1 Chemicals and Reagents). The derivatization reaction was carried out as described in Chapter 2 (2.2.2 Derivatization).

3.2.2 MEKC-LIF Instrumentation

The electrophoretic system consisted of an automatic P/ACE MDQ system (Beckman-Coulter, Fullerton, CA, USA) equipped with an external LIF detector (ZETALIF, Picometrics, Toulouse, France). The excitation was performed by a diode pumped solid-state laser (CrystaLaser, Reno, NV, USA) at a wavelength of 442 nm. A 50 µm id fused-silica capillary (Polymicro Technology, Phoenix, AZ, USA) was used (65 cm total length, 50 cm effective), with a separation voltage of 10 kV for 10 min and 20 kV for 8 min (a two-step separation). Each day, before the analyses were performed, the capillary was sequentially flushed at 20 psi with

methanol (MeOH) for 5 min, ultrapure water for 2 min, 1 mol/L hydrochloric acid for 5 min, ultrapure water for 2 min, 1 mol/L sodium hydroxide (NaOH) for 10 min, ultrapure water for 2 min and finally with the BGE for 5 min. Between analyses, the capillary was flushed at 20 psi with 1 mol/L NaOH for 3 min, with ultrapure water for 3 min and then with the BGE for 3 min. All the solutions injected onto the capillary were sterilized using a disposable 0.22 μm polyethersulfone (PES) membrane syringe filter (Millipore, Co. Cork, Ireland). Samples were introduced onto the capillary by hydrodynamic injections for 15 s at 0.7 psi. Electropherograms were acquired on Beckman 32 Karat software.

3.2.3 MEKC-LIF Method Development

The method used in this work was based on a previously reported method that was developed for the separation of several amino acids and catecholamines labeled with naphthalene-2,3-dicarboxyaldehyde (NDA) in microdialysis samples.[4] Under the conditions reported, it was possible to separate most of the analytes of interest. However, carbamathione and the internal standard (IS, 2-ABA) were not very well resolved. The effect of varying the capillary temperature was evaluated to achieve optimum resolution. Decreasing the temperature resulted in increased resolution and migration times (figure 3.1).

Figure 3.1 Effect of varying temperature on separation by MEKC-LIF.

Effect of temperature on separation of NDA-derivatized carbamathione (1), GABA (3), and Glu (4). IS (2) was 2-ABA. Electropherograms were obtained using 22.5 mmol/L LTB and 20 mmol/L LDS BGE and a two-step separation voltage (10 kV for 10 min and 20 kV for 8 min). NDA-derivatized compounds were detected using LIF detection (ex. 442 nm).

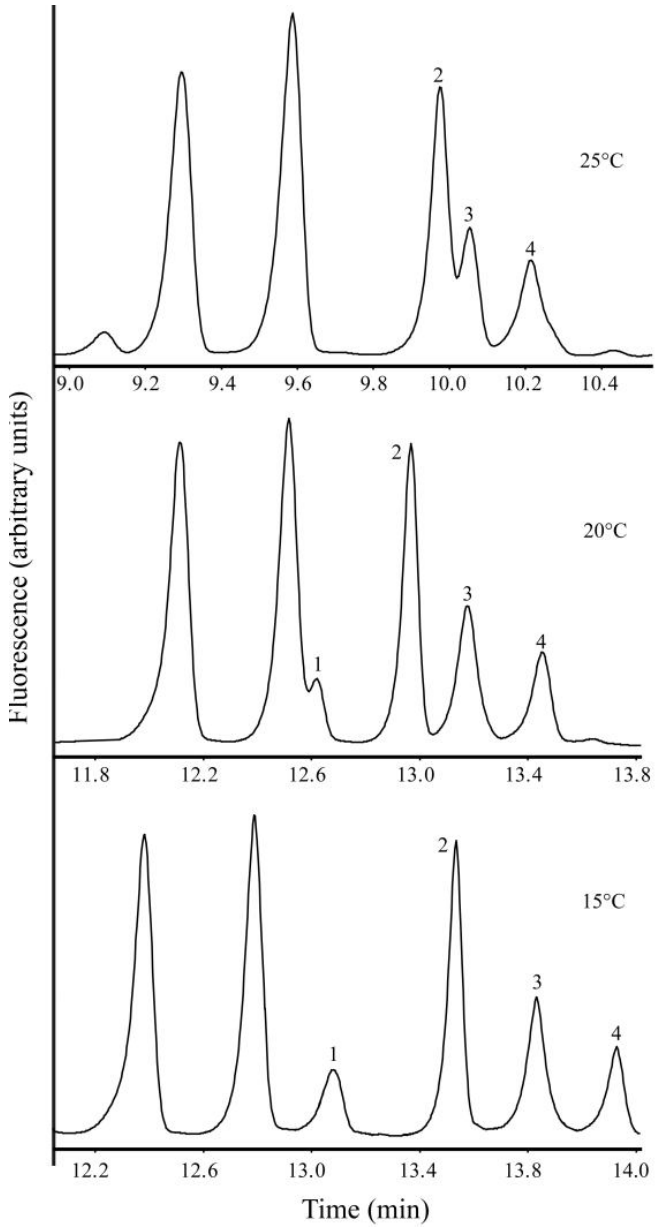

Temperatures between 15-25° C were tested and the best separation was obtained at 15° C. The resolution data at this temperature indicated good separation between standards ($R > 1.5$) for all pairs tested.

The generation of absorbance by NDA-labeled GABA, Glu, DA, and carbamathione as a function of time was tested to determine the optimum derivatization time. The results of this study are shown in figure 3.2. Samples were derivatized with NDA and were injected onto the CE system after 2.5 to 30 min. The plateaus are different for the different amino acids indicating the difference in absorbance of each of these molecules. The optimum derivatization time for GABA, Glu, DA and carbamathione was determined to be 5 min since maximum absorptions were reached at that time point (figure 3.2).

Peak identification in microdialysis samples were carried out by comparing migration times with those present in standards (figure 3.3). In addition, the observed height of the peaks of interest increased when exogenous Glu, GABA, and DA were added to the microdialysis samples. No additional peaks appeared when Glu, GABA and DA were added. Background peaks associated with NDA derivatization did not interfere with any of the analytes of interest.

Figure 3.2 Generation of absorbance at 442 nm as a function of time for GABA, Glu, DA, and carbamathione.

GABA, Glu, DA, and carbamathione (10 μmol/L) were derivatized with NDA and injected after 2.5 -30 min.

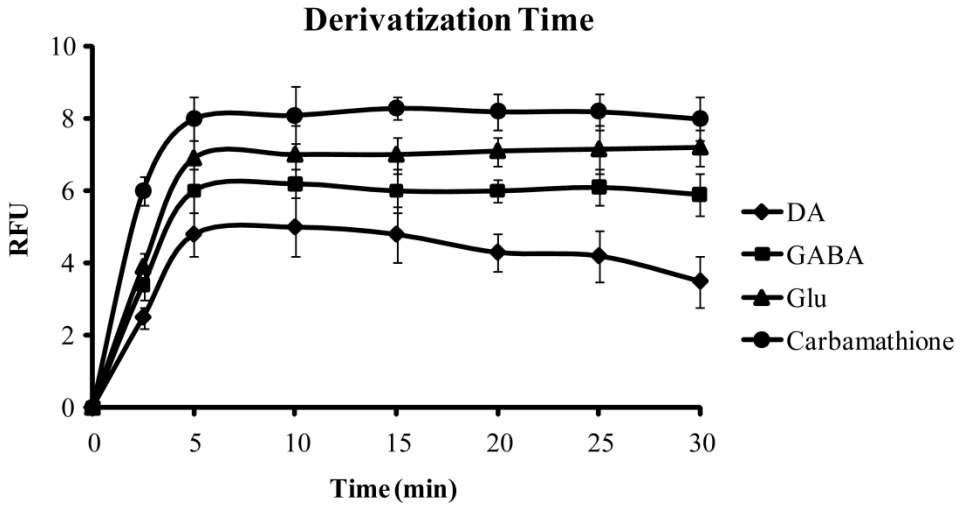

Figure 3.3 Typical MEKC-LIF electropherograms.

Electropherograms of standard solution (A) containing carbamathione (1), GABA (3), Glu (4), and DA (5) compared to dialysate obtained from rat brain (B). IS (2) was 2-ABA. Electropherograms were obtained using 22.5 mmol/L LTB and 20 mmol/L LDS BGE and a two-step separation voltage (10 kV for 10 min and 20 kV for 8 min). NDA-derivatized compounds were detected using LIF detection (ex. 442 nm).

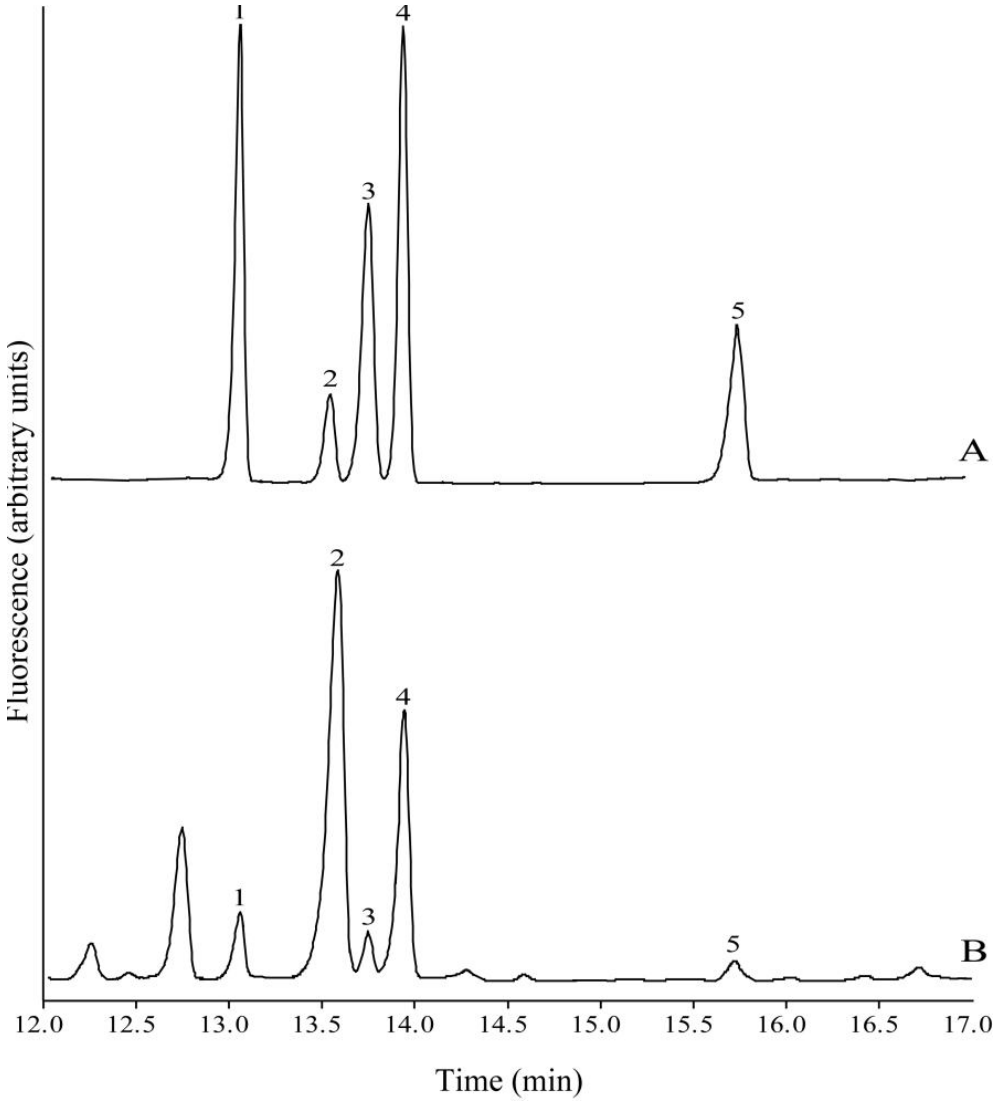

3.2.4 MEKC-LIF Method Validation Experiments

Calibration standards for method validation contained GABA prepared in a concentration range of 10^{-9}- 10^{-6} mol/L, Glu in a range of 10^{-9}- 10^{-6} mol/L, DA in a range of 10^{-10}- 10^{-7} mol/L, and carbamathione prepared in a range 10^{-8}- 10^{-5} mol/L. Calibration plots were plotted as the ratio of the area of compound of interest to area of the internal standard versus concentration (number of concentrations of each analyte, n = 5). The limits of detection and quantification were calculated as the analyte concentration that resulted in peaks with signal-to-noise ratio (S/N) of 3 and 10 respectively. Intra-day and inter-day reproducibility were determined using standards of Glu, GABA, DA, and carbamathione prepared in aCSF and microdialysis samples. The accuracy of the method was calculated from the analysis of standards in aCSF, microdialysis samples, and microdialysis samples spiked with known concentrations of standards (in triplicate).

3.2.5 LC-MS/MS Instrumentation

The chromatographic separations were performed on an Alltech Altima C-18 (50 mm x 2.1 mm i.d., 3 m particles) analytical column (Alltech Associates, Inc, Deerfield, Illinois, USA) at a flow rate of 0.3 mL/min with analysis time of 35 min. Solvent A consisted of 10 mmol/L ammonium formate, MeOH and formic

acid (99:1:0.06, v/v/v). Solvent B consisted of MeOH, 10 mmol/L ammonium formate and formic acid (99:1:0.06, v/v/v). The chromatograph consisted of a 20 min linear gradient from 95% aqueous to 95% organic followed by a 15 min re-equilibration. Five microliters of IS (5 nmol/L) was added to 5 L of the calibration standard sample and vortexed. This mixture was then diluted with 40 L of water and injected onto the LC column directly. Tandem mass spectra were acquired on a Quattro Ultima "triple" quadrupole instrument (Micromass Ltd. Manchester UK.). The electrospray source block was 80° C and probe desolvation temperature was 200° C. Argon collision gas was set to attenuate the beam by 15% ($2e^{-3}$ mbar on a gauge near the collision cell). The cone voltage was 35 V. Quadrupoles 1 and 3 were tuned to a resolution of 0.9 atomic mass units full width at half height. Mass spectrometric analysis was conducted in positive ion mode and set-up in selected reaction monitoring (SRM) mode. Data processing was performed on MassLynx version 4.1 software.

3.2.6 LC-MS/MS Method Development

SGSH was selected as the IS since it was a non-endogenous glutathione adduct. SRM acquisitions were used for sensitivity and extended dynamic range. The SRM of three transitions were recorded: m/z = 100 and m/z = 175 as products of m/z = 407.4 at 25 eV CE ($[M + H]^+$ carbamathione) and m/z = 263 as the product

of m/z = 392.4 at 10 eV CE ($[M + H]^+$ SGSH) (figure 3.4). Quantification of carbamathione was based on the sum of the integrations of the SRM traces from the two product ions.

The post-column infusion method was used to provide a qualitative assessment of matrix effects and to identify chromatographic regions most likely to experience matrix effects. Briefly, an infusion pump was used to deliver a constant amount of carbamathione into the LC stream entering the ion source of the mass spectrometer. The mass spectrometer was run in SRM mode to follow the infused analyte. Blank dialysate was then injected on the LC column. Any endogenous compound that eluted from the column would cause a variation in electrospray ionization response of carbamathione. Matrix effects were also assessed by comparison of standards in Ringer's and in water at three concentrations (5.0×10^{-9}, 1.0×10^{-7} and 5.0×10^{-6} mol/L). The post-column infusion of 1 μmol/L carbamathione challenged by the injection of blank dialysate demonstrated no significant matrix interference. The comparison of standards prepared in Ringer's and in water supported this assessment since there was no significant difference in the SRM peak areas.

Figure 3.4 Tandem mass spectrum of carbamathione after activation of $[M+H]^+$ at 25 eV CE.

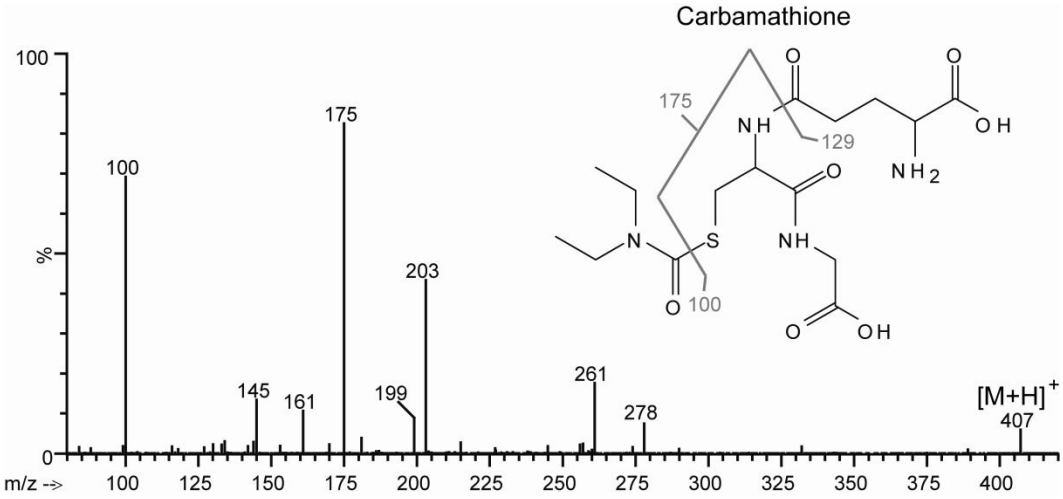

The selectivity of the method was tested by analyzing drug-free plasma dialysate. Each dialysate sample was tested using the LC-MS/MS conditions described to ensure no interference with carbamathione and the IS. No other endogenous peaks were observed (figure 3.5).

3.2.7 LC-MS/MS Method Validation Experiments

The intra-day accuracy and precision were calculated by analyzing five replicates of Ringer's solution containing carbamathione at three concentrations: 5.0×10^{-9}, 1.0×10^{-7} and 5.0×10^{-6} nmol/L. The inter-day accuracy and precision were determined by analyzing the three concentrations on five different runs.

3.2.8 Microdialysis

3.2.8.1 Brain and Vascular Probes

Microdialysis samples were obtained from the brain utilizing microdialysis probes (CMA 12 Elite) with 2 mm membranes purchased from CMA Microdialysis (North Chelmsford, MA, USA). The vascular probes were fabricated in-house.[13]

Figure 3.5 Typical LC-MS/MS chromatograms.

Chromatograms of plasma microdialysis samples showing the separation and detection of carbamathione and IS (SGSH). Chromatograms were acquired in SRM mode.

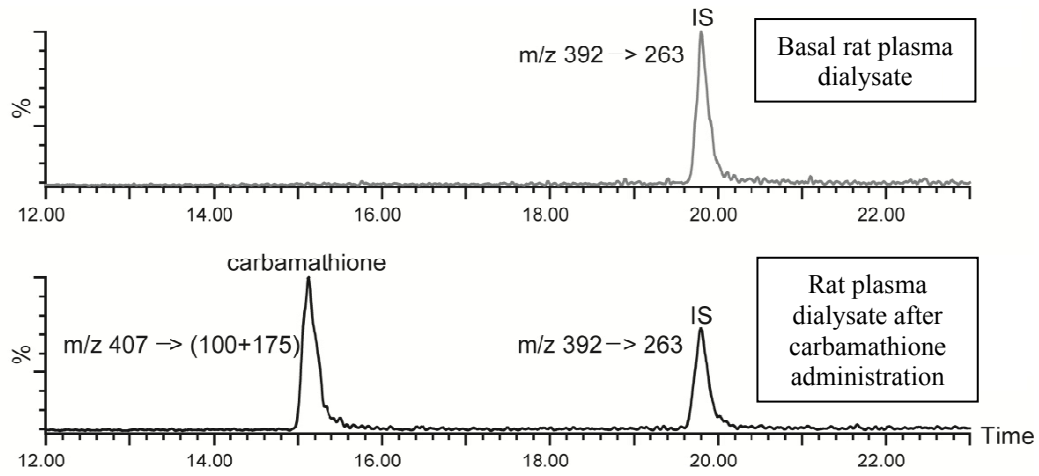

Fused silica tubing, 75 m i.d. and 150 m o.d. (Polymicro Technologies Inc., Phoenix, AZ, USA) was inserted into a 10 mm MicroRenathane surgical tubing (MRE-033), 356 m i.d. and 838 m o.d. (Braintree Scientific, Braintree, MA, USA), so that a 10 mm length is exposed. The exposed silica was then fed into a piece of regenerated cellulose dialysis fiber (AN69® HF membrane) with a 240 m i.d., 50- m wall thickness and 5 kDa molecular weight cutoff (Hospal Industrie, Meyzieu, France). This membrane was also fed into the MRE-033 and threaded one-third of the way up. The end of the membrane was cut and sealed with ultraviolet (UV) glue (UVEXS, Sunnyville, CA). The UV glue was activated under a UV light system ELC-450 (Electro-Lite Corporation, Danbury, CT, USA), with 5.0 W/cm^2 and at 365 nm for five seconds. The membrane was secured to the MRE-033 with UV glue. A small piece of plastic mesh was secured with UV glue just above the MRE-033 for the purpose of securing the probe once implanted. The probe was completed by feeding a necessary length of polyethylene tubing (PE-50), 580 m i.d. and 965 m o.d. (Fisher Scientific, Pittsburgh, PA), over the two free silica pieces and UV glued into place. The relative recovery of carbamathione through the microdialysis probes were estimated by delivery experiments.[14] Delivery experiments were carried out by perfusing 1 μmol/L of carbamathione through the microdialysis probes *in vivo* at 2 μL/min, and determining the percentage that diffused through the membrane.

3.2.8.2 Animals and Surgery

All awake experiments were carried out in accordance with the Institutional Animal Care and Use Committee (IACUC) animal protocols as described in Chapter 2 (2.2.6.2 Animals and Surgery). Sterile surgeries were conducted since all the experiments in this study involved awake animals. The microdialysis probes and surgical instruments were sterilized by ethylene oxide. The initial anesthesia and preparation of the incision sites are described in detail in Chapter 2 (2.2.6.2 Animals and Surgery).

The femoral vein of the rat was cannulated for i.v. dosing as described in Chapter 2 (2.2.6.2 Animals and Surgery). The femoral cannula was externalized through a sterile incision in the neck. All incisions were closed with stitches or surgical staples.

The jugular vein of the rat was isolated by making an incision over the right shoulder of the rat and carefully pulling the fat and tissue out of the way. Once isolated, a small nick was made in the vein with spring scissors held almost perpendicular to the vein. The vascular probe was then inserted into the vein to the vena cava. The jugular was tied above and below the probe to hold the probe in place. The probe tubing was tunneled under the skin and externalized through a

sterile incision in the neck. The jugular incision was closed with surgical staples or sutures.

The brain probes were implanted as previously described.[6] The coordinates of the insertion sites relative to the bregma line were +1.5 mm anterior, +0.9 mm lateral and −6.2 mm ventral for the nucleus accumbens shell and +3.7 mm anterior, +0.7 mm lateral and −1.0 mm ventral for the prefrontal cortex, according to the rat stereotaxic atlas.[15] Holes 1 mm in diameter were drilled through the skull at the insertion sites and intracerebral guide cannulas were lowered into the specified regions using a micromanipulator attached to the stereotaxic apparatus. The guide cannulas were positioned 2 mm above the specified regions and then affixed to the skull with dental cement. The dummy probe in the guide cannula was replaced with the CMA microdialysis probes.

After the surgical procedures, the rats were administered 0.5 to 3 mL/kg of saline subcutaneously (s.c.) to prevent dehydration. During recovery from anesthesia, the rats were placed in a rat turn equipped with a swivel arm (Bioanalytical Systems Inc., West Lafayette, IN, USA). A heating pad was placed under the rats to provide warmth during the recovery from anesthesia.

3.2.8.3 Microdialysis Sample Collection

Microdialysis samples were collected using a CMA 100 microinfusion pump and a HoneyComb fraction collector (Bioanalytical Systems Inc., West Lafayette, IN, USA). Connection of the microinjection pump and the fraction collector to the microdialysis probes was accomplished with tubing connectors (Bioanalytical Systems Inc., West Lafayette, IN, USA). After implantation, the brain probes and the vascular probes were perfused with aCSF and Ringer's solution, respectively, at 2 µL/min. The dead volume between the dialysis site and the fraction collector was also determined in order to accurately monitor the neurochemical changes. The CMA 12 Elite 2 mm brain probes had a reported outlet internal volume of 3 µL. The fluorinated ethylene propylene (FEP) tubing used to connect the syringe to the probes and the probes to the fraction collector had an internal volume of 0.12 µL/cm length. The delay was estimated to be 405 s and upon the administration of carbamathione, microdialysis samples were collected after this period of time.

3.2.8.4 In Vivo Experiments

3.2.8.4.1 Administration of 200 mg/kg Carbamathione

The collection of 5 min samples was initiated after a 24 h waiting period for awake experiments. For dosing purposes, the carbamathione dose (200 mg/kg)

was prepared by adding a few drops of 1 mol/L sodium bicarbonate solution and bringing the volume up to 1 mL with saline solution. After the i.v. administration of carbamathione through the femoral cannula, microdialysis samples were collected for 3 h. At the end of the experiments, the rats were sacrificed by placement in an isofluorane chamber for approximately 30 min. Rat brains were harvested in order to perform a histological confirmation of brain probe position.

3.2.8.4.2 Increased Temporal Resolution for Carbamathione Dose-Response

The collection of 3 min samples was initiated after a 24 h waiting period for awake experiments. After the i.v. administration of carbamathione (200 mg/kg, 50 mg/kg, and 20 mg/kg) through the femoral cannula, microdialysis samples were collected for three hours. At the end of the experiments, the rats were sacrificed by placement in an isofluorane chamber for approximately thirty minutes. Rat brains were harvested in order to perform a histological confirmation of brain probe position.

3.3 Results and Discussion

3.3.1 MEKC-LIF Method Validation Results

Validation was carried out in accordance with instructions for good laboratory practice.[16,17] Validation parameters were determined for GABA, Glu, and carbamathione in standards as well as brain microdialysis samples. The final results are shown in table 3.6. The regression coefficient of the calibration obtained with standard solutions and microdialysis samples showed good linearity and led to the routine use of only three points of the calibration curve. Limits of detection and quantification were lower than concentrations measured in microdialysis samples from the brain.

3.3.2 LC-MS/MS Method Validation Results

The carbamathione calibration curve was constructed by plotting the peak area ratio of carbamathione to the IS versus the concentration of carbamathione. The calibration curve was characterized by two different linear segments. The regression coefficient of the calibration showed good linearity (r^2 = 0.9987 over the range of 0.25-100 nmol/L and r^2 = 0.9993 over the range of 0.5-250 μmol/L). Figure 3.7 displays representative calibration curves for the low and high concentration ranges.

Table 3.6 Quantitative parameters for the analysis GABA, Glu, DA, and carbamathione in aCSF and microdialysis samples by MEKC-LIF.

aCSF	GABA	Glu	DA	Carb
Calibration Range (mol/L)	10^{-9}-10^{-6}	10^{-9}-10^{-6}	10^{-10}-10^{-7}	10^{-8}-10^{-5}
Regression Coefficient of Calibration (r^2)	0.9985	0.9990	0.9942	0.9991
Intra-assay repeatability (%RSD)[a]	8.3	7.1	8.9	6.5
Intra-day repeatability (%RSD)[a]	5.7	6.0	4.7	3.7
Inter-day repeatability (%RSD)[b]	7.2	3.5	4.2	4.9
Accuracy (%)[c]	3.2-1.8	2.9-1.4	3.3-2.0	3.6-1.8
Limits of Detection (mol/L)	1.5×10^{-9}	6.0×10^{-10}	5.0×10^{-10}	1.0×10^{-9}
Limits of Quantification (mol/L)	6.0×10^{-9}	3.0×10^{-9}	2.5×10^{-9}	5.0×10^{-9}

Microdialysis Samples	GABA	Glu	DA	Carb
Calibration Range (mol/L)[d]	10^{-9}-10^{-6}	10^{-9}-10^{-6}	10^{-10}-10^{-7}	10^{-8}-10^{-5}
Regression Coefficient of Calibration (r^2)	0.9967	0.9974	0.9905	0.9980
Intra-assay repeatability (%RSD)[a]	10.4	8.5	11.2	7.3
Intra-day repeatability (%RSD)[a]	8.2	7.5	8.3	6.1
Inter-day repeatability (%RSD)[b]	9.4	5.9	10.1	6.0
Accuracy (%)[c,d]	9.3-6.5	4.8-2.4	10.9-7.6	4.0-2.1

a. Five replicates

b. Five days, three replicates each

c. Three replicates, tested concentrations of 10^{-7}- 10^{-8} mol/L for GABA, Glu, DA and carbamathione

d. Spiked microdialysis samples

Figure 3.7 **Representative calibration curves for LC-MS/MS method.**

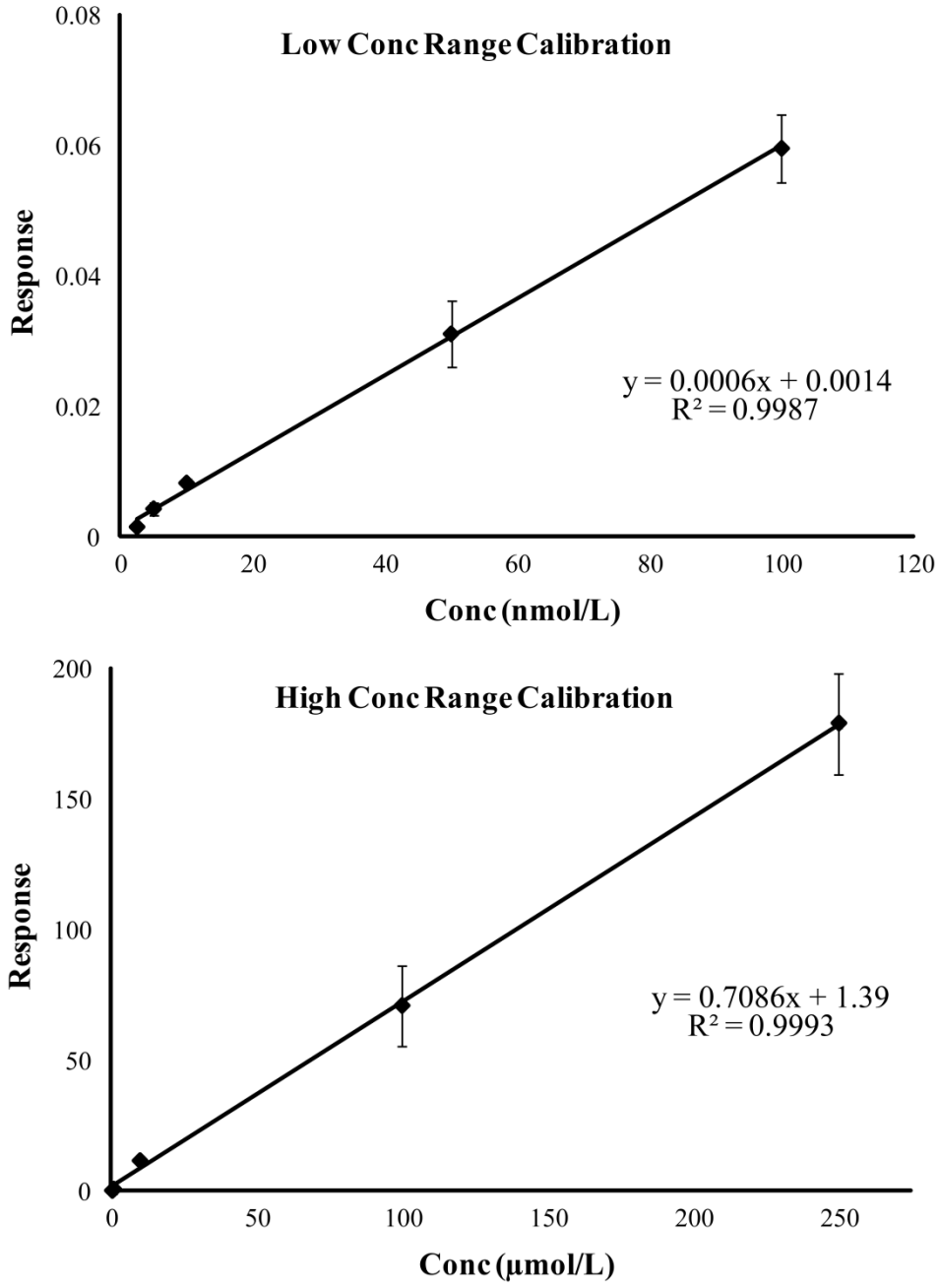

Since the LC-MS/MS method was used to detect carbamathione in plasma dialysate samples and these samples contained micromolar concentrations of carbamathione, the high concentration range calibration curve was used. The lowest limit of detection was estimated as the amount of carbamathione that resulted in a signal three times the noise (S/N $\geq$ 3) and was calculated to be 0.25 nmol/L. The lowest limit of quantification with acceptable accuracy and precision (<10%) was 1 nmol/L.

Intra-day accuracy and precision were determined by analyzing five replicates at three different concentration levels. Inter-day accuracy and precision were determined by analyzing samples at the three concentration levels, five times at each concentration. The final results are shown in table 3.8.

3.3.3 Microdialysis Probe Calibration

The characteristics of the implanted microdialysis probes were evaluated at the end of each experiment. Based on the delivery experiments, the *in vivo* extraction efficiency by delivery (EE_d) (mean ± standard error of mean [SEM], n = 3) for carbamathione was determined to be 25.8 ± 4.1% for the brain probes and 57.5 ± 10.4% for the plasma vascular probes.

Table 3.8 Quantitative parameters for the analysis of carbamathione in Ringer's solution by LC-MS/MS

Samples were analyzed at the three concentration levels, five times at each concentration.

Concentration (mol/L)		RSD (%)	
Nominal	Mean Measured	Intra-day	Inter-day
5.0×10^{-9}	4.78×10^{-9}	4.7	7.2
1.0×10^{-7}	1.04×10^{-7}	2.2	4.3
5.0×10^{-6}	4.92×10^{-6}	3.1	3.8

The concentrations of carbamathione determined in the microdialysis samples were corrected for the EE_d of the probe used. The *in vitro* extraction efficiency by recovery (EE_r) (mean ± SEM, $n = 3$) for GABA, Glu and DA was estimated to be 17.2 ± 1.8%, 13.5 ± 1.4% and 14.1 ± 1.9% respectively. The concentrations of GABA, Glu and DA were expressed as percent (mean ± SEM) of baseline concentrations in order to monitor changes from basal levels upon administration of carbamathione.

3.3.4 Histological Confirmation of Brain Probe Position

Microdialysis probe locations were examined histologically after completion of the experiments. After the rats were euthanized by isofluorane inhalation, the brains were removed and fixed in buffered formalin (10%). After localization of the microdialysis probes, the brain was sliced transversely in the coronal plane. Samples were taken from the prefrontal cortex and the nucleus accumbens. The tissues were embedded in paraffin wax and the sections cut at 5 μm and stained with hematoxylin-eosin. The sections were then examined by standard light microscopy. Only probes with at least 85% of the active dialysis membrane in the nucleus accumbens shell or prefrontal cortex were included in the study. The representative locations of microdialysis probes in the nucleus accumbens and prefrontal cortex are shown in figure 3.9.

Figure 3.9 Representative locations of microdialysis probes in nucleus accumbens shell and prefrontal cortex.

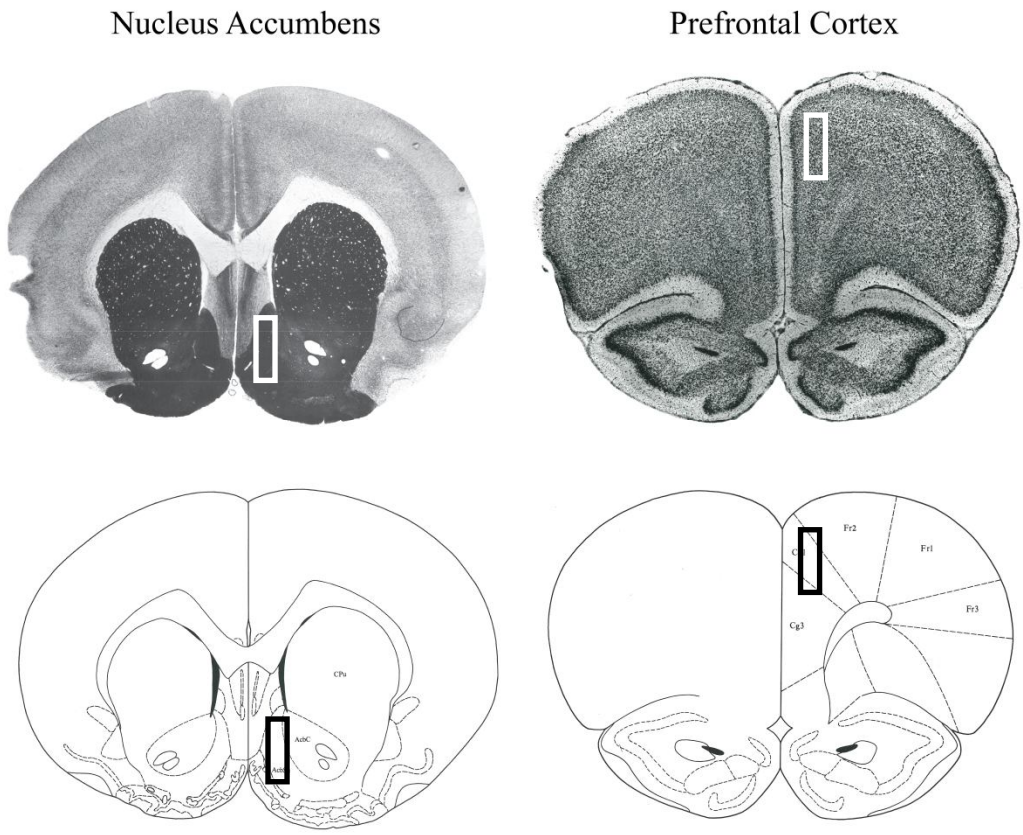

3.3.5 *In Vivo* Studies

3.3.5.1 Administration of 200 mg/kg Carbamathione and 5 min Sampling Interval

Changes in concentration of Glu, GABA, and DA were expressed as percent of the basal concentration, measured before drug or vehicle administration. An MEKC-LIF method was developed to measure the carbamathione-induced changes in GABA, Glu and DA and in the rat brain. For this purpose a 200 mg/kg dose of carbamathione was administered as an i.v. bolus dose and brain and plasma microdialysis samples were collected every 5 min. Comparison between treated and control rats were achieved on percentage transformed data using analysis of variance (ANOVA) and post-hoc comparison by Tukey-Kramer test. The level of significance was set at $P < 0.05$ for all comparisons. Data are reported as percentages of baseline and mean ± SEM.

The effect of carbamathione administration (200 mg/kg) on basal levels of GABA, Glu, and DA in the nucleus accumbens of rats is shown in figure 3.10. The basal concentrations of GABA, Glu, and DA in microdialysis samples from the nucleus accumbens were 63.5 ± 11.7 nmol/L, 2.9 ± 0.5 µmol/L, and 7.4 ± 1.8 nmol/L, respectively.

Figure 3.10 GABA, Glu, and DA in nucleus accumbens after a 200 mg/kg dose of carbamathione and 5 min sampling interval.

White squares represent experiments (n = 3) and black squares represent controls (n = 3). 0 min indicates time point of carbamathione administration (200mg/kg i.v.). * represents $P < 0.05$ versus control (ANOVA, Tukey-Kramer test).

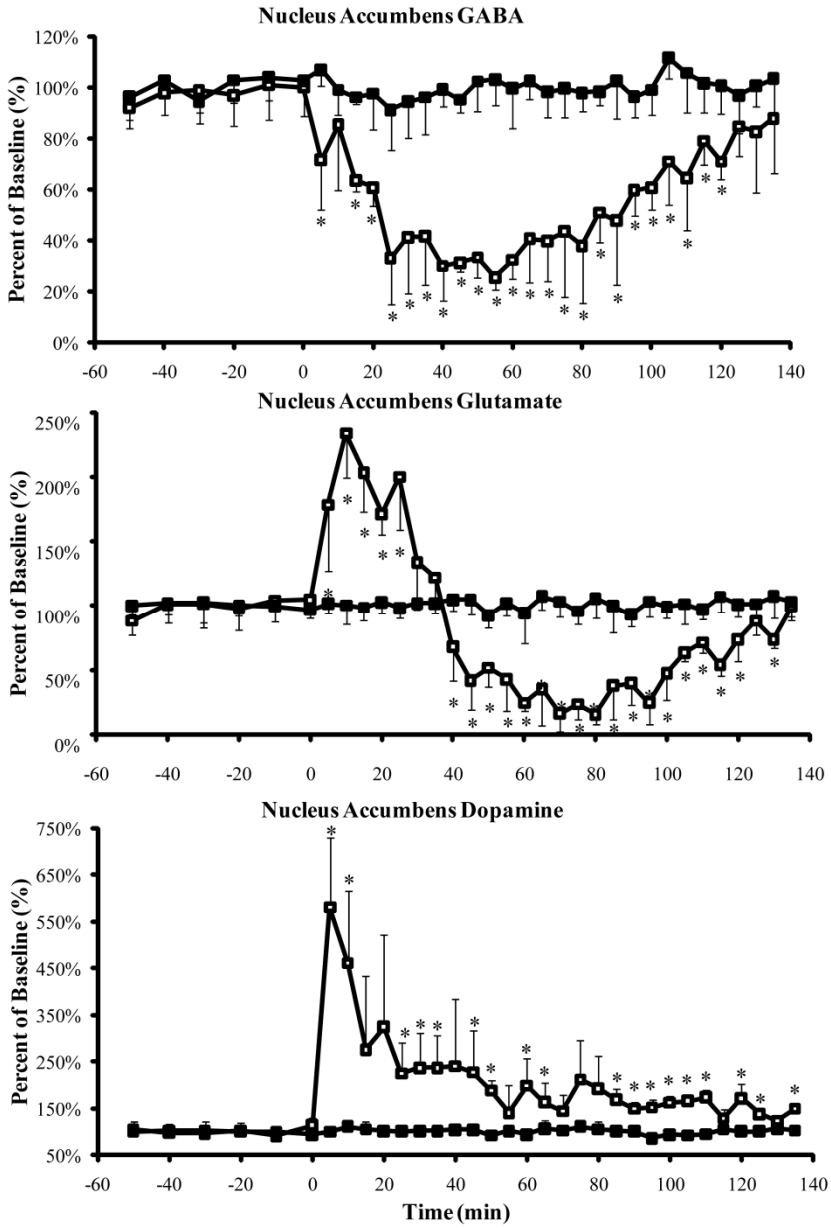

Basal GABA concentrations were significantly decreased by 28% ($P < 0.05$ Tukey-Kramer test) in the first fraction following carbamathione administration and continued to remain reduced over the next 2 h following carbamathione administration. The lowest concentration of GABA was obtained in the eleventh fraction (i.e. + 55 min) where basal GABA concentrations were significantly reduced by 74% ($P < 0.05$ Tukey-Kramer test).

Basal Glu concentrations were significantly increased by 78% ($P < 0.05$ Tukey-Kramer test) in the first 5 min fraction after carbamathione administration. The increase in Glu concentration from basal levels continued over the next 30 min after carbamathione administration with a peak increase of 133% ($P < 0.05$ Tukey-Kramer test) at the third fraction (i.e. + 15 min). However, during the next 10 min Glu concentration was reduced by 32% ($P < 0.05$ Tukey-Kramer test) and continued to remain reduced over the next 95 min. The lowest concentration of Glu was obtained in the sixteenth fraction (i.e. + 80 min) where basal Glu concentrations were significantly reduced by 84% ($P < 0.05$ Tukey-Kramer test).

Basal DA concentrations were significantly increased by 480% ($P < 0.05$ Tukey-Kramer test) in the first fraction following carbamathione administration, and continued to remain increased over the next 2 h.

The effect carbamathione administration (200 mg/kg) on basal levels of GABA, Glu, and DA in the prefrontal cortex of rats is shown in figure 3.11. The basal concentrations of GABA, Glu, and DA in microdialysis samples from the prefrontal cortex were 49.8 ± 8.4 nmol/L, 2.4 ± 0.3 μmol/L, and 3.8 ± 0.5 nmol/L, respectively.

Basal GABA concentrations were significantly decreased by 5% ($P < 0.05$ Tukey-Kramer test) in the first fraction following carbamathione administration. The GABA levels continued to remain reduced over the next 2 h following carbamathione administration. The lowest concentration of GABA was obtained in the ninth fraction (i.e. + 45 min) where basal GABA concentrations were significantly reduced by 62% ($P < 0.05$ Tukey-Kramer test).

Basal Glu concentrations were significantly increased by 113% ($P < 0.05$ Tukey-Kramer test) in the first 5 min fraction after carbamathione administration. The increase in Glu concentration from basal levels continued over the next 10 min after carbamathione administration. However, during the next 5 min Glu concentration was reduced by 23% ($P < 0.05$ Tukey-Kramer test) and continued to remain reduced over the next 80 min. The lowest concentration of Glu was obtained in the tenth fraction (i.e. + 50 min) where basal Glu concentrations were significantly reduced by 60% ($P < 0.05$ Tukey-Kramer test).

Figure 3.11 GABA, Glu, and DA in prefrontal cortex after a 200 mg/kg dose of carbamathione and 5 min sampling interval.

White squares represent experiments (n = 3) and black squares represent controls (n = 3). 0 min indicates time point of carbamathione administration (200mg/kg i.v.). * represents $P < 0.05$ versus control (ANOVA, Tukey-Kramer test).

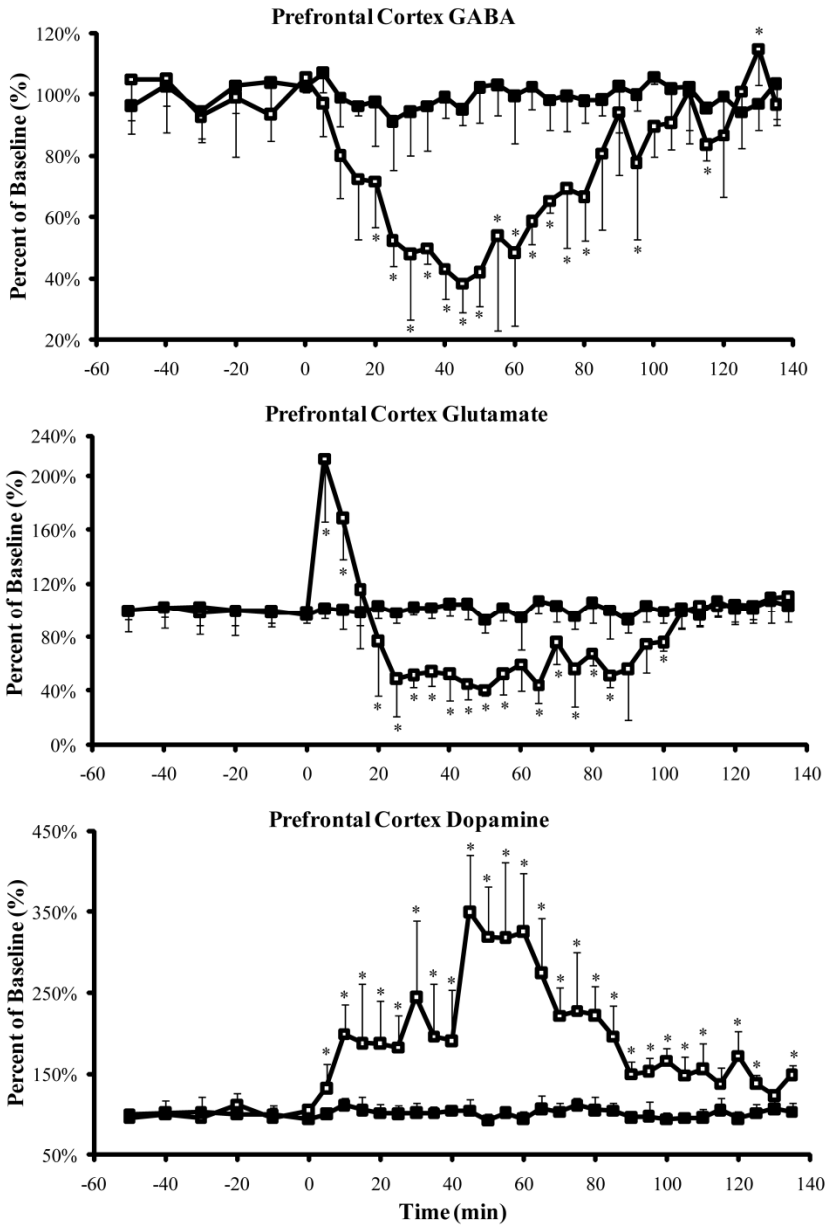

Basal DA concentrations were significantly increased by 32% ($P < 0.05$ Tukey-Kramer test) in the first fraction following carbamathione administration, and continued to remain increased over the next 2 h. The highest concentration of DA was obtained in the ninth fraction (i.e. + 45 min) where basal DA concentrations were significantly reduced by 250% ($P < 0.05$ Tukey-Kramer test).

Figure 3.12 shows concentration in brain microdialysis samples and plasma microdialysis samples versus time profile for carbamathione after administration of carbamathione (200 mg/kg i.v., $n = 3$). Carbamathione concentrations in the plasma and the brain increased to a peak at 5 and 10 min, respectively after administration and then proceeded to fall exponentially. The pharmacokinetic parameters of carbamathione in brain are given in table 3.13. The elimination constants for carbamathione in the brain and plasma are very close in value which suggests passive diffusion across the blood-brain barrier. It is also important to note that the half-lives of carbamathione in the plasma, prefrontal cortex and nucleus accumbens are 4.81 ± 0.97, 4.31 ± 0.59 and 4.19 ± 0.66 min respectively. The sample collection time of 5 min was more than the estimated half-lives of carbamathione. This suggests that the collection time may have to be decreased in order to obtain the relevant PK and PD data on carbamathione.

Figure 3.12 Carbamathione concentration versus time profile after 200 mg/kg dose of carbamathione and 5 min sampling interval.

Concentration of carbamathione in rat brain following carbamathione administration (200 mg/kg i.v., *n* = 3). Microdialysis samples were collected every 5 min. Data shown as concentration (mean ± SEM).

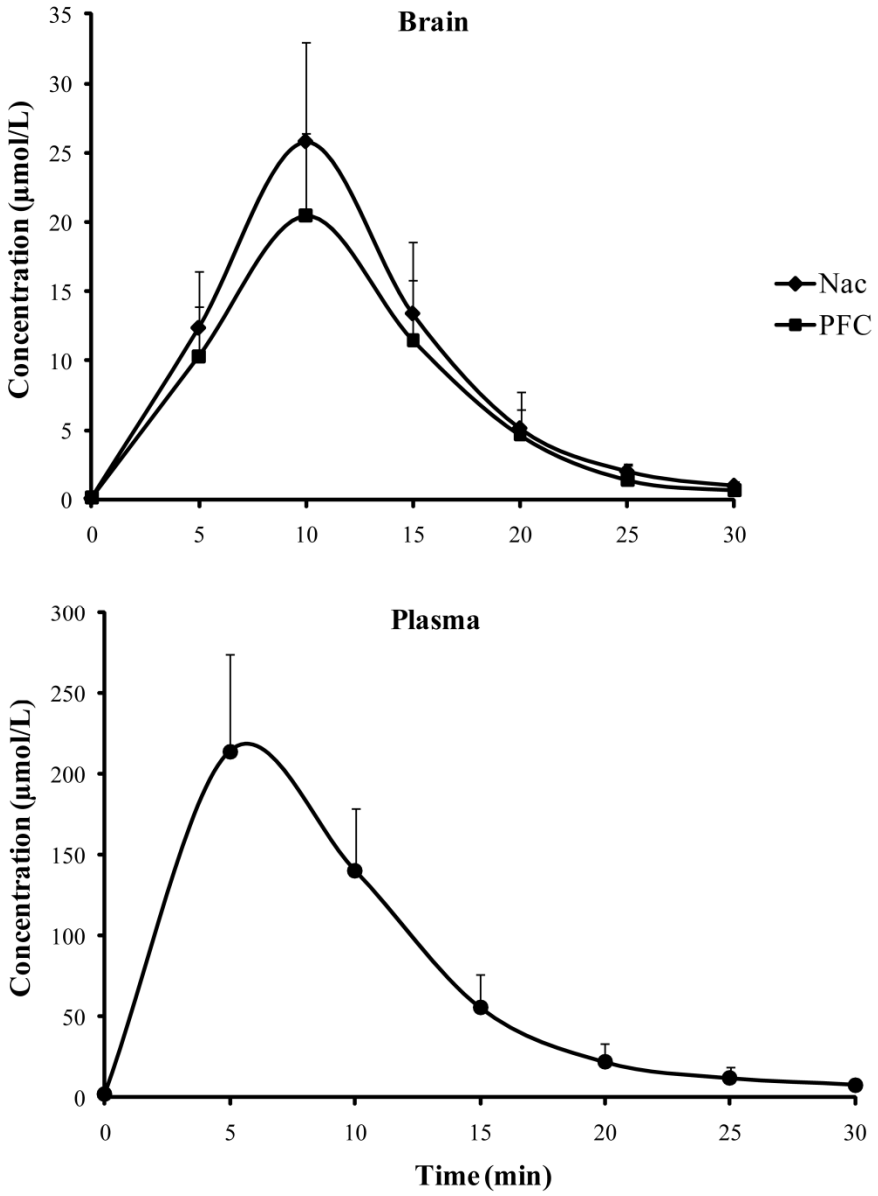

Table 3.13 Pharmacokinetic paramaters of carbamathione with 5 min sampling interval.

Pharmacokinetic parameters of carbamathione in rat brain following carbamathione administration (200 mg/kg i.v., n = 3) and 5 min sample collection. Data expressed as mean ± SEM.

200 mg/kg	C_{max}	t_{max}	$t_{1/2}$	K_{elim}	AUC
PFC	20.4 ± 3.6	7.5± 2.5	4.31 ± 0.59	0.16 ± 0.02	252 ± 81
NAc	25.8 ± 4.1	7.5± 2.5	4.19 ± 0.66	0.17 ± 0.02	308 ± 87
Plasma	213 ± 37	2.5± 2.5	4.81 ± 0.97	0.15 ± 0.03	2310 ± 628

PFC= Prefrontal Cortex

NAc=Nucleus Accumbens

C_{max} = maximum concentration (µmol/L)

t_{max} = time to maximum concentration (min)

$t_{1/2}$ = elimination half-life (min)

K_{elim} = elimination constant (1/min)

AUC = area under the dialysate concentration versus time profile (µmol/L min)

3.3.5.2 Increased Temporal Resolution for Carbamathione Dose-Response

The MEKC-LIF method developed was applied to a 200 mg/kg i.v. dose of carbamathione followed by a 5 min sample collection interval. The sampling rate was later increased to 3 min sample collections to obtain important PK and PD data related with three doses (200 mg/kg, 50 mg/ kg, and 20 mg/kg i.v.) of carbamathione. Data are given as mean ± SEM. Two-way ANOVA with repeated measures over time was used to compare neurotransmitter levels between treatments and within treatments over time. Post hoc comparisons were made using Fisher's least significant difference (LSD) test. The level of significance was set as at least $P < 0.05$ for all comparisons.

Figure 3.14 shows the effect of three doses of carbamathione (200 mg/kg, 50 mg/kg, and 20 mg/kg i.v.) on basal GABA levels in the nucleus accumbens. Carbamathione produced a significant decrease (19%-40%, $P < 0.05$) in extracellular basal GABA concentrations 6-12 min after dosing and remained decreased for the next 80-96 min. The lowest concentrations (23%-77%, $P < 0.05$) were obtained 45-63 min after dosing. Two-way ANOVA for repeated measures over time for the data shown in figure 3.14 revealed a significant main effect of treatment ($F_{3,47} = 21.37$, $P < 0.05$), a significant interaction between treatment and time interaction ($F_{45,705} = 9.13$, $P < 0.05$), and a trend towards a main effect of time ($F_{15,705} = 17.69$, $P < 0.05$).

Figure 3.14 GABA levels in the nucleus accumbens after carbamathione administration and 3 min sampling interval.

Data reported as percentages of baseline. 0 min indicates time point of carbamathione administration (n=5). * $P < 0.05$, compared to the 20 mg/kg dose using Fisher's LSD test. # $P < 0.05$, compared to the 50 mg/kg dose using Fisher's LSD test.

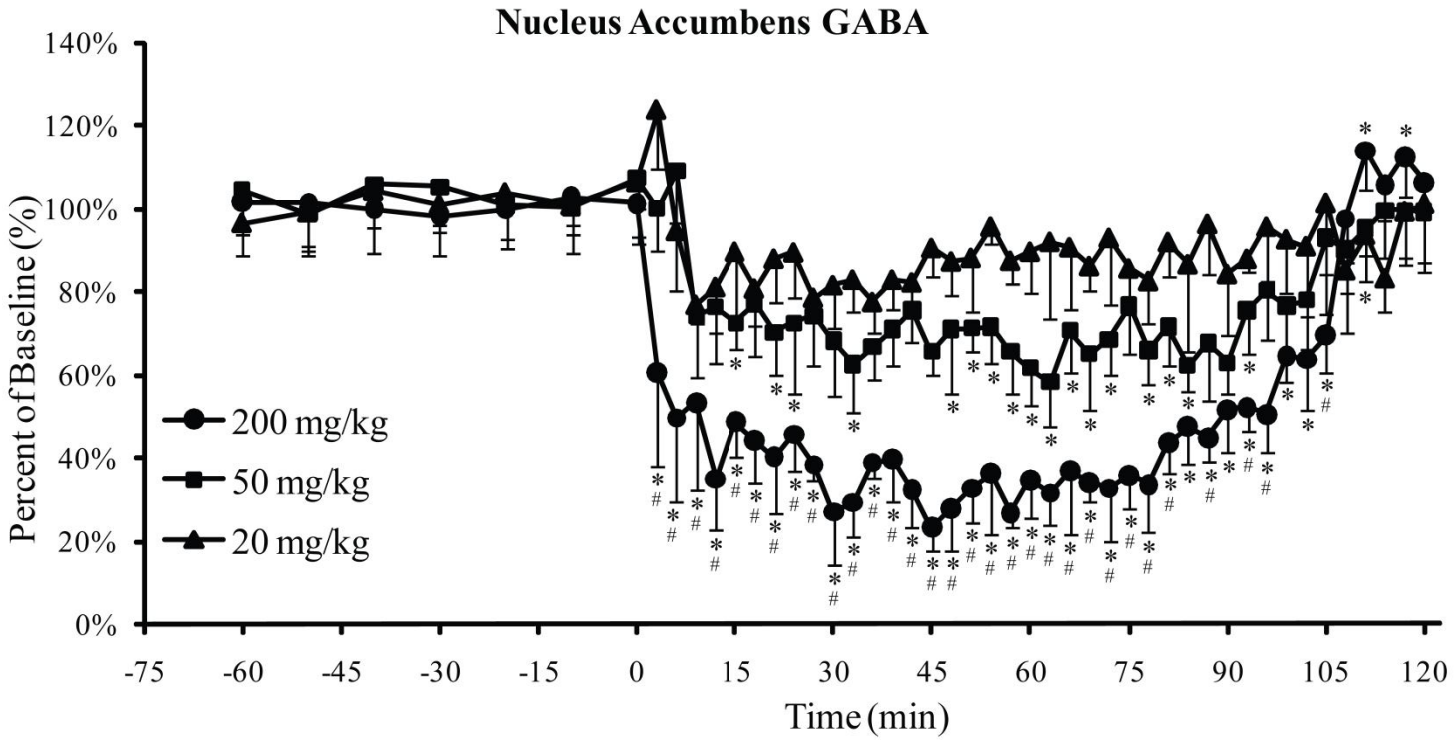

Figure 3.15 shows the effect of three doses of carbamathione (200 mg/kg, 50 mg/kg, and 20 mg/kg i.v.) on basal Glu levels in the nucleus accumbens. Extracellular basal Glu concentrations were significantly increased (10%-51 %, $P < 0.05$) in the first 3-6 min after carbamathione administration and continued to remain elevated over the next 27-39 min with the peak concentrations (29%-101 %, $P < 0.05$) occurring 6-9 min after dosing. There was later a significant decrease (26%-84%, $P < 0.05$) in Glu concentrations for the next 66 min. Two-way ANOVA for repeated measures over time for the data shown in figure 3.15 revealed a statistically significant main effect of time ($F_{15,705} = 15.20$, $P < 0.05$) and a significant interaction between treatment and time ($F_{45,705} = 5.41$, $P < 0.05$), but no significant main effect of treatment ($F_{3,47} = 0.48$, $P < 0.05$).

Figure 3.16 shows the effect of three doses of carbamathione (200 mg/kg, 50 mg/kg, and 20 mg/kg i.v.) on basal DA levels in the nucleus accumbens. Carbamathione produced a significant increase (54%-260%, $P < 0.05$) in extracellular basal DA concentrations 3-6 min after dosing and remained elevated for the next 75-100 min. The peak increase (95%-616%, $P < 0.05$) in basal DA levels occurred 15-21 min after dosing.

Figure 3.15 GABA levels in the nucleus accumbens after carbamathione administration and 3 min sampling interval.

Data reported as percentages of baseline. 0 min indicates time point of carbamathione administration (n=5). * $P < 0.05$, compared to the 20 mg/kg dose using Fisher's LSD test. # $P < 0.05$, compared to the 50 mg/kg dose using Fisher's LSD test.

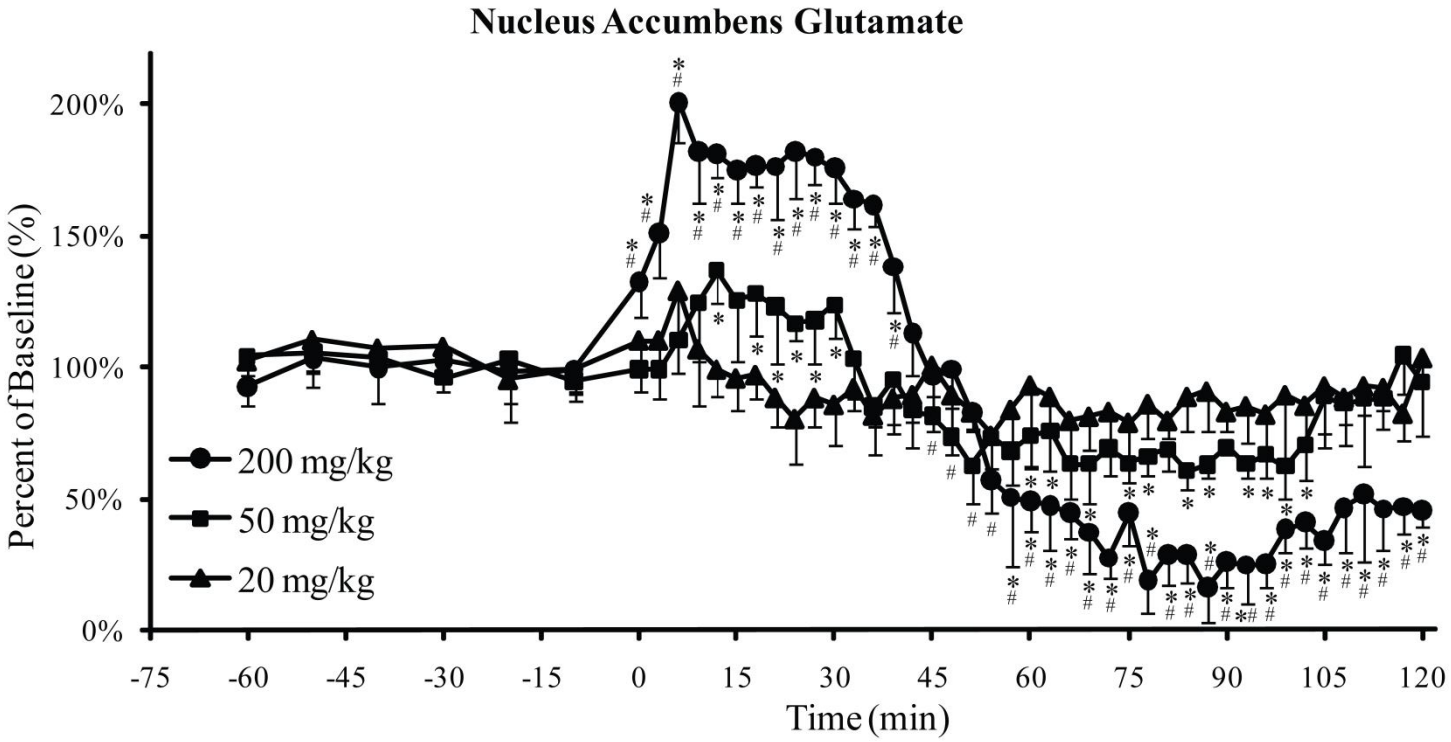

Figure 3.16 DA levels in the nucleus accumbens after carbamathione administration and 3 min sampling interval.

Data reported as percentages of baseline. 0 min indicates time point of carbamathione administration (n=5). * $P < 0.05$, compared to the 20 mg/kg dose using Fisher's LSD test. # $P < 0.05$, compared to the 50 mg/kg dose using Fisher's LSD test.

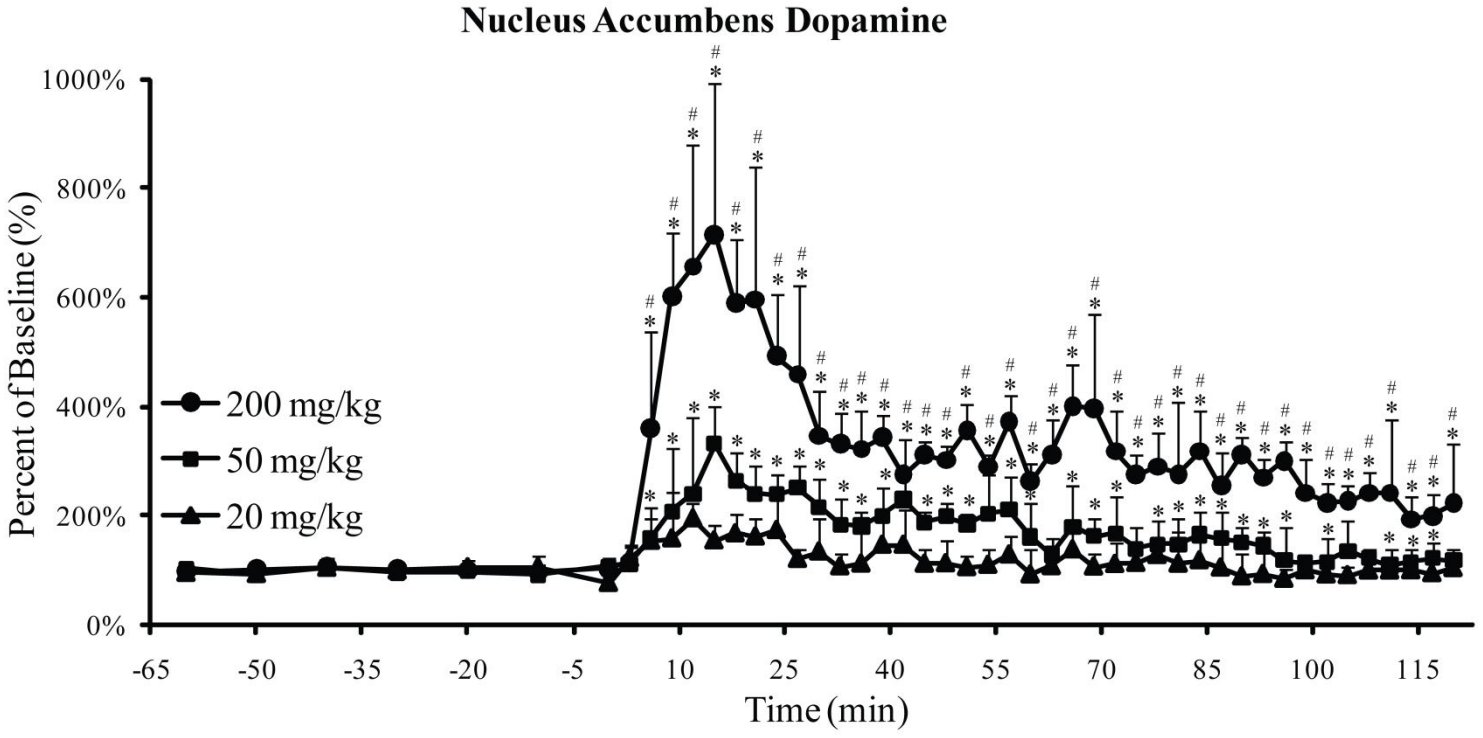

Two-way ANOVA for repeated measures over time for the data shown in figure 3.16 revealed a significant main effect of treatment ($F_{3,47}$ = 28.59, P < 0.05), a significant interaction between treatment and time interaction ($F_{45,705}$ = 6.49, P < 0.05), and a trend towards a main effect of time ($F_{15,705}$ = 13.61, P < 0.05).

Figure 3.17 shows the effect of three doses of carbamathione (200 mg/kg, 50 mg/kg, and 20 mg/kg i.v.) on basal GABA levels in the prefrontal cortex. Carbamathione produced a significant decrease (15%-48%, P < 0.05) in extracellular basal GABA concentrations 3-6 min after dosing and remained decreased for the next 90-96 min. The lowest concentrations (29%-81%, P < 0.05) were obtained 53-75 min after dosing. Two-way ANOVA for repeated measures over time for the data shown in figure 3.17 revealed a significant main effect of treatment ($F_{3,47}$ = 23.03, P < 0.05), a significant interaction between treatment and time interaction ($F_{45,705}$ = 9.52, P < 0.05), and a trend towards a main effect of time ($F_{15,705}$ = 19.83, P < 0.05).

Figure 3.18 shows the effect of three doses of carbamathione (200 mg/kg, 50 mg/kg, and 20 mg/kg i.v.) on basal Glu levels in the prefrontal cortex.

Figure 3.17 GABA levels in the prefrontal cortex after carbamathione administration and 3 min sampling interval.

Data reported as percentages of baseline. 0 min indicates time point of carbamathione administration (n=5). * $P < 0.05$, compared to the 20 mg/kg dose using Fisher's LSD test. # $P < 0.05$, compared to the 50 mg/kg dose using Fisher's LSD test.

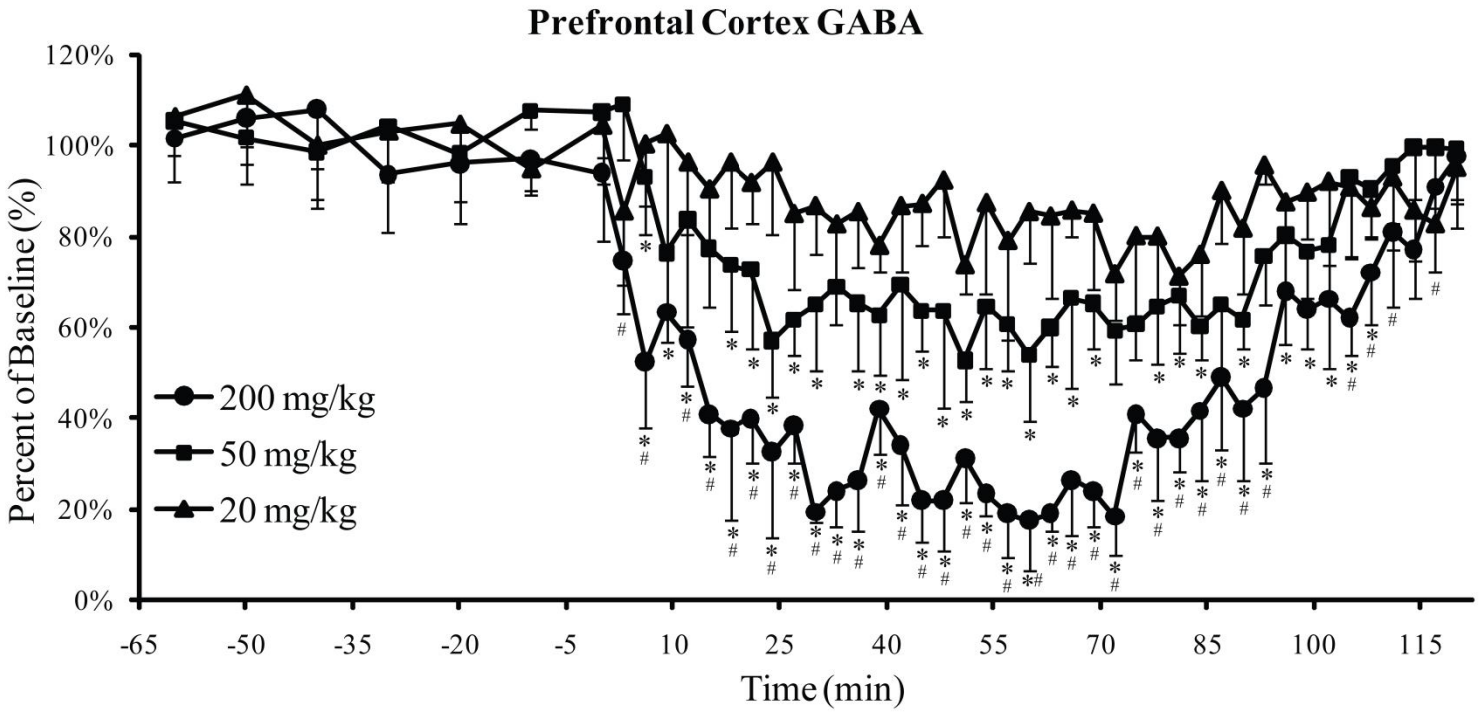

Figure 3.18 Glu levels in the prefrontal cortex after carbamathione administration and 3 min sampling interval.

Data reported as percentages of baseline. 0 min indicates time point of carbamathione administration (n=5). * $P < 0.05$, compared to the 20 mg/kg dose using Fisher's LSD test. # $P < 0.05$, compared to the 50 mg/kg dose using Fisher's LSD test.

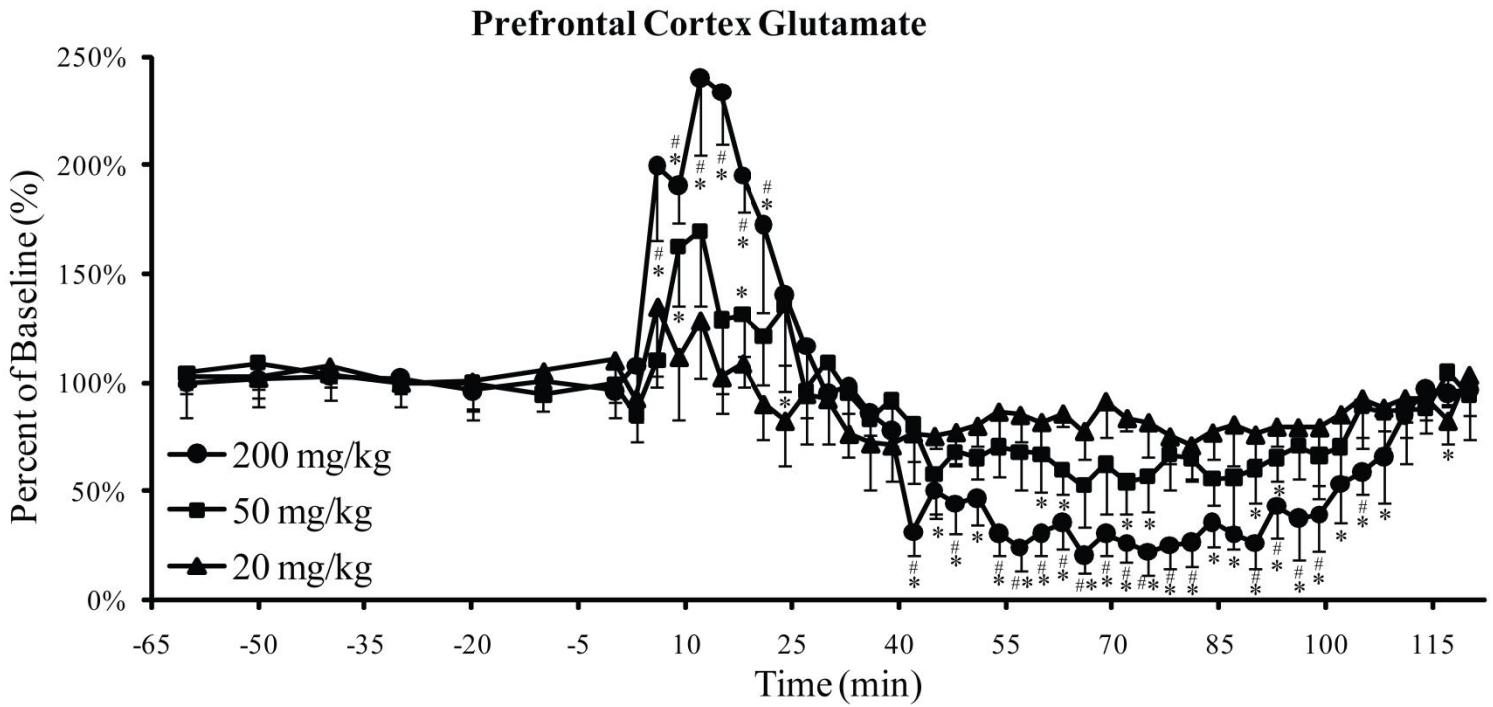

Extracellular basal Glu concentrations were significantly increased (11%-100 %, $P < 0.05$) in the first 3-6 min after carbamathione administration and continued to remain elevated over the next 12-18 min with the peak concentrations (35%-140 %, $P < 0.05$) occurring 9-12 min after dosing. There was later a significant decrease (29%-79%, $P < 0.05$) in Glu concentrations for the next 78-90 min. Two-way ANOVA for repeated measures over time for the data shown in figure 3.18 revealed a statistically significant main effect of time ($F_{15,705} = 24.2$, $P < 0.05$) and a significant interaction between treatment and time ($F_{45,705} = 3.84$, $P < 0.05$), but no significant main effect of treatment ($F_{3,47} = 0.67$, $P < 0.05$).

Figure 3.19 shows the effect of three doses of carbamathione (200 mg/kg, 50 mg/kg, and 20 mg/kg i.v.) on basal DA levels in the prefrontal cortex. Carbamathione produced a significant increase (11-87%, $P < 0.05$) in extracellular basal DA concentrations 3-6 min after dosing and remained elevated for the next 90-114 min. The peak increase (66-395%, $P < 0.05$) in basal DA levels occurred 48-72 min after dosing. Two-way ANOVA for repeated measures over time for the data shown in figure 3.19 revealed a significant main effect of treatment ($F_{3,47} = 42.03$, $P < 0.05$), a significant interaction between treatment and time interaction ($F_{45,705} = 3.23$, $P < 0.05$), and a trend towards a main effect of time ($F_{15,705} = 8.46$, $P < 0.05$).

Figure 3.19 DA levels in the prefrontal cortex after carbamathione administration and 3 min sampling interval.

Data reported as percentages of baseline. 0 min indicates time point of carbamathione administration (n=5). * $P < 0.05$, compared to the 20 mg/kg dose using Fisher's LSD test. # $P < 0.05$, compared to the 50 mg/kg dose using Fisher's LSD test.

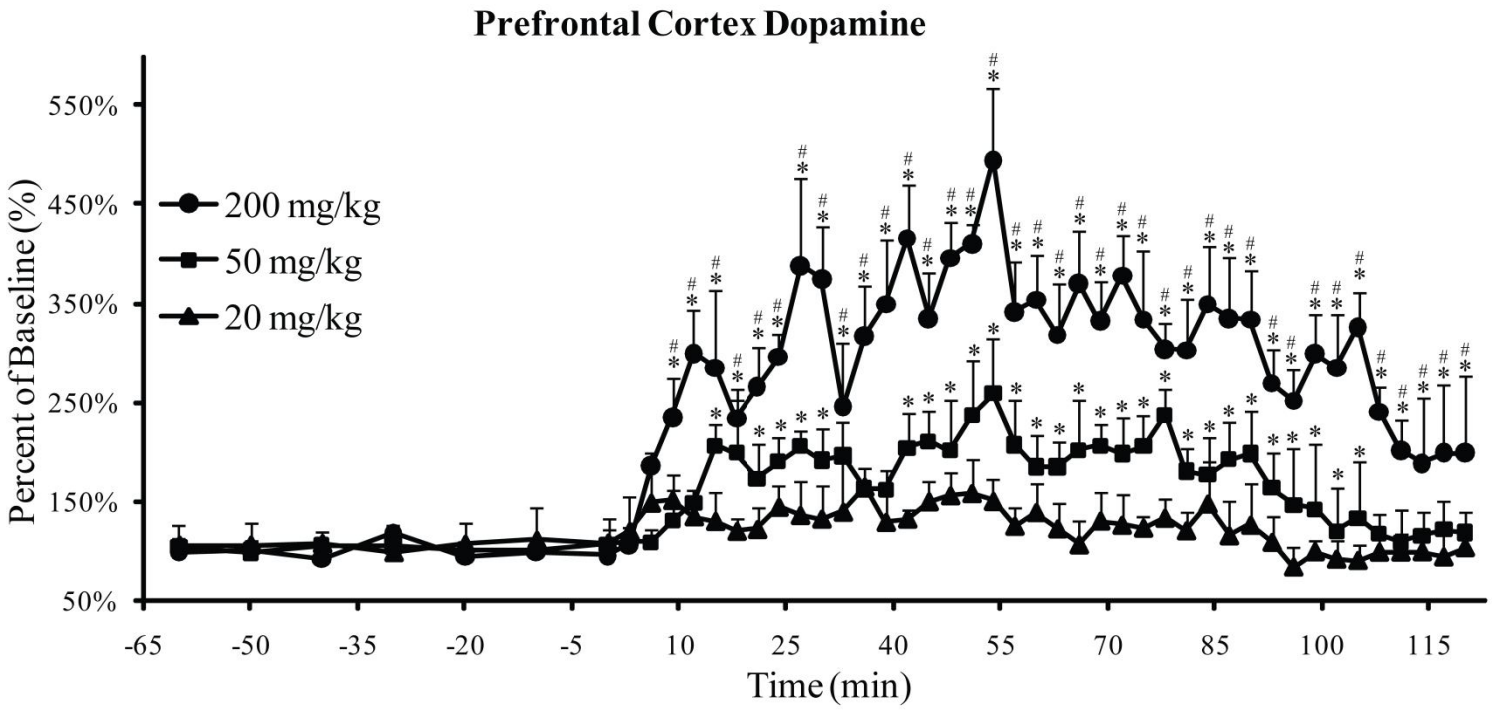

Figure 3.20 shows concentration in brain microdialysis samples and plasma microdialysis samples versus time profile for carbamathione after the i.v. administration of carbamathione (200 mg/kg, 50 mg/kg, and 20 mg/kg). Carbamathione concentrations in the plasma and the brain increased to a peak after 3 and 6 min, respectively and then proceeded to fall exponentially. The pharmacokinetic parameters of carbamathione in brain are given in table 3.21. It is important to note that the values for the half-life of carbamathione in the brain and plasma obtained by 3 min sampling are very close to those obtained by 5 min sampling (see table 3.13). The values obtained for the elimination constants by 3 min sampling were also very close to those obtained by 5 min sampling. These results suggest that 5 min sampling was sufficient to obtain the relevant PK and PD data for carbamathione.

3.4 Discussion

The results from this study show that carbamathione crossed the blood-brain barrier (BBB) and administration of carbamathione was correlated with a dose-dependent change in GABA, Glu, and DA. This finding has implications for carbamathione as a possible pharmacological agent in alcohol and cocaine addiction.

Figure 3.20 Carbamathione concentration versus time profile after three doses carbamathione and 3 min sampling interval.

Concentration of carbamathione in rat brain following carbamathione administration (200 mg/kg, 50 mg/kg, 20 mg/kg i.v., *n* = 5). Microdialysis samples were collected every 3 min. Data shown as concentration (mean ± SEM).

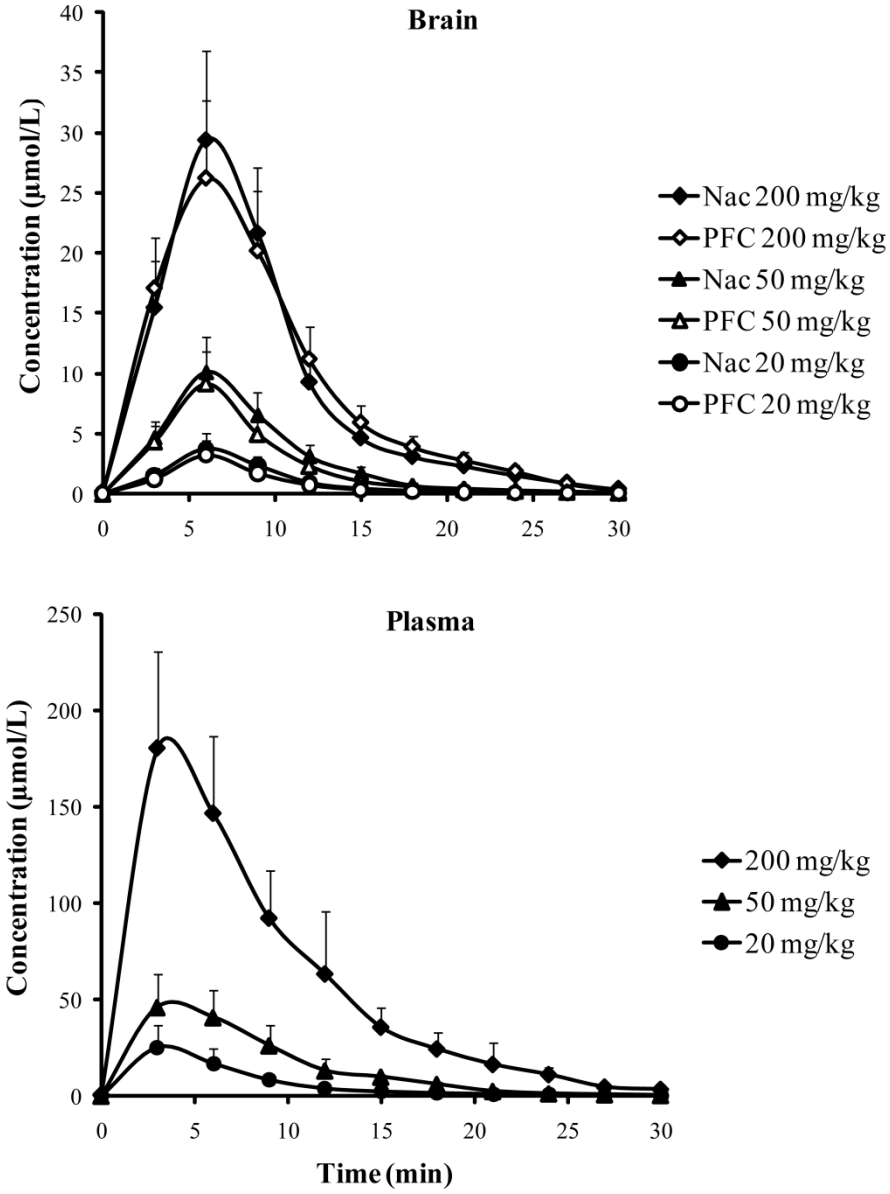

Table 3.21 Pharmacokinetic paramaters of carbamathione with 3 min sampling interval.

Pharmacokinetic parameters of carbamathione in rat brain following carbamathione administration (200 mg/kg, 50 mg/kg, and 20 mg/kg i.v., n = 5) and 3 min sample collection. Data expressed as mean ± SEM.

Dose	C_{max}	t_{max}	$t_{1/2}$	K_{elim}	AUC
200 mg/kg PFC	26.2 ± 6.5	4.5 ± 1.5	4.15 ± 0.37	0.17 ± 0.02	273 ± 66
200 mg/kg NAc	29.4 ± 7.3	4.5 ± 1.5	4.10 ± 0.48	0.16 ± 0.02	270 ± 67
200 mg/kg Plasma	182 ± 47	1.5 ± 1.5	4.67 ± 0.41	0.15 ± 0.03	1854 ± 458
50 mg/kg PFC	9.24 ± 2.64	4.5 ± 1.5	4.14 ± 0.58	0.17 ± 0.03	71.1 ± 21.3
50 mg/kg NAc	10.1 ± 3.0	4.5 ± 1.5	4.05 ± 0.57	0.17 ± 0.02	84.1 ± 25.2
50 mg/kg Plasma	45.9 ± 9.4	1.5 ± 1.5	4.37 ± 0.44	0.16 ± 0.03	447 ± 124
20 mg/kg PFC	3.25 ± 0.43	4.5 ± 1.5	4.17 ± 0.67	0.17 ± 0.03	23.7 ± 6.3
20 mg/kg NAc	3.72 ± 0.54	4.5 ± 1.5	4.09 ± 0.71	0.17 ± 0.03	29.1 ± 8.1
20 mg/kg Plasma	25.2 ± 8.3	1.5 ± 1.5	4.34 ± 0.55	0.16 ± 0.04	183 ± 70

PFC= Prefrontal Cortex

NAc=Nucleus Accumbens

C_{max} = maximum concentration (µmol/L)

t_{max} = time to maximum concentration (min)

$t_{1/2}$ = elimination half-life (min)

K_{elim} = elimination constant (1/min)

AUC = area under the dialysate concentration versus time profile (µmol/L min)

Alcohol exerts its reinforcing properties through a set of effects on multiple neurotransmitter systems that includes agonism or potentiating $GABA_A$, and antagonism at the Glu receptors. Alcohol reduces the pace of brain activity in part by decreasing the excitatory actions of Glu at the *N*-methyl-*D*-aspartic acid (NMDA) receptor. Alcohol also causes the release of DA (i.e., stimulant-like properties), and may exert some of its acute positively reinforcing properties by its effects on dopaminergic systems.[18-21] The reinforcing properties and abuse liability of cocaine is primarily mediated by its binding action at the DA reuptake transporter, which leads to an increase in DA. Both cocaine and alcohol also cause an increase in DA transmission by an indirect pathway in which GABAergic interneurons that normally inhibit DA neurons are inhibited. In one study, the administration of vigabatrin, a drug that enhances brain GABA levels abolished a cocaine cue-induced increase in brain DA levels.[22] The dopaminergic pathways in the nucleus accumbens and prefrontal cortex are the main sites in the brain that mediate alcohol and cocaine reinforcement. Dopaminergic activity in the nucleus accumbens is regulated by glutamatergic and GABAergic inputs from the prefrontal cortex.[19-21]

Administration of carbamathione was correlated with an initial increase in extracellular Glu concentration and a subsequent decrease after 30 min. This initial increase was statistically greater in the nucleus accumbens than in the

prefrontal cortex. This is interesting because this increase and decrease can be correlated with the PK of carbamathione in the brain (figure 3.20). This suggests that the initial increase may be due to carbamathione, which is a partial NMDA antagonist. The subsequent decrease may be due to a metabolite that is formed after carbamathione. The fact that carbamathione may act as a partial NMDA antagonist with effects that do not last very long may prove to be an advantage in the treatment of cocaine and alcohol addiction. Glu receptor antagonists have been used in the treatment of both alcohol and cocaine addiction.[18,23-25] Acamprosate, a drug approved by the FDA for alcohol dependency, has been proposed to act on the glutamatergic system. In particular, it has been demonstrated that acamprosate acts through the attenuation of a 'hyperglutamatergic state' that underlies acute and protracted alcohol withdrawal, and is associated with alcohol craving and relapse. This mode of action of acamprosate suggests that the blockade of Glu receptors could reduce relapse and craving. In fact, memantine and neramexane, both NMDA blockers, can attenuate cue-induced craving in a dose-dependent fashion in alcohol-dependent patients by producing alcohol-like effects. This provides a new concept in replacement therapy for alcoholism.[25] Another study showed that delivering cues associated with cocaine during self-administration training reliably reinstated active lever responding after extinction and systemic administration of Glu antagonists significantly attenuated cue-induced reinstatement.[26] Glutamatergic signaling

between the prefrontal cortex and nucleus accumbens has been demonstrated to be essential for cue-induced drug seeking behavior. Pharmacological agents capable of reducing glutamatergic signaling within these regions may potentially provide a mechanism through which to promote abstinence.[27,28]

Administration of carbamathione was correlated with an increase in DA levels in the brain. The increase of DA in the nucleus accumbens was more pronounced than the increase in the prefrontal cortex. This difference was statistically significant. This is expected since carbamathione also appeared to decrease GABA in the prefrontal cortex which usually inhibits DA in the nucleus accumbens. The DA efflux evoked by carbamathione appeared to be reversible over time which seems to exclude short-term cytotoxic implications. The role of DA in mediating the rewarding effects of drugs of abuse has been well established. DA has been demonstrated to play a significant role in the development of craving and withdrawal when alcohol and cocaine are abused. Replacement treatments for cocaine dependence involve replacing cocaine's effects at the DA reuptake transporter and replacing postsynaptic DA with DA agonists. [18,19,29-31] Among the DA-enhancing agents, amantadine has shown some promise in treating patients with cocaine dependence, but this has not been a reliable finding. Another replacement approach involves substituting amphetamine for cocaine as an agonist since it has been shown to reduce cocaine

use in cocaine dependent patients. This would be similar to replacing heroin with methadone.[18] Another study demonstrated that the acute administration of a dopamine antagonist significantly decreased alcohol intake and cue/alcohol-triggered reinstatement of alcohol-seeking behavior in a model of oral alcohol self-administration in mice.[32] Carbamathione is a promising pharmacological agent since the drugs that enhance dopaminergic function have been also shown to reduce the effects of withdrawal from alcohol and cocaine.[7,18,33,34]

Administration of carbamathione was correlated with a dose-dependent decrease in extracellular GABA levels in the nucleus accumbens and the prefrontal cortex. The decrease of GABA in the prefrontal cortex was greater than the decrease in the nucleus accumbens at 57-72 min after carbamathione administration. This difference was statistically significant. As discussed previously, chronic alcohol and cocaine use have demonstrated effects on GABAergic transmission in the nucleus accumbens, disinhibiting DA neurons in this area as well as GABAergic receptor expression and binding characteristics.[18,35] GABA agonists such as baclofen have been shown to reduce the reinforcing effects of several different classes of abused drugs in animal models under a variety of conditions. In addition clinical trials have also shown baclofen to be promising in treating cocaine addiction and alcoholism.[30] Other approaches to altering GABA neurotransmission include the use of anticonvulsants. The exact pharmacology of

these drugs is not fully understood but most also affect the glutamatergic system. Anticonvulsants, such as valproate, tiagabine and topiramate, have shown promise in treating cocaine addiction and alcoholism. Since carbamathione appeared to decrease GABA with a concurrent increase in DA, an effect seen with both alcohol and cocaine, carbamathione may lead to the decrease in craving for alcohol or cocaine. Disulfiram was observed to have an anti-craving property in clinical trials for the treatment of alcohol and cocaine addiction.[36,37] The effect of carbamathione on GABA levels further supports a possible role for carbamathione in replacement therapy for alcohol and cocaine addiction.

Microdialysis provided important information pertaining to the extracellular levels of neurotransmitters in the brain as well as the PK of carbamathione. However, one of the drawbacks of the microdialysis technique is that it does not provide information about the mechanism of action of carbamathione. Previous studies with disulfiram may provide some mechanistic information on the data obtained in this investigation. Vaccari *et al.*, 1996 demonstrated that disulfiram administration led to DA release from striatal vesicles and inhibited the vesicular uptake of [^{3}H]DA.[38] Studies from the same laboratory also demonstrated that disulfiram evoked a vesicular efflux of Glu and an *in vivo* striatal release of Glu.[39] These studies may explain some of the changes observed in Glu and DA levels in the brain after carbamathione administration in this study since carbamathione is a

metabolite of disulfiram. Nagendra *et al.*, 1997 showed that carbamathione was formed when *S*- methyl *N, N*-diethylthiocarbamate sulfone (DETC-$MeSO_2$), a metabolite of disulfiram, carbamoylated glutathione. Carbamathione was suggested to cross the BBB and carbamoylate brain Glu receptor *in vivo*.[40] This suggests that carbamathione or a metabolite after carbamathione may be responsible for the changes observed in brain neurotransmitters after disulfiram or carbamathione administration.

It is interesting to note that administration of carbamathione was correlated with an effect on multiple neurotransmitter systems. Most of the pharmacotherapy for alcoholism and cocaine abuse usually target a single neurotransmitter system and multi-drug therapy appeared to be more efficacious that administration of a single drug.[18,19,30] The effect of carbamathione on multiple neurotransmitters may indicate the presence of one or more other metabolites that are formed after carbamathione.

3.5 Conclusions

The work in this chapter showed the application of a MEKC-LIF method for the simultaneous detection of GABA, Glu, DA, and carbamathione in rat brain dialysate and an LC-MS/MS method for the detection of carbamathione in plasma

dialysate. The analytical methods were validated and exhibited good linearity, accuracy and reproducibility with nanomolar and sub-nanomolar detection limits. The administration of three doses of carbamathione was correlated with changes in the brain neurotransmitter systems in awake rats. Administration of carbamathione was correlated with dose-dependent changes in GABA, Glu, and DA in both the prefrontal cortex and nucleus accumbens. Carbamathione was also determined in plasma dialysate and allowed the determination of PK parameters. Although carbamathione administration was correlated with changes in brain neurotransmitters, the mechanism by which this occurred remains unknown. Future studies will focus on elucidating this mechanism by studying selectively inhibiting disulfiram metabolism and investigating whether changes in brain neurotransmitters were observed.

3.6 References

1 Le Moal, M. & Koob, G. F. Drug addiction: Pathways to the disease and pathophysiological perspectives. *European Neuropsychopharmacology* **17**, 377-393, (2007).

2 Tseng, H. M., Li, Y. & Barrett, D. A. Profiling of amine metabolites in human biofluids by micellar electrokinetic chromatography with laser-induced fluorescence detection. *Anal Bioanal Chem* **388**, 433-439, (2007).

3 Freed, A. L. & Lunte, S. M. Separation of naphthalene-2,3-dicarboxaldehyde-derivatized-substance P and its metabolites by micellar electrokinetic chromatography. *Electrophoresis* **21**, 1992-1996, (2000).

4 Siri, N., Lacroix, M., Garrigues, J. C., Poinsot, V. & Couderc, F. HPLC-fluorescence detection and MEKC-LIF detection for the study of amino acids and catecholamines labelled with naphthalene-2,3-dicarboxyaldehyde. *Electrophoresis* **27**, 4446-4455, (2006).

5 Ueda, T., Mitchell, R., Kitamura, F., Metcalf, T., Kuwana, T. & Nakamoto, A. Separation of Naphthalene-2,3-Dicarboxaldehyde-Labeled Amino-Acids by High-Performance Capillary Electrophoresis with Laser-Induced Fluorescence Detection. *Journal of Chromatography* **593**, 265-274, (1992).

6 Kaul, S., Williams, T. D., Lunte, C. E. & Faiman, M. D. LC-MS/MS determination of carbamathione in microdialysis samples from rat brain and plasma. *J Pharm Biomed Anal* **51**, 186-191, (2010).

7 Huang, M., Li, Z., Dai, J., Shahid, M., Wong, E. H. & Meltzer, H. Y. Asenapine increases dopamine, norepinephrine, and acetylcholine efflux in the rat medial prefrontal cortex and hippocampus. *Neuropsychopharmacology* **33**, 2934-2945, (2008).

8 Benturquia, N., Parrot, S., Sauvinet, V., Renaud, B. & Denoroy, L. Simultaneous determination of vigabatrin and amino acid neurotransmitters in brain microdialysates by capillary electrophoresis with laser-induced fluorescence detection. *J Chromatogr B Analyt Technol Biomed Life Sci* **806**, 237-244, (2004).

9 Moghaddam, B., Adams, B., Verma, A. & Daly, D. Activation of glutamatergic neurotransmission by ketamine: A novel step in the pathway from NMDA receptor blockade to dopaminergic and cognitive disruptions associated with the prefrontal cortex. *Journal of Neuroscience* **17**, 2921-2927, (1997).

10 Maganti, S. A. *A proposed new mechanism of action for disulfiram in alcohol and cocaine addiction* M.S. thesis, University of Kansas, (2006).

11 Jin, L., Davis, M. R., Hu, P. & Baillie, T. A. Identification of novel glutathione conjugates of disulfiram and diethyldithiocarbamate in rat bile

by liquid chromatography-tandem mass spectrometry. Evidence for metabolic activation of disulfiram in vivo. *Chemical research in toxicology* **7**, 526-533, (1994).

12 Schloss, J. V. Therapeutic Compositions. U.S.A. patent (2007).

13 Davies, M. I. & Lunte, C. E. Microdialysis sampling for hepatic metabolism studies. Impact of microdialysis probe design and implantation technique on liver tissue. *Drug Metab Dispos* **23**, 1072-1079, (1995).

14 Zhao, Y. P., Liang, X. Z. & Lunte, C. E. Comparison of Recovery and Delivery in-Vitro for Calibration of Microdialysis Probes. *Analytica Chimica Acta* **316**, 403-410, (1995).

15 Paxinos, G. & Watson, C. *The Rat Brain in Stereotaxic Coordinates*. (Academic Press, 1982).

16 Karnes, H. T., Shiu, G. & Shah, V. P. Validation of bioanalytical methods. *Pharm Res* **8**, 421-426, (1991).

17 O'Shea, T. J., Weber, P. L., Bammel, B. P., Lunte, C. E., Lunte, S. M. & Smyth, M. R. Monitoring excitatory amino acid release in vivo by microdialysis with capillary electrophoresis-electrochemistry. *J Chromatogr* **608**, 189-195, (1992).

18 Ross, S. & Peselow, E. Pharmacotherapy of Addictive Disorders. *Clin Neuropharmacol* **32**, 277-289, (2009).

19 Jupp, B. & Lawrence, A. J. New horizons for therapeutics in drug and alcohol abuse. *Pharmacol Therapeut* **125**, 138-168, (2010).

20 Volkow, N. D., Fowler, J. S., Wang, G. J., Baler, R. & Telang, F. Imaging dopamine's role in drug abuse and addiction. *Neuropharmacology* **56 Suppl 1**, 3-8, (2009).

21 Koob, G. F. & Le Moal, M. Review. Neurobiological mechanisms for opponent motivational processes in addiction. *Philos Trans R Soc Lond B Biol Sci* **363**, 3113-3123, (2008).

22 Gerasimov, M. R., Schiffer, W. K., Gardner, E. L., Marsteller, D. A., Lennon, I. C., Taylor, S. J. C., Brodie, J. D., Ashby, C. R. & Dewey, S. L. GABAergic blockade of cocaine-associated cue-induced increases in nucleus accumbens dopamine. *European Journal of Pharmacology* **414**, 205-209, (2001).

23 Uys, J. D. & LaLumiere, R. T. Glutamate: The New Frontier in Pharmacotherapy for Cocaine Addiction. *Cns Neurol Disord-Dr* **7**, 482-491, (2008).

24 Torregrossa, M. M., Tang, X. C. & Kalivas, P. W. The glutamatergic projection from the prefrontal cortex to the nucleus accumbens core is required for cocaine-induced decreases in ventral pallidal GABA. *Neurosci Lett* **438**, 142-145, (2008).

25 Spanagel, R. & Kiefer, F. Drugs for relapse prevention of alcoholism: ten years of progress. *Trends Pharmacol Sci* **29**, 109-115, (2008).

26 Backstrom, P. & Hyytia, P. Ionotropic and metabotropic glutamate receptor antagonism attenuates cue-induced cocaine seeking. *Neuropsychopharmacology* **31**, 778-786, (2006).

27 Gass, J. T. & Olive, M. F. Glutamatergic substrates of drug addiction and alcoholism. *Biochemical Pharmacology* **75**, 218-265, (2008).

28 Heilig, M. & Egli, M. Pharmacological treatment of alcohol dependence: Target symptoms and target mechanisms. *Pharmacol Therapeut* **111**, 855-876, (2006).

29 Le Foll, B., Gallo, A., Le Strat, Y., Lu, L. & Gorwood, P. Genetics of dopamine receptors and drug addiction: a comprehensive review. *Behav Pharmacol* **20**, 1-17, (2009).

30 Nutt, D. & Lingford-Hughes, A. Addiction: the clinical interface. *Brit J Pharmacol* **154**, 397-405, (2008).

31 Koob, G. F. & Le Moal, M. Addiction and the brain antireward system. *Annu Rev Psychol* **59**, 29-53, (2008).

32 Heidbreder, C. Selective Antagonism at Dopamine D-3 Receptors as a Target for Drug Addiction Pharmacotherapy: A Review of Preclinical Evidence. *Cns Neurol Disord-Dr* **7**, 410-421, (2008).

33 Karila, L., Gorelick, D., Weinstein, A., Noble, F., Benyamina, A., Coscas, S., Blecha, L., Lowenstein, W., Martinot, J. L., Reynaud, M. & Lepine, J. P. New treatments for cocaine dependence: a focused review. *Int J Neuropsychoph* **11**, 425-438, (2008).

34 Kreek, M. J., LaForge, K. S. & Butelman, E. Pharmacotherapy of addictions. *Nat Rev Drug Discov* **1**, 710-726, (2002).

35 Enoch, M. A. The role of GABA(A) receptors in the development of alcoholism. *Pharmacol Biochem Be* **90**, 95-104, (2008).

36 Petrakis, I. L., Poling, J., Levinson, C., Nich, C., Carroll, K. & Rounsaville, B. Naltrexone and disulfiram in patients with alcohol dependence and comorbid psychiatric disorders. *Biol Psychiatry* **57**, 1128-1137, (2005).

37 de Sousa, A. & de Sousa, A. An open randomized study comparing disulfiram and acamprosate in the treatment of alcohol dependence. *Alcohol and alcoholism (Oxford, Oxfordshire)* **40**, 545-548, (2005).

38 Vaccari, A., Ferraro, L., Saba, P., Ruiu, S., Mocci, I., Antonelli, T. & Tanganelli, S. Differential mechanisms in the effects of disulfiram and diethyldithiocarbamate intoxication on striatal release and vesicular transport of glutamate. *J Pharmacol Exp Ther* **285**, 961-967, (1998).

39 Vaccari, A., Saba, P. L., Ruiu, S., Collu, M. & Devoto, P. Disulfiram and diethyldithiocarbamate intoxication affects the storage and release of striatal dopamine. *Toxicol Appl Pharmacol* **139**, 102-108, (1996).

40 Nagendra, S. N., Faiman, M. D., Davis, K., Wu, J. Y., Newby, X. & Schloss, J. V. Carbamoylation of brain glutamate receptors by a disulfiram metabolite. *The Journal of biological chemistry* **272**, 24247-24251, (1997).

4 INHIBITION OF DISULFIRAM METABOLISM AND ITS EFFECT ON BRAIN NEUROTRANSMITTERS

4.1 Introduction

In Chapter 3, the pharmacokinetics (PK) and pharmacodynamics (PD) of carbamathione were determined in a dose-dependent manner. The next step in the development of carbamathione as a potential pharmacological agent for alcohol and/or cocaine addiction was to demonstrate *in vivo* the relationship between carbamathione and disulfiram. This is an important step since disulfiram is approved by the U.S. Food and Drug Administration and has been used as a deterrent in alcoholism for over 60 years. There are several clinical studies with disulfiram, but none at the present time with carbamathione. It is thus important to establish the relationship between the changes in brain neurotransmitters after disulfiram administration and carbamathione. This chapter describes a laboratory-built micellar electrokinetic chromatography coupled with laser-induced fluorescence (MEKC-LIF) system used to determine the relationship between carbamathione and disulfiram administration, and the brain neurotransmitters.

4.1.1 Background and Significance

Although substantial progress has been made in understanding the molecular basis of alcohol and cocaine addiction, complete knowledge of the neural substrates

associated with drug abuse is still not definitive. Therefore there is no medication specifically approved to treat cocaine addiction.[1] The possibility of developing a drug that treats the craving aspect of addiction regardless of the substance being abused is an exciting one that warrants further study. Recent use of disulfiram in alcohol and cocaine addiction suggests that it can curb some of the craving effects of these addictions.[2-5] However, carbamathione offers many advantages over disulfiram as an anti-addiction drug. First, carbamathione does not inhibit aldehyde dehydrogenase ($ALDH_2$), so the unpleasant effects caused by disulfiram are eliminated. Second, disulfiram requires bioactivation by several cytochrome P450 enzymes, and there are several drugs and food items that can inhibit these enzymes. Third, several disulfiram metabolites are known to be toxic and may contribute to some of the reported adverse effects associated with disulfiram. Carbamathione does not form any of these toxic intermediates.[6]

4.1.2 Specific Aims of Research

The MEKC-LIF method used in Chapter 3 was modified and optimized for a laboratory-built system. In the method described in Chapter 3, a temporal resolution of 5 min was determined to be sufficient to obtain relevant PK and PD data. The goal of this research was to apply an MEKC-LIF method to determine the changes in rat brain neurotransmitters as related to the administration of

disulfiram and an inhibitor of disulfiram metabolism. Disulfiram metabolism can be inhibited by a non-specific cytochrome P450 enzyme inhibitor such as *N*-benzylimidazole (NBI). The administration of NBI with disulfiram should thus prevent disulfiram from being metabolized to carbamathione and block any neurochemical effect. Our hypothesis was that carbamathione is the proposed active metabolite of disulfiram and the administration of NBI with carbamathione should not have an effect on carbamathione-induced changes in brain neurotransmitters. Carbamathione does not require cytochrome P450 enzymes for activation. Thus even if a metabolite of carbamathione is responsible for the changes observed in brain neurotransmitters, NBI administration would not interfere with the formation of the metabolite. It would also indicate that if a metabolite is formed in the brain, it is not a cytochrome P450 metabolite.

4.2 Experimental

4.2.1 Chemicals and Reagents

In addition to the chemicals used in Chapter 2 and 3 (2.2.1 & 3.2.1 Chemicals and Reagents), disulfiram, NBI, and fluorescein were purchased from Sigma (St. Louis, MO, USA). Artificial cerebrospinal fluid (aCSF) was prepared as described in Chapter 2 (2.2.1 Chemicals and Reagents). Ringer's solution was prepared as described in Chapter 3 (3.2.1 Chemicals and Reagents). Standard

solutions of amino acids and carbamathione were prepared as previously described in Chapter 3 (3.2.1 Chemicals and Reagents). The background electrolyte (BGE) consisted of 22.5 mmol/L lithium tetraborate (LTB) (pH 9.2), 25 mmol/L lithium dodecylsulfate (LDS) and 10% methanol (MeOH). The borate buffer for derivatization was prepared as described in Chapter 2 (2.2.1 Chemicals and Reagents). The derivatization reaction was carried out as described in Chapter 2 (2.2.2 Derivatization).

4.2.2 Laboratory–Built MEKC-LIF Instrumentation

The laboratory-built electrophoretic system was set up as shown in figure 4.1. A high voltage direct-current power supply (CZE 1000R, Spellman High Voltage Electronics, Hauppauge, NY) was used and was capable of delivering 0-30 kV. The separations were performed on a 50 μm id fused-silica capillary (Polymicro Technology, Phoenix, AZ, USA) suspended between two electrodes that were immersed in reservoirs filled with the BGE. The length of the fused-silica capillary was 65 cm (50 cm effective). The capillary and the inlet electrode reservoir were enclosed in a Plexiglass box (made of polymethyl methacrylate) with an interlock safety system. The outlet electrode reservoir was part of the fluorescence detector (ZETALIF, Picometrics, Toulouse, France).

Figure 4.1 Schematic diagram of laboratory-built MEKC-LIF system.[7]

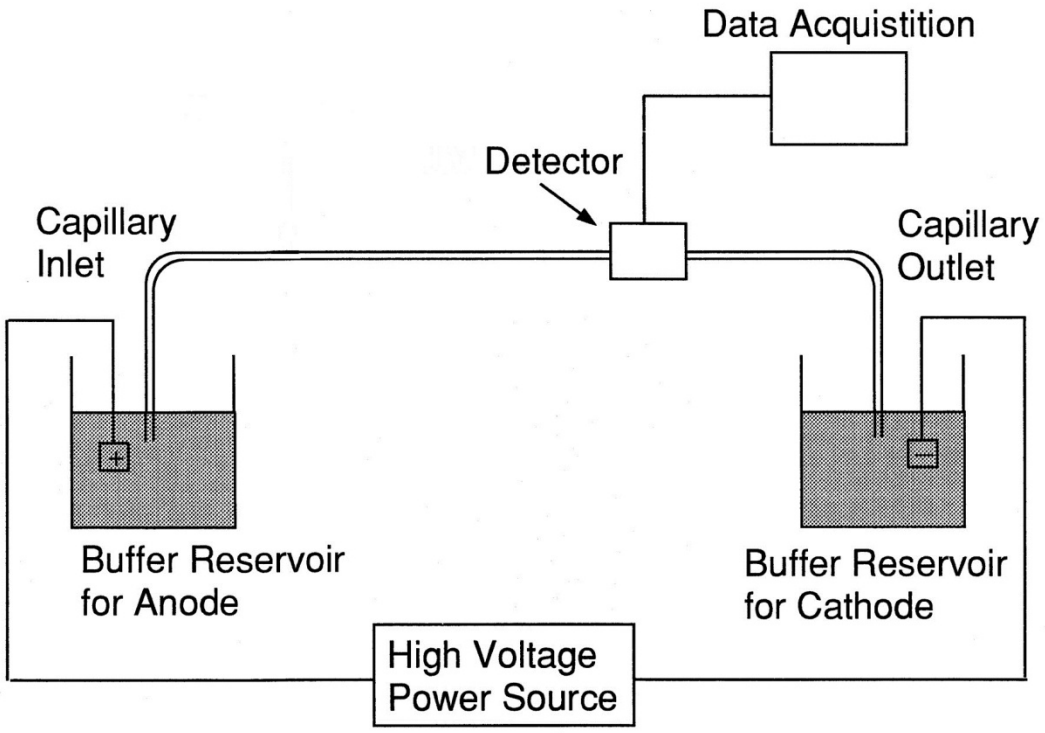

Excitation was performed by a diode pumped solid-state laser (CrystaLaser, Reno, NV, USA) at an excitation wavelength of 442 nm. An on-column optical cell was made by removing the polyimide coating from a short section of the fused-silica capillary. The incident laser beam was aligned to its optimum position by adjusting the position of collecting optics between the capillary and the detector. A 1 μmol/L solution of fluorescein in ultrapure water was used for alignment until maximum absorbance was observed.

Hydrodynamic injections were performed by a laboratory-built pressure injection system. An argon gas tank (Lindweld, Lincoln, NE, USA) was set up with a pressure regulator (Fisher Scientific, Pittsburgh, PA, USA). A union-T was used to connect the regulator to a three-way valve that controlled the flow of pressure to the sample vial. The three-way valve was connected to a solenoid valve with an electronic timer. The capillary and the electrode were inserted through gas-tight septa on sample or buffer vials. To make a hydrodynamic injection, the sample vial was pressurized (at a pressure set by the pressure regulator) for the predetermined amount of time.

Each day, before the analyses were performed, the capillary was sequentially flushed at 20 psi with MeOH for 5 min, ultrapure water for 5 min, 1 mol/L hydrochloric acid (HCl) for 10 min, ultrapure water for 5 min, 1 mol/L sodium

hydroxide (NaOH) for 20 min, ultrapure water for 5 min, and finally with the BGE for 10 min. Between analyses, the capillary was flushed at 20 psi with 1 mol/L NaOH for 2.5 min, with ultrapure water for 1.5 min and then with the BGE for 2.5 min. All the solutions injected onto the capillary were sterilized using a disposable 0.22 μm polyethersulfone (PES) membrane syringe filter (Millipore, Co. Cork, Ireland). Each day, an Ohm's law test was performed to establish that there was a linear relationship between the applied electric field and the current within the capillary. Electropherograms were acquired on Chrom&Spec version 1.5 software (Ampersand International,Inc., Beachwood, OH, USA).

4.2.3 Method Development

As described in Chapter 3, the BGE consisted of 22.5 mmol/L LTB (pH 9.2) and 20 mmol/L LDS and the capillary temperature was reduced to 15° C to optimize the separation. However, with the laboratory-built MEKC-LIF system used for these studies it is difficult to reproducibly cool the capillary to this temperature. Therefore, experiments to optimize the separation buffer were carried out by varying the concentration of the surfactant and adding MeOH to increase the viscosity of the BGE.

Experiments to optimize the separation buffer were carried out using standards of gamma-amino butyric acid (GABA), glutamate (Glu), dopamine (DA), and carbamathione. Figure 4.2 displays the effect of increasing the surfactant concentration. Increasing the concentration of LDS resulted in shorter analysis times and improved peak shapes, but it also led to loss of resolution. Figure 4.3 shows the effect of adding MeOH to the BGE. Addition of increasing amounts of MeOH resulted in improved resolution and peak shapes, but also in longer analysis times. Figure 4.3 shows that 10% MeOH produced improved resolution without greatly lengthening the analysis time. Once this observation was made, it was important to study the effect of varying the concentration of the surfactant in the presence of 10% MeOH. Figure 4.4 displays the results of this experiment. The run buffer ultimately chosen for the separation consisted of 22.5 mmol/L LTB (pH 9.2), 25 mmol/L LDS and 10% MeOH because it represented a good compromise between run time and peak resolution with good peak shape. The resolution data with this buffer indicated good separation between standards ($R >$ 1.5) for all pairs tested.

Figure 4.2 Effect of varying the concentration of the surfactant on separation.

Effect of varying LDS concentration on separation of NDA-derivatized carbamathione (1), GABA (2), IS (3), Glu (4), and DA (5). IS was 2-ABA. Electropherograms were obtained using 22.5 mmol/L LTB and varying concentrations of LDS under a 15 kV voltage. NDA-derivatized compounds were detected using LIF detection (ex. 442 nm).

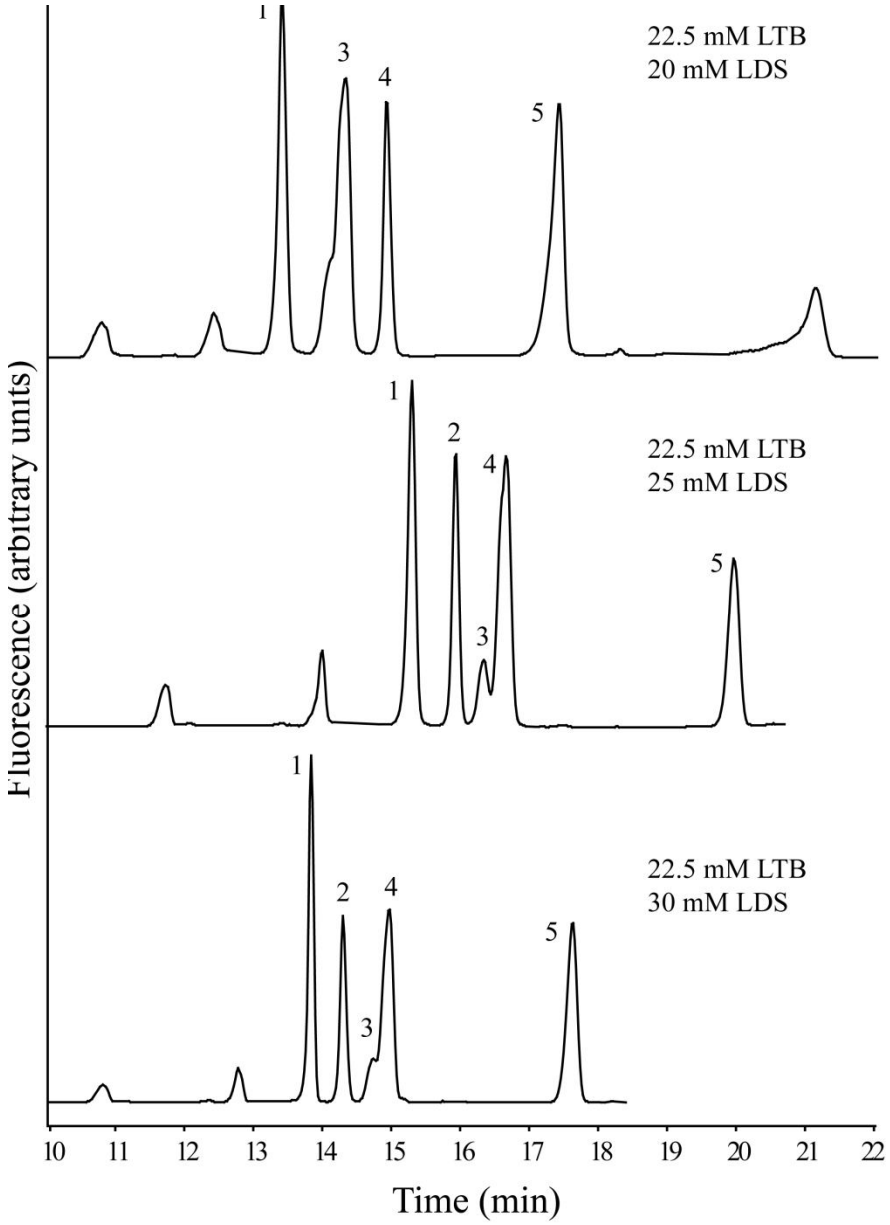

Figure 4.3 Effect of adding MEOH to BGE on separation.

Effect of adding varying amounts of MeOH on separation of NDA-derivatized carbamathione (1), GABA (2), IS (3), Glu (4), and DA (5). IS was 2-ABA. Electropherograms were obtained using 22.5 mmol/L LTB and 20 mmol/L LDS with varying methanol compositions under a 15 kV voltage. NDA-derivatized compounds were detected using LIF detection (ex. 442 nm).

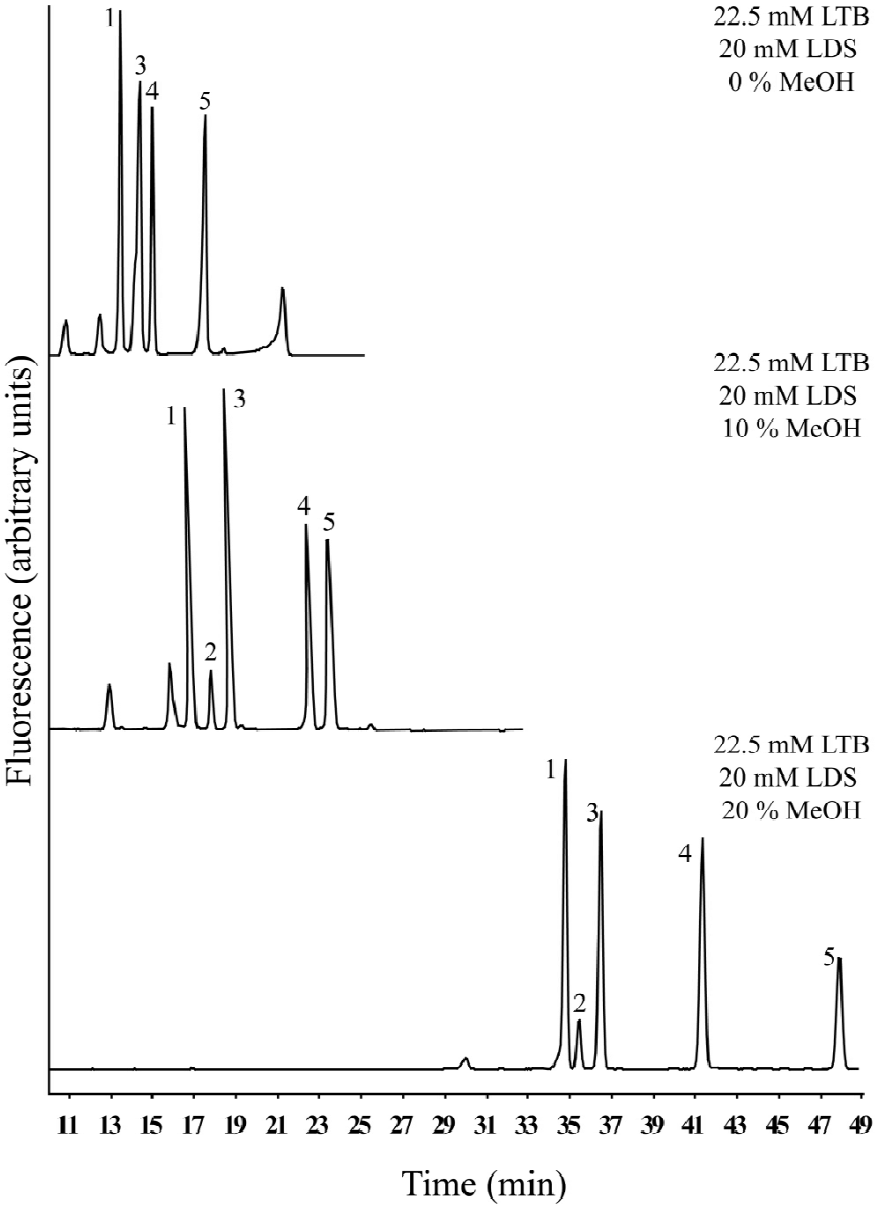

Figure 4.4 Effect of varying the concentration of the surfactant on separation.

Effect of varying LDS concentration on separation of NDA-derivatized carbamathione (1), GABA (2), IS (3), Glu (4), and DA (5). IS was 2-ABA. Electropherograms were obtained using 22.5 mmol/L LTB and 10 % MeOH with varying concentrations of LDS under a 15 kV voltage. NDA-derivatized compounds were detected using LIF detection (ex. 442 nm).

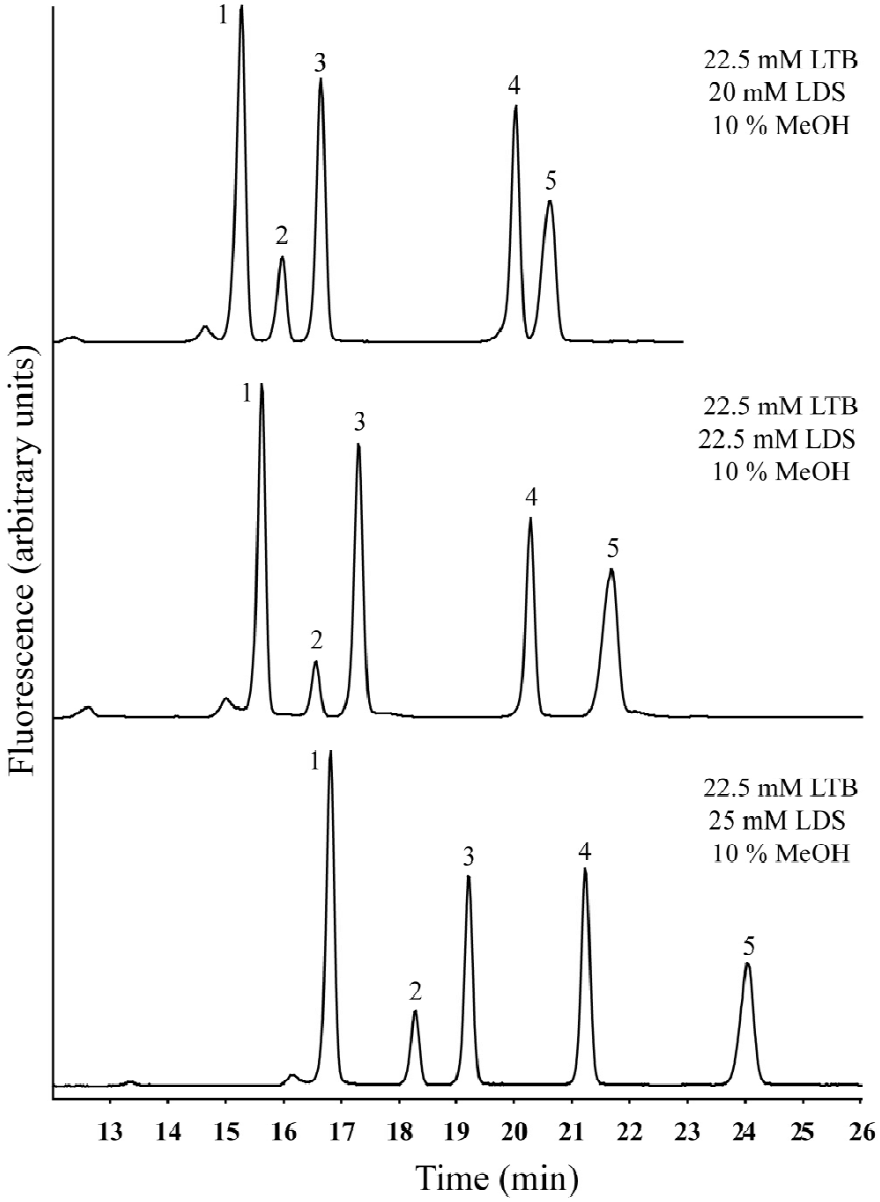

As described in Chapter 3 (3.2.2 MEKC-LIF Instrumentation), samples were introduced onto the capillary by hydrodynamic injections for 15 s at 0.7 psi. However, the pressure regulator used in the laboratory-built pressure injection system could not accurately reproduce pressures below 5 psi. The hydrodynamic injection described in Chapter 2 represented an injection volume of 17.09 μL and a sample plug that was 1.34% of capillary length. A hydrodynamic injection at 5 psi with varying times of injection was investigated. A 2 s injection at 5 psi was chosen as it was a good compromise between separation and sensitivity. This hydrodynamic injection represented an injection volume of 16.27 μL and a sample plug that was 1.27% of capillary length.

In Chapter 3 (3.2.2 MEKC-LIF Instrumentation) a two-step separation voltage (10 kV for 10 min and 20 kV for 8 min) was described. Since the change in voltage at 10 min would have to be performed manually on a laboratory-built MEKC-LIF system, the separation voltage was re-evaluated. Voltages between 10-30 kV were tested and the best separation was obtained at 15 kV.

Peak identification in microdialysis samples were carried out by comparing migration times to those present in standards. During this study it was observed that the IS (2-ABA) co-migrated with an endogenous peak. A new IS (AAP) was used since it did not co-migrate with any endogenous peak or interfere with any of

the standards. Figure 4.5 displays electropherograms obtained for standards, microdialysis samples and microdialysis sample spiked with standards. The observed height of the peaks of interest increased when exogenous Glu, GABA, DA, and carbamathione were added to the microdialysis samples. No additional peaks appeared when Glu, GABA, DA, and carbamathione were added. Background peaks associated with NDA derivatization did not interfere with any of the analytes of interest.

In summary, separations were carried out using BGE consisting of 22.5 mmol/L LTB and 25 mmol/L LDS (10% MeOH) at a running voltage of 15 kV in 65 x 50 μm id fused-silica capillary (50 cm effective). Separations were performed at room temperature (25° C). Figure 4.5 shows a typical electropherogram of derivatized microdialysis sample from the rat brain.

4.2.4 Method Validation Experiments

Calibration standards for method validation contained GABA prepared in concentration range of 10^{-9}- 10^{-6} mol/L, Glu prepared in a range of 10^{-9}- 10^{-6} mol/L, DA in a range of 10^{-10}- 10^{-7} mol/L and carbamathione prepared in a range of 10^{-8}- 10^{-5} mol/L.

Figure 4.5 Typical MEKC-LIF electropherograms.

Electropherograms of standard solution (A) containing NDA-derivatized carbamathione (1), GABA (2), IS (3), Glu (4), and DA (5) compared to dialysate obtained from rat brain (C) and dialysate spiked with standards (B). IS (3) was AAP. Electropherograms were obtained using 22.5 mmol/L LTB and 25 mmol/L LDS (10% MeOH) as BGE under a 15 kV voltage. NDA-derivatized compounds were detected using LIF detection (ex. 442 nm).

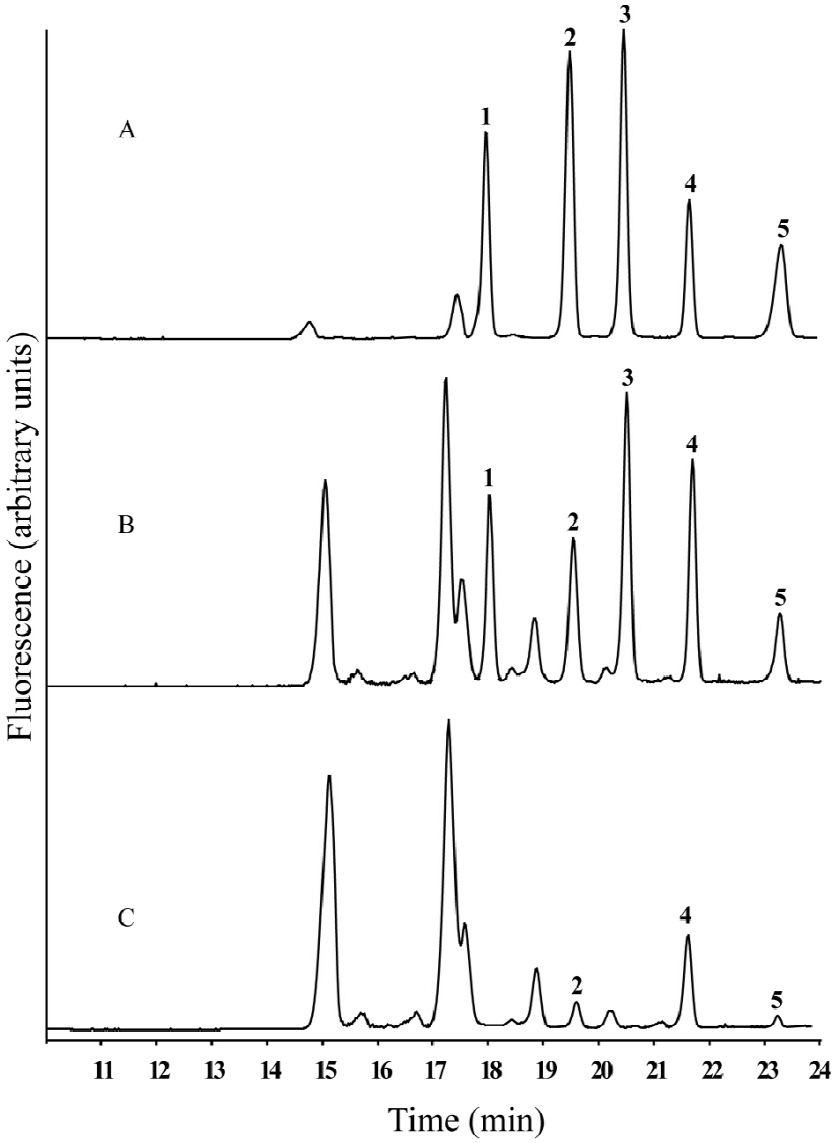

Calibration plots were plotted as the ratio of the area of compound of interest to area of the internal standard versus concentration (number of concentrations of each analyte, n = 5). The limits of detection and quantification were calculated as the analyte concentration that resulted in peaks with signal-to-noise ratio (S/N) of 3 and 10 respectively. Intra-day and inter-day reproducibility were determined using standards of Glu, GABA, DA, and carbamathione prepared in aCSF and microdialysis samples. The accuracy of the method was calculated from the analysis of standards in aCSF, microdialysis samples and microdialysis samples spiked with known concentrations of standards (in triplicate).

4.2.5 Microdialysis

4.2.5.1 Brain and Vascular Probes

Brain microdialysis probes (CMA 12 Elite) with 2 mm membranes were purchased from CMA Microdialysis (North Chelmsford, MA, USA). The fabrication of vascular probes in-house and the relative recovery of carbamathione through the microdialysis probes were as described in Chapter 3 (3.2.8.1 Brain and Vascular Probes).

4.2.5.2 Animals and Surgery

All awake experiments were carried out in accordance with Institutional Animal Care and Use Committee (IACUC) animal protocols as described in Chapter 2 (2.2.6.2 Animals and Surgery). Sterile surgeries were conducted as described in Chapter 3 (3.2.8.2 Animals and Surgery). The initial anesthesia and preparation of the incision sites are described in detail in Chapter 2 (2.2.6.2 Animals and Surgery).

An intraperitoneal (i.p.) cannula (PE-50) was implanted into the abdomen for dosing purposes. The cannula was sterilized by ethylene oxide. A small area at the back of the neck and the lower abdomen was shaved and disinfected. The animal was then transferred to a sterile field and draped. A small incision was made in the skin and then through the muscle at the mid-line of the abdomen. Five to ten cm of the cannula was inserted into the abdominal cavity so that the end of the cannula lies between the small intestine and the ventral cavity wall. The cannula was held in place by suturing it to the edge of the opening in the muscle wall. The muscle incision was sutured and the free end of the cannula was externalized through a sterile incision at the back of the neck. The abdominal skin incision was sutured and the incision at the back of the neck closed with suture or tissue glue.

Microdialysis probes were implanted into brain nucleus accumbens as described in Chapter 2 (2.2.6.2 Animals and Surgery) and into the jugular vein as described in Chapter 3 (3.2.8.2 Animals and Surgery). After the surgical procedures, the rats were administered 0.5 to 3 mL/kg of saline subcutaneously (s.c.) and placed in a rat turn with a heating pad to facilitate recovery from anesthesia.

4.2.5.3 Microdialysis Sample Collection

Microdialysis samples were collected as described in Chapter 3 (3.2.8.3 Microdialysis Sample Collection). After implantation, the brain probes and the vascular probes were perfused with aCSF and Ringer's solution, respectively, at 2 µL/min. The dead volume between the dialysis site and the fraction collector was also determined in order to accurately monitor the neurochemical changes as described in Chapter 3 (3.2.8.3 Microdialysis Sample Collection).

4.2.5.4 In Vivo Experiments

The collection of 5 min samples was initiated after a 24 h waiting period for awake experiments. For dosing purposes, the carbamathione dose (200 mg/kg) was prepared by adding a few drops of 1 mol/L sodium bicarbonate solution and bringing the volume up to 1 mL with saline solution. The disulfiram dose (200 mg/kg) was prepared as suspension in saline solution. The NBI dose (20 mg/kg)

was prepared by adding saline, a few drops of 0.1 mol/L HCl solution and sonicating the solution. After the i.p. administration of carbamathione, disulfiram, or NBI through the i.p. cannula, microdialysis samples were collected for 3 h. At the end of the experiments, the rats were sacrificed by placement in an isofluorane chamber for approximately 30 min. Rat brains were harvested in order to perform a histological confirmation of brain probe position as described in Chapter 2 (2.3.3 Histological Confirmation of Brain Probe Position).

4.3 Results and Discussion

4.3.1 Method Validation Results

Validation was carried out in accordance with instructions for good laboratory practice.[8,9] Validation parameters were determined for GABA, Glu, DA, and carbamathione in standards as well as brain microdialysis samples. The final results are shown in table 4.6. The regression coefficient of the calibration obtained with standard solutions and microdialysis samples showed good linearity and led to the routine use of only three points of the calibration curve. A complete calibration curve was obtained every time the capillary was changed. Limits of detection and quantification were lower than concentrations measured in microdialysis samples from the brain.

Table 4.6 Quantitative parameters for the analysis GABA, Glu, DA, and carbamathione in aCSF and microdialysis samples.

aCSF	GABA	Glu	DA	Carb
Calibration Range (mol/L)	10^{-9}-10^{-6}	10^{-9}-10^{-6}	10^{-10}-10^{-7}	10^{-8}-10^{-5}
Regression Coefficient of Calibration (r^2)	0.9999	0.9988	0.9902	0.9992
Intra-day repeatability (%RSD)[a]	9.6	3.9	10.4	7.7
Inter-day repeatability (%RSD)[b]	5.8	8.1	9.5	9.1
Accuracy (%)[c]	4.2-2.1	6.3-3.4	8.0-5.9	4.1-2.6
Limits of Detection (mol/L)	6.0×10^{-9}	1.0×10^{-8}	5.0×10^{-9}	1.0×10^{-8}
Limits of Quantification (mol/L)	3.0×10^{-8}	3.0×10^{-7}	2.5×10^{-8}	5.0×10^{-7}

Microdialysis Samples	GABA	Glu	DA	Carb
Calibration Range (mol/L)[d]	10^{-9}-10^{-6}	10^{-9}-10^{-6}	10^{-10}-10^{-7}	10^{-8}-10^{-5}
Regression Coefficient of Calibration (r^2)	0.9983	0.9909	0.9800	0.9976
Intra-day repeatability (%RSD)[a]	10.2	9.8	12.3	9.2
Inter-day repeatability (%RSD)[b]	8.4	8.1	9.9	9.7
Accuracy (%)[c,d]	10.3-6.9	9.5-6.4	10.0-6.1	8.5-5.1

a. Five replicates

b. Five days, three replicates each

c. Three replicates, tested concentration of 10^{-7} mol/L for GABA, Glu, DA and carbamathione

d. Spiked microdialysis samples

4.3.2 *In Vivo* Studies

In this study, all the agents were administered i.p. This was done in order to be consistent since disulfiram is extremely insoluble in water and saline solution and has to be administered as a suspension. Linear regression analysis was performed to test the existence of a statistically significant linearity for the calibration curves. Changes in concentration of Glu, GABA, and DA were expressed as percent of the basal concentration, measured before drug or vehicle administration. Data are given as mean ± standard error of mean (SEM). Comparison between treated and control rats were achieved on percentage transformed data using analysis of variance (ANOVA) and post-hoc comparison by Tukey-Kramer test. The level of significance was set at $P < 0.05$ for all comparisons.

4.3.2.1 Pharmacokinetic Studies

4.3.2.1.1 Administration of Disulfiram (200 mg/kg i.p.)

Figure 4.7 shows concentration in brain nucleus accumbens microdialysis samples and plasma microdialysis samples versus time profile for carbamathione after the i.p. administration of disulfiram (200 mg/kg, n = 3). Carbamathione concentrations in the plasma and the brain increased to a peak at 90 and 95 min after administration, respectively and then proceeded to fall.

Figure 4.7 Carbamathione concentration versus time profile after a 200 mg/kg dose of disulfiram.

Concentration of carbamathione in rat brain nucleus accumbens following disulfiram administration (200 mg/kg i.p., n = 3). Microdialysis samples were collected every 5 min. Data shown as concentration (mean ± SEM).

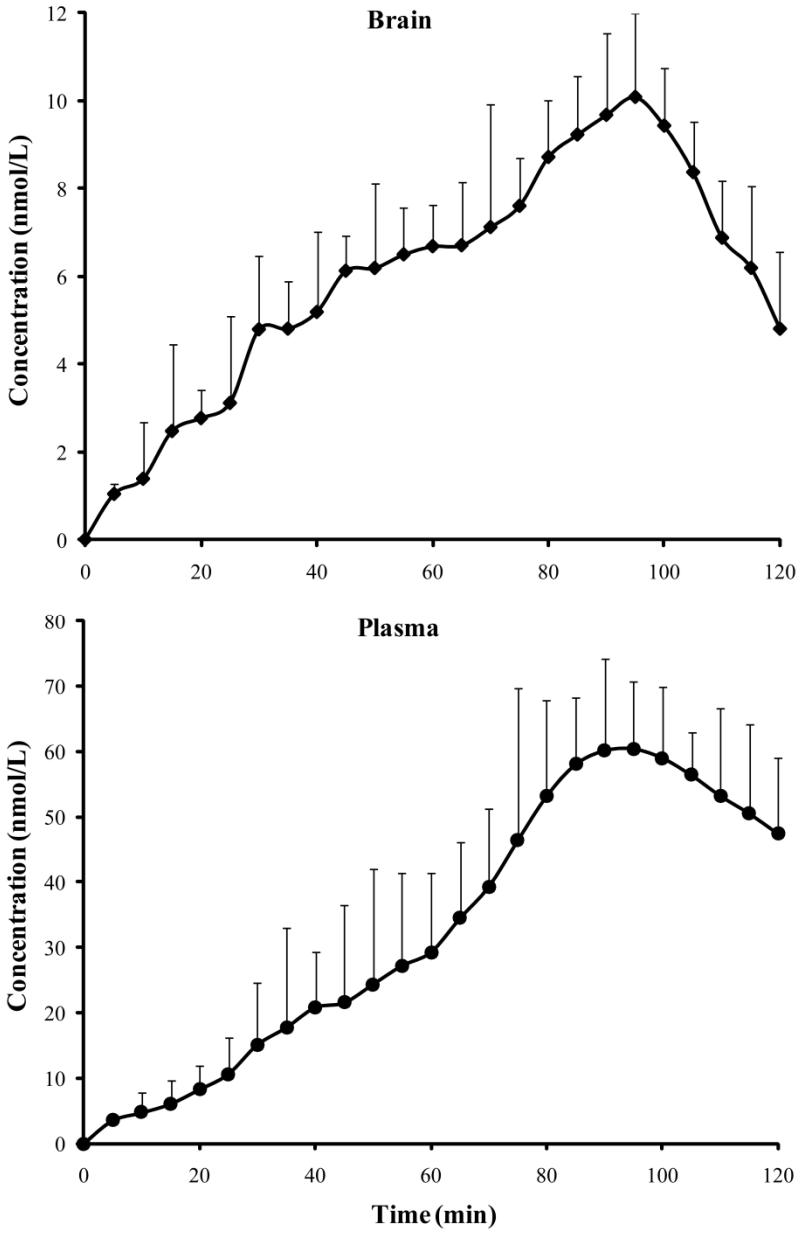

As expected, there was a slow increase in carbamathione concentrations since disulfiram was administered i.p. In addition, the clearance of carbamathione could not be monitored completely due to this long distribution phase. The C_{max} for carbamathione concentrations after disulfiram administration in the plasma and the brain nucleus accumbens were 61.1 ± 10.2 nmol/L and 10.0 ± 1.9 nmol/L respectively. In comparison, the C_{max} for carbamathione concentrations after the intravenous (i.v.) administration of the lowest dose of carbamathione (20 mg/kg i.v.) in the plasma and the brain nucleus accumbens were 25.2 ± 8.3 μmol/L and 3.72 ± 0.54 μmol/L respectively (see table 3.21). Interestingly, the ratio of the C_{max} for carbamathione in the brain to the C_{max} for carbamathione in the plasma remained very similar regardless of dose or route of administration. The area under the dialysate concentration versus time profile (AUC) for carbamathione in the brain nucleus accumbens and plasma after the administration of disulfiram (200 mg/kg i.p.) were 729 ± 174 nmol/L min and 4.05 ± 1.30 μmol/L min. A 200 mg/kg dose of carbamathione and a 200 mg/kg dose of disulfiram are approximately equimolar. Therefore, a percent conversion of disulfiram to carbamathione can be estimated for the administration of disulfiram based on carbamathione concentrations in the plasma and brain. It was determined to be less than 1% of disulfiram was ultimately converted to carbamathione.

4.3.2.1.2 Administration of NBI (20 mg/kg i.p.) and Disulfiram (200 mg/kg i.p.)

NBI (20 mg/kg i.p.) was administered 30 min prior to administration of saline vehicle or disulfiram (200 mg/kg i.p.) and 30 min after administration in order to ensure maximum inhibition of cytochrome P450. This dosing scheme has been used in previous studies into the metabolites of disulfiram.[10] Carbamathione concentrations in the microdialysis samples from the brain nucleus accumbens were determined to be below the limits of detection for the MEKC-LIF system. Liquid chromatography- tandem mass spectrometric (LC-MS/MS) analysis of microdialysis samples from the plasma indicated that the concentrations of carbamathione detected were less than 1 nmol/L in comparison with a C_{max} of 61.1 ± 10.2 nmol/L after disulfiram administration alone. These results suggest that NBI was successful in inhibiting the formation of carbamathione from disulfiram by inhibiting cytochrome P450. Cytochrome P450 enzymes appear to be essential for disulfiram to be ultimately converted to carbamathione.

4.3.2.1.3 Administration of NBI (20 mg/kg i.p.) and Carbamathione (200 mg/kg i.p.)

The effect of dosing NBI (20 mg/kg) in combination with carbamathione (200 mg/kg) was also evaluated. Figure 4.8 shows concentration in brain nucleus accumbens microdialysis samples and plasma microdialysis samples versus time profile for carbamathione after the i.p. administration of carbamathione (200 mg/kg, $n = 3$) following NBI administration. Carbamathione concentrations in the plasma and the brain nucleus accumbens increased to a peak at 15 and 25 min after administration, respectively and then proceeded to fall exponentially. The PK parameters of carbamathione in brain nucleus accumbens are given in table 4.9. It must be pointed out that the PK of the clearance of carbamathione from the plasma and brain nucleus accumbens was similar to the values previously obtained after the i.v. administration of carbamathione alone (see tables 3.13 and 3.21). For instance, the AUC for carbamathione concentrations in the brain nucleus accumbens and plasma after carbamathione administration (200 mg/kg i.v.) were 308 ± 81 μmol/L min and 2310 ± 628 μmol/L min, respectively (table 3.13). In comparison, the AUC for carbamathione concentrations in the brain nucleus accumbens and plasma after dosing a combination of NBI (20 mg/kg i.p.) and carbamathione (200 mg/kg i.p.) were 244 ± 84 μmol/L min and 1990 ± 501 μmol/L min, respectively. This indicated that NBI did not interfere with the PK of carbamathione.

Figure 4.8 Carbamathione concentration versus time profile after a 200 mg/kg dose of carbamathione.

Concentration of carbamathione in rat brain nucleus accumbens following carbamathione administration (200 mg/kg i.p., n = 3). Microdialysis samples were collected every 5 min. Data shown as concentration (mean ± SEM).

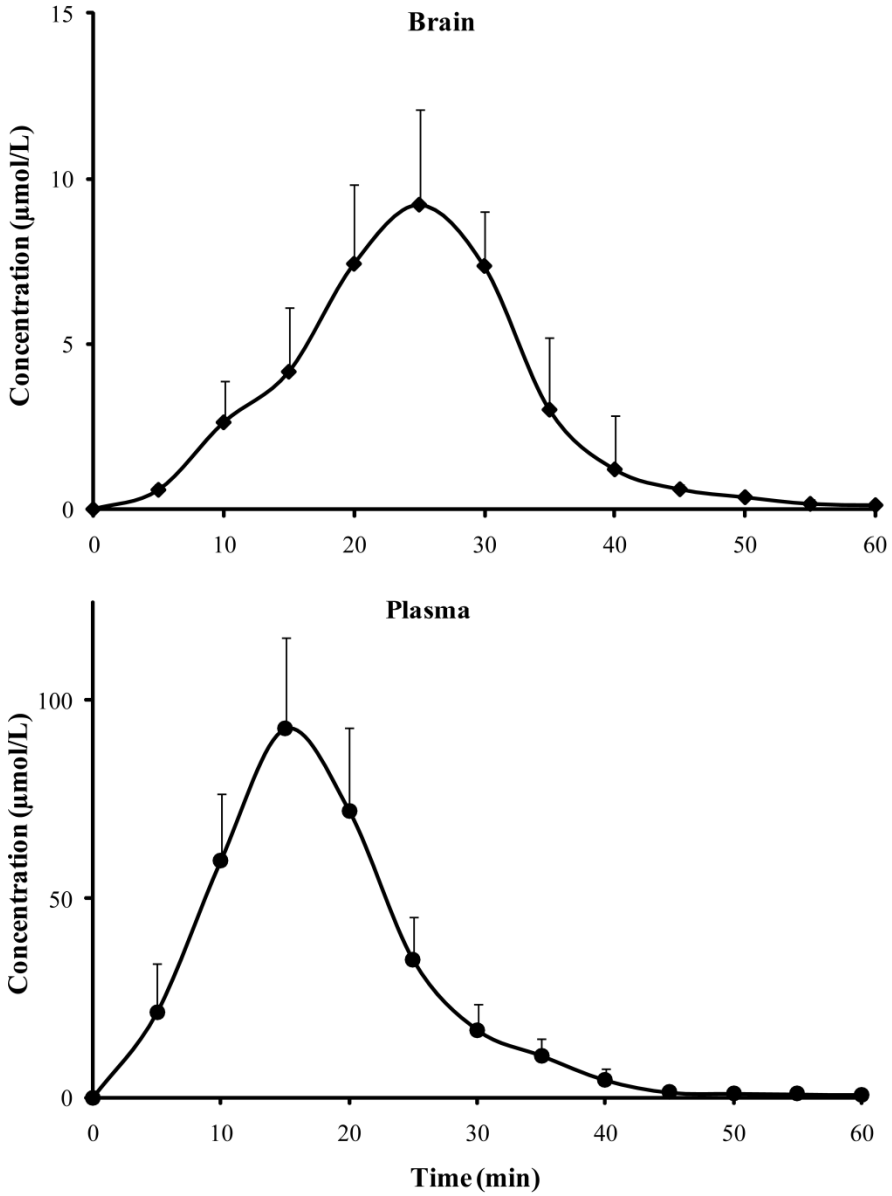

Table 4.9 Pharmacokinetic paramaters of carbamathione with 5 min sampling interval.

Pharmacokinetic parameters of carbamathione in rat brain nucleus accumbens following carbamathione administration (200 mg/kg i.p., n = 3) and 5 min sample collection. Data expressed as mean ± SEM.

200 mg/kg	C_{max}	t_{max}	$t_{1/2}$	K_{elim}	AUC
Brain	9.21 ± 1.87	22.5± 2.5	4.38 ± 0.52	0.14 ± 0.03	244 ± 84
Plasma	93.8 ± 16.5	12.5± 2.5	4.94 ± 1.05	0.15 ± 0.03	1990 ± 501

C_{max} = maximum concentration (µmol/L)

t_{max} = time to maximum concentration (min)

$t_{1/2}$ = elimination half-life (min)

K_{elim} = elimination constant (1/min)

AUC = area under the dialysate concentration versus time profile (µmol/L min)

4.3.2.2 Pharmacodynamic Studies

4.3.2.2.1 Administration of Disulfiram (200 mg/kg i.p.)

The effect of disulfiram administration (200 mg/kg i.p.) on basal levels of GABA, Glu, and DA in the rat brain nucleus accumbens is shown in figure 4.10. Microdialysis samples from the brain nucleus accumbens and plasma were analyzed utilizing the laboratory-built MEKC-LIF system described in this chapter and the LC-MS/MS described in Chapter 3 (3.2.5 LC-MS/MS Instrumentation).

Basal Glu concentrations were significantly increased by 29% ($P < 0.05$ Tukey-Kramer test) at the ninth fraction 5 (i.e. + 45 min) after disulfiram administration. The increase in Glu concentration from basal levels continued over the next 30 min after carbamathione administration with a peak increase of 35% ($P < 0.05$ Tukey-Kramer test) at the fifteenth fraction (i.e. + 75 min). However, during the next 10 min Glu concentration was reduced by 12% ($P < 0.05$ Tukey-Kramer test) and continued to remain reduced over the next 30 min. The lowest concentration of Glu was obtained in the twenty-third fraction (i.e. + 115 min) where basal Glu concentrations were significantly reduced by 20 % ($P < 0.05$ Tukey-Kramer test).

Figure 4.10 GABA, Glu, and DA in rat brain nucleus accumbens after a 200 mg/kg dose of disulfiram.

White squares represent experiments (n = 3) and black squares represent controls (n = 3). 0 min indicates time point of disulfiram administration (200 mg/kg i.p.). * represents $P < 0.05$ versus control (ANOVA, Tukey-Kramer test).

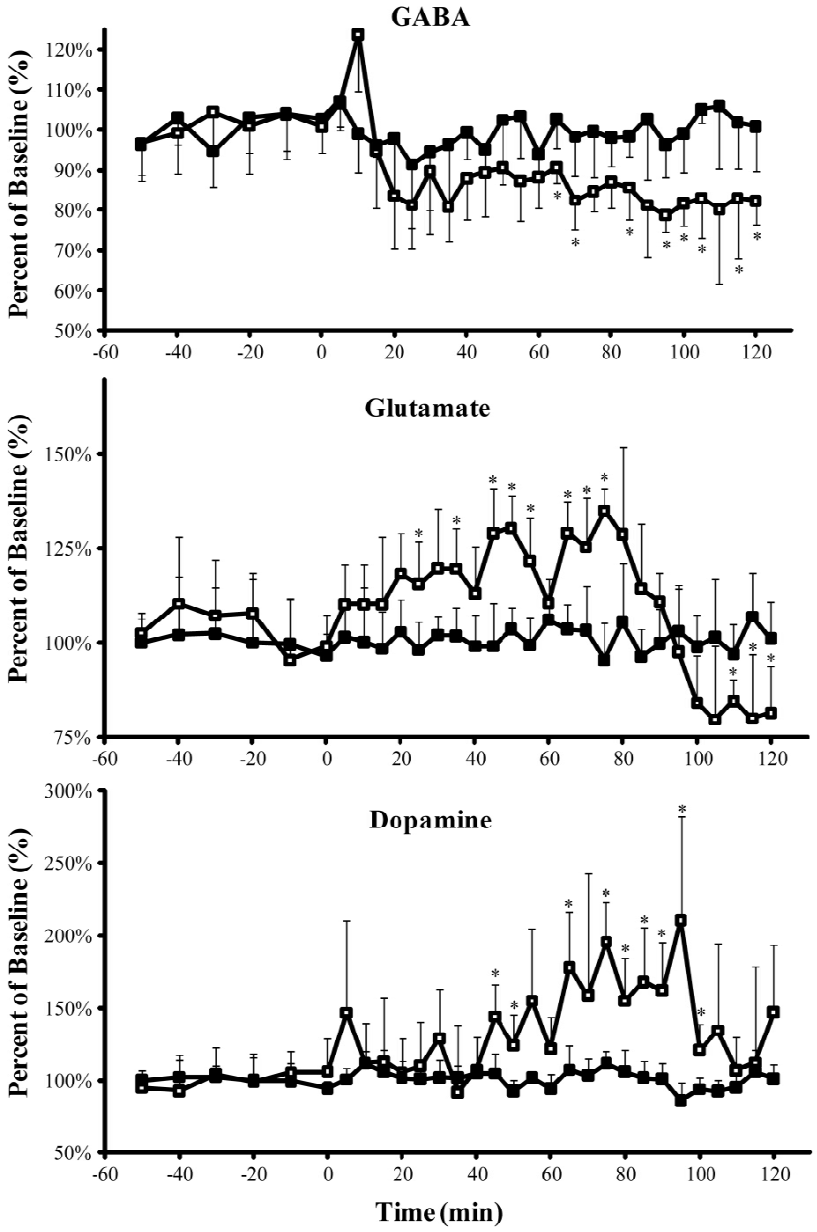

Basal GABA concentrations were significantly increased by 23% ($P < 0.05$ Tukey-Kramer test) in the first fraction following disulfiram administration. However, basal GABA levels decreased in the next 10 min and continued to remain reduced over the next 2 h following disulfiram administration. The lowest concentration of GABA was obtained in the nineteenth fraction (i.e. + 95 min) where basal GABA concentrations were significantly reduced by 22 % ($P < 0.05$ Tukey-Kramer test).

Basal DA concentrations were significantly increased by 45% ($P < 0.05$ Tukey-Kramer test) in the ninth fraction (i.e. + 45 min) following disulfiram administration, and continued to remain increased over the next 75 min. The highest concentration was obtained in the nineteenth fraction (i.e. + 95 min) where basal DA concentrations were significantly increased by 111 % ($P < 0.05$ Tukey-Kramer test).

After disulfiram administration, the neurotransmitters concentrations did not appear to change to the same extent as the changes in neurotransmitter concentration when the lowest dose (20 mg/kg) of carbamathione was administered. This may be because only a small percentage of disulfiram was metabolized to carbamathione (<1%).

4.3.2.2.2 Administration of NBI (20 mg/kg i.p.) and Disulfiram (200 mg/kg i.p.)

The comparison between the effect of NBI (20 mg/kg i.p.) alone and the effect of NBI (20 mg/kg i.p.) in combination with disulfiram administration (200 mg/kg i.p.) on basal levels of GABA, Glu, and DA in the rat brain nucleus accumbens is shown in figure 4.11. NBI was administered 30 min prior to administration of saline vehicle or disulfiram and 30 min after administration in order to ensure maximum inhibition of cytochrome P450. This dosing scheme has been used in previous studies on the inhibition of disulfiram metabolism.[10] Microdialysis samples from the brain nucleus accumbens and plasma were analyzed utilizing the laboratory-built MEKC-LIF system described in this chapter and the LC-MS/MS described in Chapter 3 (3.2.5 LC-MS/MS Instrumentation).

As seen in figure 4.11, there was no statistical difference in GABA, Glu, or DA levels following administration of NBI and NBI in combination with disulfiram ($P < 0.05$ Tukey-Kramer test). There was a slight increase in DA and Glu upon injection of either NBI or DA. However, this increase was not statistically significant ($P < 0.05$ Tukey-Kramer test). These results also indicate that the inhibition of cytochrome P450 blocked the changes observed in brain neurotransmitters when disulfiram was administered alone.

Figure 4.11 GABA, Glu, and DA in rat brain nucleus accumbens after after a 200 mg/kg dose of disulfiram and a 20 mg/kg dose of NBI.

White squares represent experiments with disulfiram and NBI administration (n = 3) and black squares represent controls (n = 3). 0 min indicates time point of disulfiram administration (200 mg/kg i.p.). Arrows indicate time points of NBI administration (20 mg/kg i.p.).

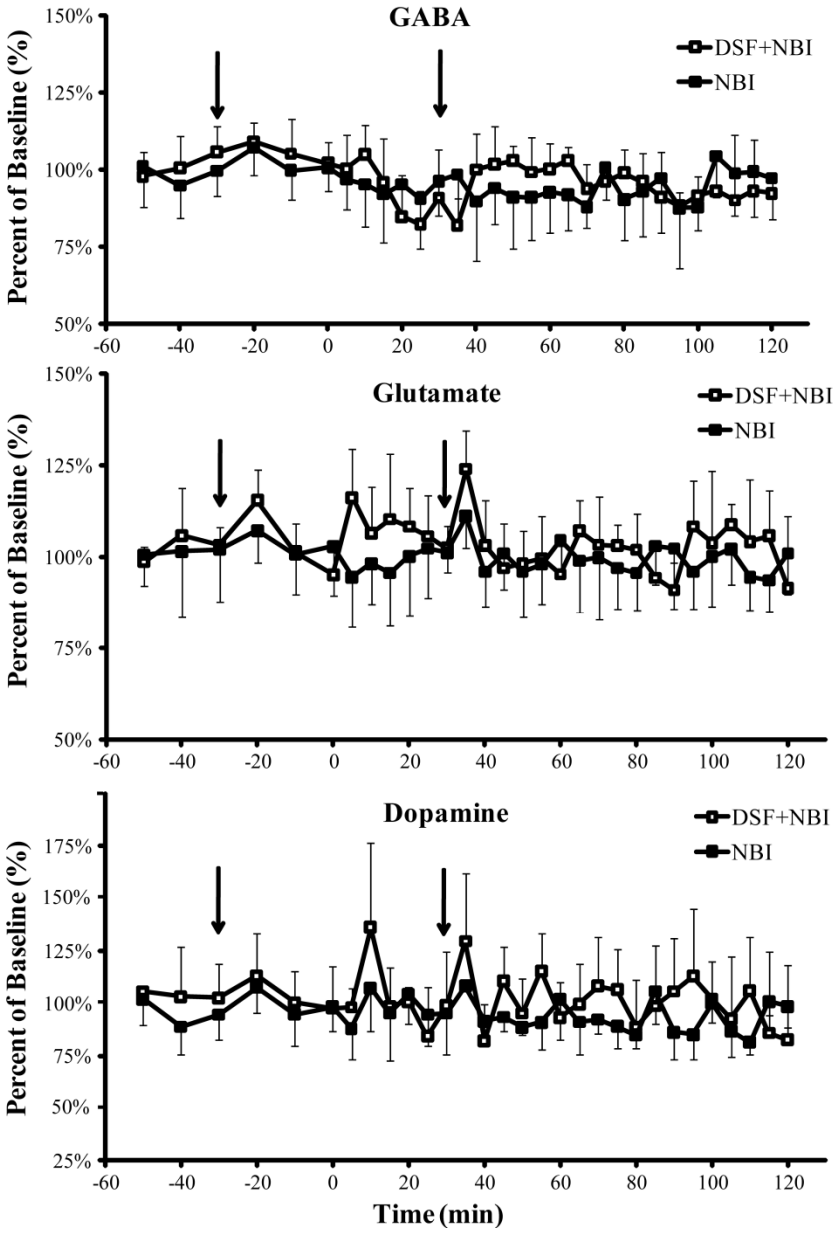

This suggests that the changes observed in neurotransmitter levels after disulfiram administration may be due to carbamathione or a metabolite formed after carbamathione formation. An important experiment that can be used to confirm this finding is the administration of carbamathione in combination with NBI.

4.3.2.2.3 Administration of NBI (20 mg/kg i.p.) and Carbamathione (200 mg/kg i.p.)

The comparison between the effect of NBI (20 mg/kg i.p.) alone and the effect of NBI (20 mg/kg i.p.) in combination with carbamathione administration (200 mg/kg i.p.) on basal levels of GABA, Glu, and DA in the rat brain nucleus accumbens is shown in figure 4.12. NBI was administered 30 min prior to administration of saline vehicle or carbamathione and 30 min after administration in order to ensure maximum inhibition of cytochrome P450. Microdialysis samples from the brain and plasma were analyzed utilizing the laboratory-built CE system described in this chapter and the LC-MS/MS described in Chapter 3 (3.2.5 LC-MS/MS Instrumentation).

There was a significant difference in the neurotransmitter levels observed between the administration of NBI alone and NBI in combination with carbamathione.

Figure 4.12 GABA, Glu, and DA in rat brain nucleus accumbens after after a 200 mg/kg dose of carbamathione and a 20 mg/kg dose of NBI.

White squares represent experiments with carbamathione administration (n = 3) and black squares represent controls (n = 3). 0 min indicates time point of carbamathione administration (200 mg/kg i.p.). Arrows indicate time points of NBI administration (20 mg/kg i.p.).

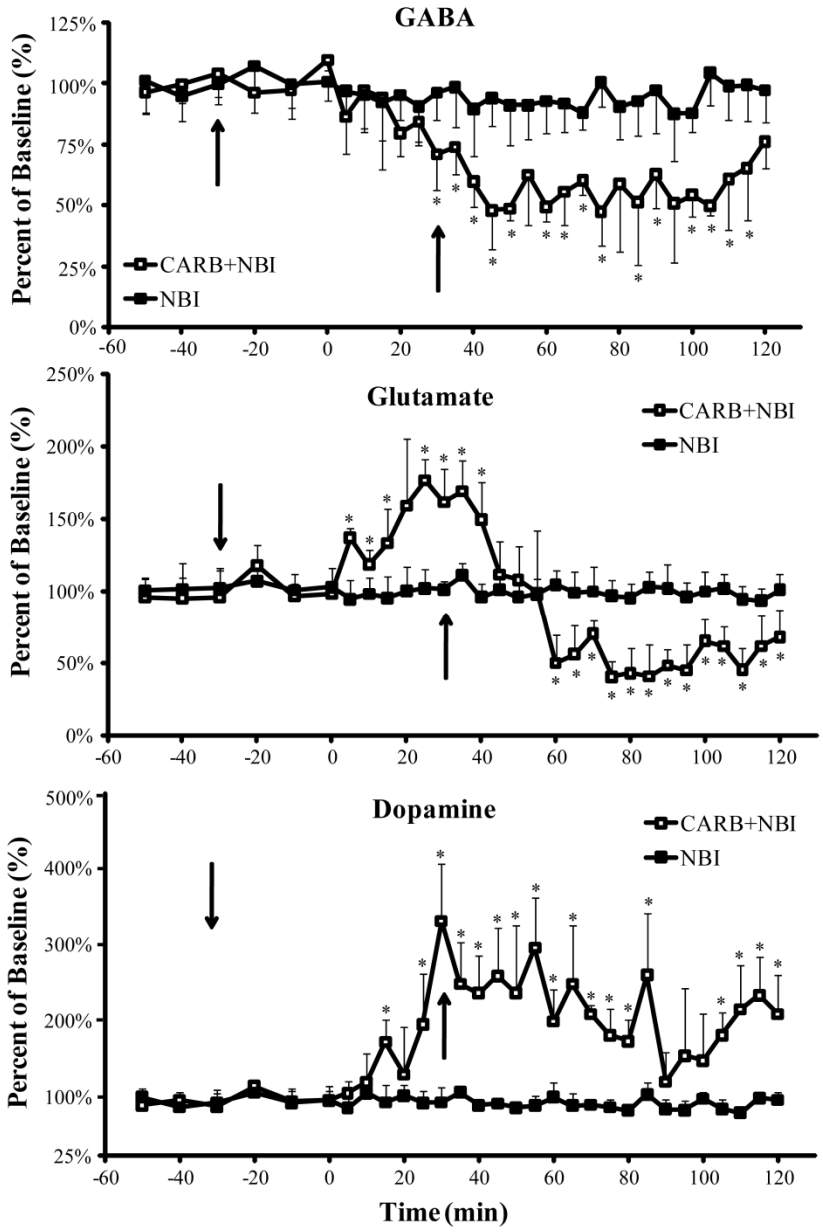

Basal Glu concentrations were significantly increased by 36% ($P < 0.05$ Tukey-Kramer test) in the first 5 min fraction after carbamathione administration. The increase in Glu concentration from basal levels continued over the next 50 min after carbamathione administration with a peak increase of 77% ($P < 0.05$ Tukey-Kramer test) at the fifth fraction (i.e. + 25 min). However, during the next 30 min Glu concentration was reduced by 50% ($P < 0.05$ Tukey-Kramer test) and continued to remain reduced over the next 65 min. The lowest concentration of Glu was obtained in the fifteenth fraction (i.e. + 75 min) where basal Glu concentrations were significantly reduced by 60% ($P < 0.05$ Tukey-Kramer test).

Basal GABA concentrations were significantly decreased by 14% ($P < 0.05$ Tukey-Kramer test) in the first fraction following carbamathione administration and continued to remain reduced over the next 2 h following carbamathione administration. The lowest concentration of GABA was obtained in the fifteenth fraction (i.e. + 75 min) where basal GABA concentrations were significantly reduced by 53% ($P < 0.05$ Tukey-Kramer test).

Basal DA concentrations were significantly increased by 21% ($P < 0.05$ Tukey-Kramer test) in the first fraction following carbamathione administration, and continued to remain increased over the next 2 h. The highest concentration of DA

was obtained in the sixth fraction (i.e. + 30 min) where basal DA concentrations were significantly increased by 232% ($P < 0.05$ Tukey-Kramer test).

Since administration of carbamathione in combination with NBI restored the changes in neurotransmitter observed with carbamathione and disulfiram alone, these changes may be attributed to carbamathione or a metabolite that is formed after carbamathione rather than to disulfiram.

4.4 Discussion

These studies demonstrated that carbamathione was produced from disulfiram since it was detected in the brain after disulfiram administration but was not detected when an inhibitor of disulfiram metabolism was administered. This suggests that disulfiram has to be bioactivated during the phase I metabolism before carbamathione is formed from by glutathione conjugation in phase II metabolism (see figure 1.4). Phase I metabolism involved cytochrome P450 enzymes and phase II metabolism involved the carbamoylation of glutathione. These studies suggest that the changes observed in GABA, Glu, and DA are due to carbamathione and not disulfiram or any of the intermediate metabolites of disulfiram.

Disulfiram has been observed to be efficacious in clinical trials investigating the treatment of cocaine and alcohol addiction.[4,5,11,12] The findings in the present study suggest that this efficacy may be attributed to carbamathione since it crosses the BBB and its administration was correlated with changes in brain neurotransmitters. Disulfiram administration also appeared to be correlated with changes in brain GABA, Glu, and DA levels, albeit to a much lesser degree than carbamathione administration. This may be because disulfiram is slowly absorbed and forms several metabolites before ultimately forming carbamathione. Thus the percentage of disulfiram that is metabolized to carbamathione is very low. When disulfiram metabolism was inhibited, there were no statistically significant changes observed in the brain GABA, Glu, and DA levels. However, when carbamathione was administered after NBI administration, statistically significant changes in the brain GABA, Glu, and DA levels were found, and these changes were similar to those observed after carbamathione and disulfiram administration. Since NBI did not appear to have an effect on carbamathione administration, cytochrome P450 enzymes do not appear to be involved in the possible formation of metabolites after carbamathione.

4.5 Conclusions

The work in this chapter showed the development of a laboratory-built MEKC-LIF method for the simultaneous detection of GABA, Glu, DA, and carbamathione in rat brain dialysate. The analytical method was validated and exhibited good linearity, accuracy, and reproducibility with nanomolar detection limits. This method was applied to the study of the effect of disulfiram on brain GABA, Glu and DA levels in the presence of a cytochrome P450 inhibitor. The administration of disulfiram (200 mg/kg, i.p.) was correlated with changes in the brain GABA, Glu, and DA systems in awake rats. Administration of an inhibitor of disulfiram metabolism, NBI (20 mg/kg, i.p.) in combination with disulfiram attenuated the changes observed in brain GABA, Glu, and DA levels. Administration of carbamathione (200 mg/kg, i.p.) in combination with NBI restored the changes observed in brain GABA, Glu, and DA levels as shown previously (figure 3.10).

4.6 References

1 Kenna, G. A., Nielsen, D. M., Mello, P., Schiesl, A. & Swift, R. M. Pharmacotherapy of dual substance abuse and dependence. *Cns Drugs* **21**, 213-237, (2007).

2 Gossop, M. & Carroll, K. M. Disulfiram, cocaine, and alcohol: two outcomes for the price of one? *Alcohol and alcoholism (Oxford, Oxfordshire)* **41**, 119-120, (2006).

3 Williams, S. H. Medications for treating alcohol dependence. *American family physician* **72**, 1775-1780, (2005).

4 de Sousa, A. & de Sousa, A. An open randomized study comparing disulfiram and acamprosate in the treatment of alcohol dependence. *Alcohol and alcoholism (Oxford, Oxfordshire)* **40**, 545-548, (2005).

5 Carroll, K. M., Fenton, L. R., Ball, S. A., Nich, C., Frankforter, T. L., Shi, J. & Rounsaville, B. J. Efficacy of disulfiram and cognitive behavior therapy in cocaine-dependent outpatients: a randomized placebo-controlled trial. *Archives of general psychiatry* **61**, 264-272, (2004).

6 Faiman, M. D., Artman, L. & Maziasz, T. Diethyldithiocarbamic-Acid Methyl-Ester Distribution, Elimination, and Ld50 in the Rat after Intraperitoneal Administration. *Alcoholism-Clinical and Experimental Research* **7**, 307-311, (1983).

7 Glynn, J. R., Jr., Belongia, B. M., Arnold, R. G., Ogden, K. L. & Baygents, J. C. Capillary Electrophoresis Measurements of Electrophoretic Mobility for Colloidal Particles of Biological Interest. *Appl Environ Microbiol* **64**, 2572-2577, (1998).

8 Karnes, H. T., Shiu, G. & Shah, V. P. Validation of bioanalytical methods. *Pharm Res* **8**, 421-426, (1991).

9 O'Shea, T. J., Weber, P. L., Bammel, B. P., Lunte, C. E., Lunte, S. M. & Smyth, M. R. Monitoring excitatory amino acid release in vivo by microdialysis with capillary electrophoresis-electrochemistry. *J Chromatogr* **608**, 189-195, (1992).

10 Hart, B. W. & Faiman, M. D. Bioactivation of S-methyl N,N-diethylthiolcarbamate to S-methyl N,N-diethylthiolcarbamate sulfoxide. Implications for the role of cytochrome P450. *Biochem Pharmacol* **46**, 2285-2290, (1993).

11 Karila, L., Gorelick, D., Weinstein, A., Noble, F., Benyamina, A., Coscas, S., Blecha, L., Lowenstein, W., Martinot, J. L., Reynaud, M. & Lepine, J. P. New treatments for cocaine dependence: a focused review. *Int J Neuropsychoph* **11**, 425-438, (2008).

12 Petrakis, I. L., Poling, J., Levinson, C., Nich, C., Carroll, K. & Rounsaville, B. Naltrexone and disulfiram in patients with alcohol

dependence and comorbid psychiatric disorders. *Biol Psychiatry* **57**, 1128-1137, (2005).

5 *IN VIVO* MICRODIALYSIS AND UPLC-MS/MS FOR MONITORING A METABOLITE OF CARBMATHIONE

5.1 Introduction

In the previous chapters, capillary electrophoresis (CE) methods were used to detect brain gamma-amino butyric acid (GABA), glutamate (Glu), dopamine (DA) and carbamathione in microdialysis samples from the brain. In addition, a liquid chromatography-tandem mass spectrometric (LC-MS/MS) method was developed for the analysis of carbamathione in microdialysis samples from the plasma. These methods were used to elucidate carbamathione pharmacokinetics (PK) and pharmacodynamics (PD). It was demonstrated that both disulfiram and carbamathione administration led to changes in these brain neurotransmitters, but carbamathione led to a much greater change. However, carbamathione was cleared from the brain after 35 min and these changes in neurotransmitters continued for 2 h after carbamathione administration. One explanation for this was the possible formation of other metabolites of carbamathione with longer half-lives. This chapter describes an ultra-performance liquid chromatography-tandem mass spectrometric (UPLC-MS/MS) method that was developed in the Williams, Stobaugh and Faiman laboratories (University of Kansas, Lawrence, KS). This method was originally developed to detect carbamathione in plasma samples that were precipitated by perchloric acid. During one of the studies

conducted, an unknown metabolite later identified as the *N*-acetyl cysteine (NAC) conjugate of carbamathione was discovered in the plasma samples. This UPLC-MS/MS method was used to detect carbamathione and the NAC conjugate of carbamathione in microdialysis samples.

5.1.1 Specific Aims of Research

Figure 5.1 displays the structures of carbamathione and a NAC conjugate of carbamathione (*S*- methyl *N, N*-diethylthiocarbamate-*N*-acetyl cysteine [DETC-NAC]). The goal of this research was to apply the previously developed UPLC-MS/MS method to determine the concentration of carbamathione and DETC-NAC in the nucleus accumbens and prefrontal cortex of a rat brain after the administration of disulfiram. Microdialysis samples from the plasma were also analyzed for these compounds. The purpose of this study was to determine whether DETC-NAC was detected in the brain after administration of disulfiram and to quantify the concentrations detected. Since this was an exploratory study, samples collection times were extended to 15 min and samples were collected for over 5 h.

Figure 5.1 Structures of carbamathione, DETC-NAC and diisopropyl carbamathione.

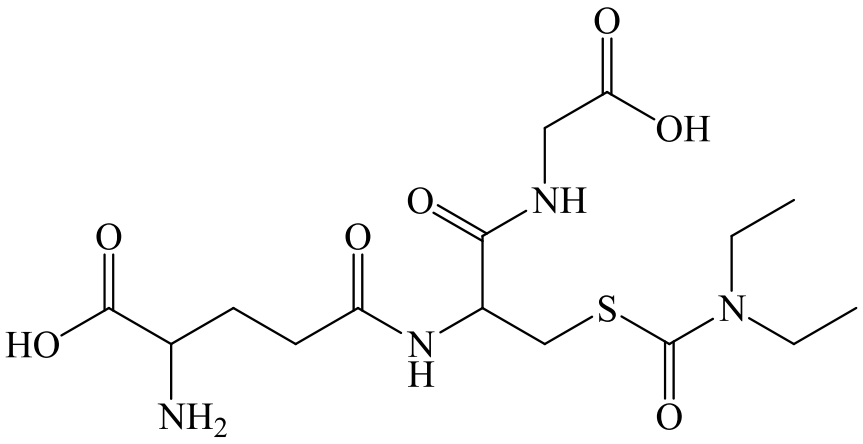

Carbamathione
M.W. 406 g/mol

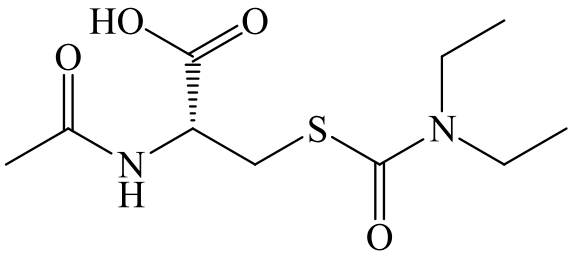

DETC-NAC
M.W. 262 g/mol

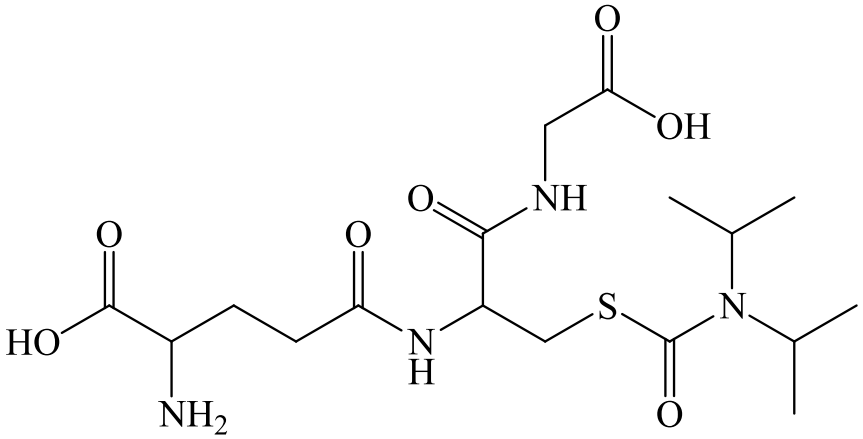

Diisopropyl carbamathione
M.W. 432 g/mol

5.2 Experimental

5.2.1 Chemicals and Reagents

The chemicals and manufacturers were stated in Chapter 2, 3 and 4 (2.2.1, 3.2.1 & 4.2.1 Chemicals and Reagents). Ringer's solution was prepared as described in Chapter 3 (3.2.1 Chemicals and Reagents). Standard solutions of carbamathione were prepared as described in Chapter 3 (3.2.1 Chemicals and Reagents). DETC-NAC and the internal standard (IS), diisopropyl carbamathione, were synthesized in the Stobaugh laboratory. The structure of the diisopropyl carbamathione is shown in figure 5.1. A stock solution of 1 mmol/L DETC-NAC (molecular weight [M.W.] 262 g/mol) and 1 mmol/L diisopropyl carbamathione were provided by the Stobaugh laboratory.

5.2.2 UPLC-MS/MS Instrumentation

The chromatographic separations were performed on an Phenomenex Kinetex C-18 (50 mm x 2.1 mm i.d., 1.7 m, 100 Á) analytical column (Phenomenex, Torrance, CA, USA) at a flow rate of 0.4 mL/min with analysis time of 10 min. Solvents were delivered by a Waters Acquity UPLC system (Waters Corporation, Milford, MA, USA). Solvent A consisted of ultrapure water, methanol (MeOH), and formic acid (99:1:0.1, v/v/v). Solvent B consisted of MeOH, water and formic acid (99:1:0.1, v/v/v). The chromatograph consisted of a 6.5 min gradient

followed by a 1.5 min re-equilibration. The gradient used is given in table 5.2. A built-in diverter valve on the mass spectrometer was used to switch between waste and the mass spectrometer after 2 min. Tandem mass spectra were acquired on a Quattro Ultima "triple" quadrupole instrument (Micromass Ltd., Manchester, UK.). The probe capillary was optimized at 2.8 kV, and the desolvation and source temperatures were set to 250° C and 100° C, respectively. The cone gas flow rate was optimized at 49 L/h, and the desolvation and nebulizer gas flow rate was adjusted for maximum signal of analyte. Argon was used for collision-induced dissociation and the cell vacuum was set at 2.23×10^{-3} mbar. Quadrupoles 1 and 3 were tuned to a resolution of 0.8 atomic mass units full width at half height. Selected reaction monitoring (SRM) parameters including precursor ions, product ions and collision energy are given in table 5.3. Mass spectrometric analysis was conducted in positive ion mode. Data processing was performed on MassLynx version 4.1 software.

5.2.3 UPLC-MS/MS Method Development

Diisopropyl carbamathione (IS) was synthesized since it was a non-endogenous glutathione adduct that was very similar in structure to carbamathione. Quantification of carbamathione and DETC-NAC was based on the ratio of the integrations of the SRM traces to the integration of the SRM trace from the IS.

Table 5.2 UPLC-MS/MS Gradient.

Time (min)	Solvent A	Solvent B
0.20	95.0%	5.0%
4.50	47.7%	52.3%
4.51	20.0%	80.0%
6.50	20.0%	80.0%
6.51	95.0%	5.0%
8.00	95.0%	5.0%

Table 5.3 SRM parameters for the UPLC-MS/MS method.

Analyte	Precursor ion (m/z)	Product ion (m/z)	Cone voltage (V)	Collision energy (V)
DETC-NAC	263.0	100.0	25	15
Carbamathione	407.1	100.1	35	30
IS	435.0	128.0	35	30

The post-column infusion method was used to provide a qualitative assessment of matrix effects and to identify chromatographic regions most likely to experience matrix effects. Briefly, an infusion pump was used to deliver a constant amount of carbamathione and DETC-NAC into the liquid chromatography (LC) stream entering the ion source of the mass spectrometer. The mass spectrometer was run in SRM mode to follow the infused analytes. Blank dialysate was then injected on the LC column. Any endogenous compound that eluted from the column would cause a variation in electrospray ionization (ESI) response of carbamathione or DETC-NAC. The post-column infusion of 1 μmol/L carbamathione and 1 μmol/L DETC-NAC challenged by the injection of blank dialysate demonstrated no significant matrix interference. The comparison of standards prepared in Ringer's and in water supported this assessment since there was no significant difference in the SRM peak areas. The selectivity of the method was tested by analyzing drug-free plasma dialysate. Each dialysate sample was tested using the UPLC-MS/MS conditions described to ensure no interference with carbamathione and the IS. No other endogenous peaks were observed.

5.2.4 Preparation of Standards and Calibration Curves

DETC-NAC and carbamathione standards were prepared by serially diluting the stock solutions with Ringer's solution. Calibration standards contained DETC-

NAC and carbamathione prepared in concentrations of 1, 5, 10, 50, and 100 nmol/L. Calibration plots were plotted as the ratio of the area of compound of interest to area of the internal standard versus concentration. Calibration curves were plotted every day (n = 5).

5.2.5 Sample Preparation

Twenty µL of standard solution or microdialysis sample was placed in an autosampler vial with a glass liner. Fifty nmol/L IS was prepared in 1% formic acid. Forty µL of this solution was added to the standard or microdialysis sample. The autosampler was set up to make 50 µL injections.

5.2.6 Microdialysis

5.2.6.1 Brain and Vascular Probes

Brain microdialysis probes (CMA 12 Elite) with 2 mm membranes were purchased from CMA Microdialysis (North Chelmsford, MA, USA). The vascular probes were fabricated in-house as described in Chapter 3 (3.2.8.1 Brain and Vascular Probes). Delivery experiments were carried out by perfusing 1 µmol/L carbamathione and DETC-NAC through the microdialysis probes *in vivo* at 2 µL/min, and determining the percentage that diffused through the membrane.

5.2.6.2 Animals and Surgery

All awake experiments were carried out in accordance with Institutional Animal Care and Use Committee (IACUC) animal protocols as described in Chapter 2 (2.2.6.2 Animals and Surgery). Sterile surgeries were conducted as described in Chapter 3 (3.2.8.2 Animals and Surgery). The initial anesthesia and preparation of the incision sites are described in detail in Chapter 2 (2.2.6.2 Animals and Surgery) and Chapter 3(3.2.8.2 Animals and Surgery).

An intraperitoneal (i.p.) cannula was implanted into the abdomen the rat as described in Chapter 4 (4.2.5.2 Animals and Surgery). The i.p. cannula was externalized through a sterile incision in the neck. All incisions were closed with stitches or surgical staples. Microdialysis probes were implanted into the brain nucleus accumbens, brain prefrontal cortex and into the jugular vein as described in Chapter 3 (3.2.8.2 Animals and Surgery). After the surgical procedures, the rats were administered 0.5 to 3 mL/kg of saline subcutaneously (s.c.) and placed in a rat turn with a heating pad to facilitate recovery from anesthesia.

5.2.6.3 Microdialysis Sample Collection

Microdialysis samples were collected as described in Chapter 3 (3.2.8.3 Microdialysis Sample Collection). After implantation, the brain probes and the

vascular probes were perfused with Ringer's solution at 2 µL/min. The dead volume between the dialysis site and the fraction collector was also determined in order to accurately monitor the neurochemical changes as described in Chapter 3 (3.2.8.3 Microdialysis Sample Collection).

5.2.6.4 In Vivo Experiments

The collection of 15 min samples was initiated after a 24 h waiting period for awake experiments. For dosing purposes, the disulfiram dose (200 mg/kg) was prepared as described in Chapter 4 (4.2.5.4 *In Vivo* Experiments). After the i.p. administration of disulfiram through the i.p. cannula, microdialysis samples were collected for six hours. At the end of the experiments, the rats were sacrificed by placement in an isofluorane chamber for approximately thirty minutes. Rat brains were harvested in order to perform a histological confirmation of brain probe position as described in Chapter 3 (3.3.4 Histological Confirmation of Brain Probe Position).[1]

5.3 Results and Discussion

5.3.1 UPLC-MS/MS Calibration Results

The carbamathione calibration curve was constructed by plotting the peak area ratio of carbamathione or DETC-NAC to the IS versus the concentration of carbamathione or DETC-NAC. The regression coefficient of the calibration showed good linearity ($r^2 = 0.9996$ for carbamathione and $r^2 = 0.9997$ for DETC-NAC). Figure 5.4 displays representative calibration curves for DETC-NAC and carbamathione over a concentration range of 1-100 nmol/L.

5.3.2 Microdialysis Probe Calibration

The characteristics of the implanted microdialysis probes were evaluated at the end of each experiment. Based on the delivery experiments, the *in vivo* extraction efficiency by delivery (EE_d) (mean ± standard error of mean [SEM], $n = 3$) for carbamathione was determined to be 24.3 ± 4.4% for the brain probes and 50.0 ± 9.4% for the plasma vascular probes. Based on the delivery experiments, the *in vivo* EE_d (mean ± SEM, $n = 3$) for DETC-NAC was determined to be 53.7 ± 9.8% for the brain probes and 81.3 ± 10.8% for the plasma vascular probes.

Figure 5.4 **Representative calibration curves for UPLC-MS/MS method.**

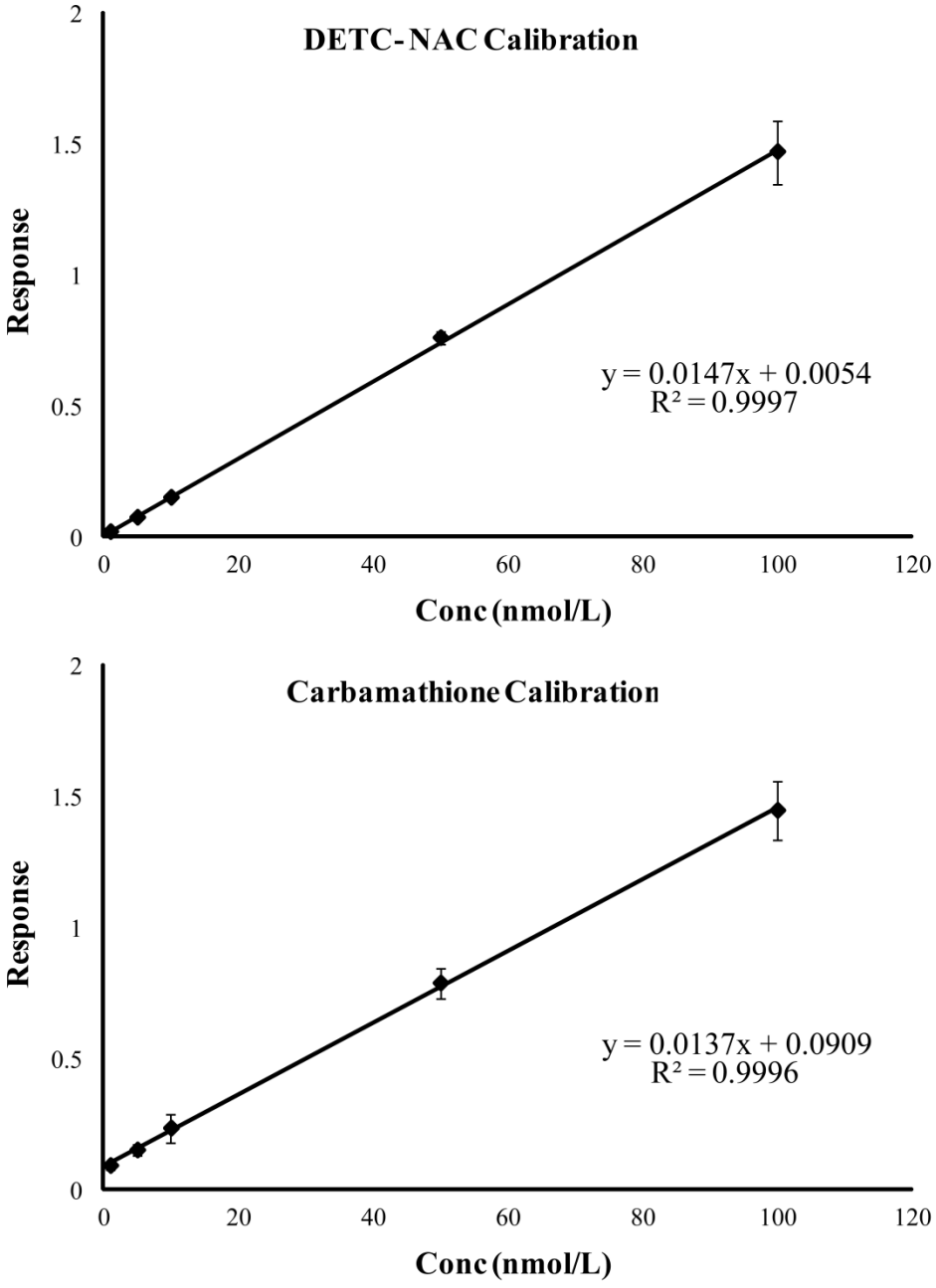

5.3.3 *In Vivo* Studies

Figure 5.5 shows the concentration in plasma microdialysis samples versus time profile for carbamathione and DETC-NAC after the i.p. administration of disulfiram (200 mg/kg, n = 3). Figure 5.6 shows the concentration in the brain nucleus accumbens microdialysis samples versus time profile for carbamathione and DETC-NAC after the i.p. administration of disulfiram (200 mg/kg, n = 3). Figure 5.7 shows the concentration in the brain prefrontal cortex microdialysis samples versus time profile for carbamathione and DETC-NAC after the i.p. administration of disulfiram (200 mg/kg, n = 3).

Carbamathione and DETC-NAC appear to have similar distribution curves in the plasma. Carbamathione had a C_{max} of 148.4 ± 41.1 nmol/L at 285 min after disulfiram administration. DETC-NAC had a C_{max} of 86.7 ± 14.2 nmol/L at 300 min after disulfiram administration. This indicated that DETC-NAC was still increasing in concentration at the last collection and had not reached its true C_{max}. The area under the dialysate concentration versus time profile (AUC) for carbamathione in the brain nucleus accumbens, brain prefrontal cortex and plasma after the administration of disulfiram (200 mg/kg i.p.) were 1.75 ± 0.83 μmol/L min, 2.20 ± 1.82 μmol/L min and 31.8 ± 14.9 μmol/L min.

Figure 5.5 Carbamathione and DETC-NAC concentration versus time profile after 200 mg/kg dose of disulfiram and 15 min sampling interval in plasma dialysate.

Concentrations of carbamathione and DETC-NAC in rat plasma following disulfiram administration (200 mg/kg i.p., n = 3). Microdialysis samples were collected every 15 min. Data shown as concentration (mean ± SEM).

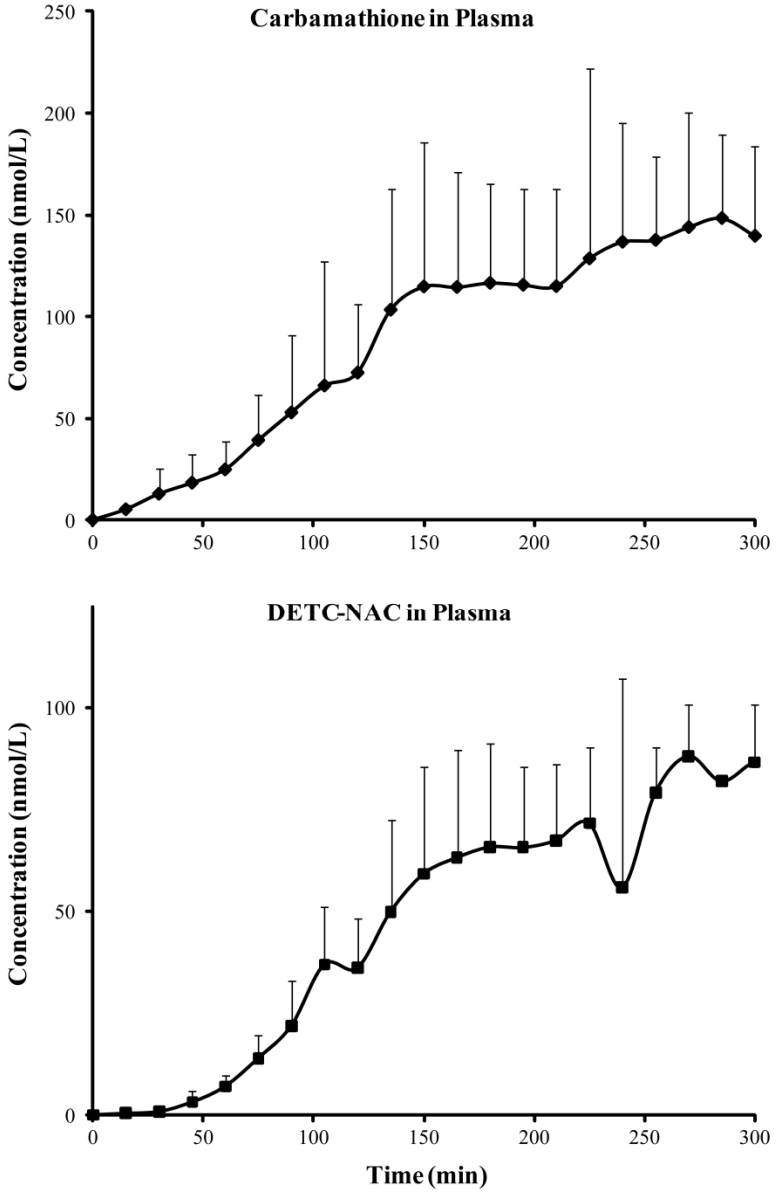

Figure 5.6 Carbamathione and DETC-NAC concentration versus time profile after 200 mg/kg dose of disulfiram and 15 min sampling interval in brain dialysate.

Concentrations of carbamathione and DETC-NAC in rat brain nucleus accumbens following disulfiram administration (200 mg/kg i.p., n = 3). Microdialysis samples were collected every 15 min. Data shown as concentration (mean ± SEM).

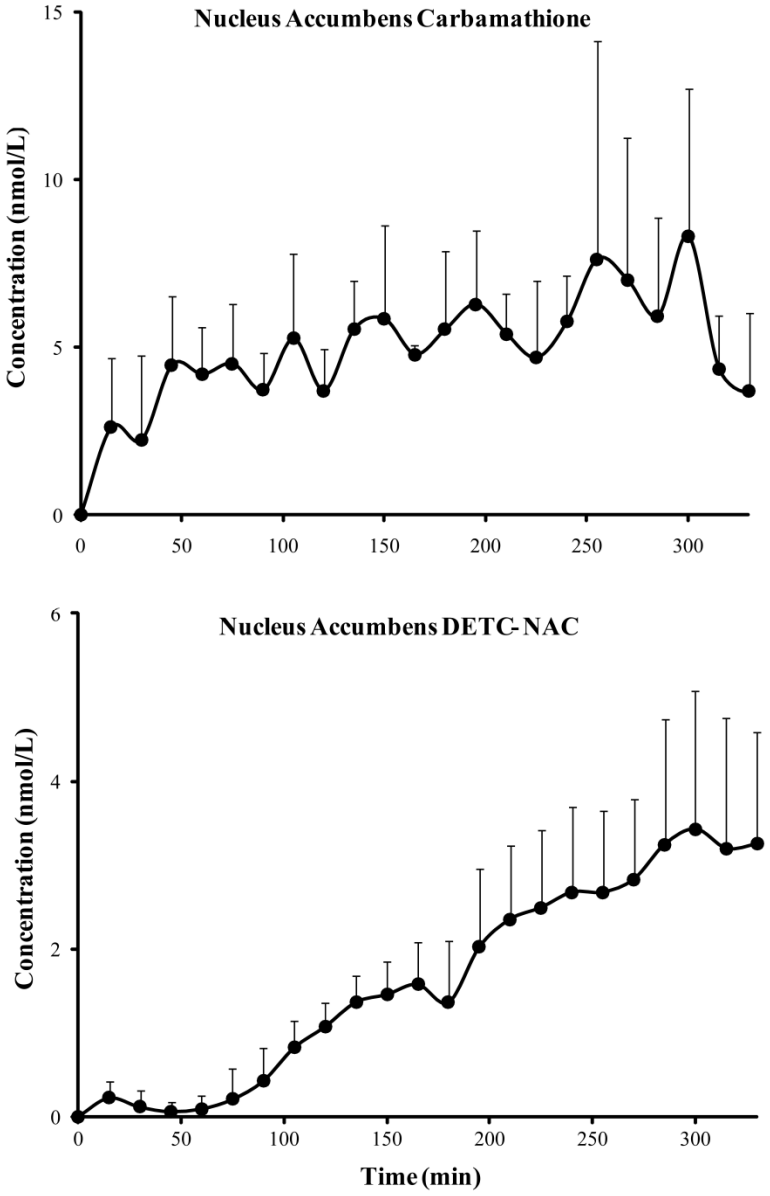

Figure 5.7 Carbamathione and DETC-NAC concentration versus time profile after 200 mg/kg dose of disulfiram and 15 min sampling interval in brain dialysate.

Concentrations of carbamathione and DETC-NAC in rat brain prefrontal cortex following disulfiram administration (200 mg/kg i.p., n = 3). Microdialysis samples were collected every 15 min. Data shown as concentration (mean ± SEM).

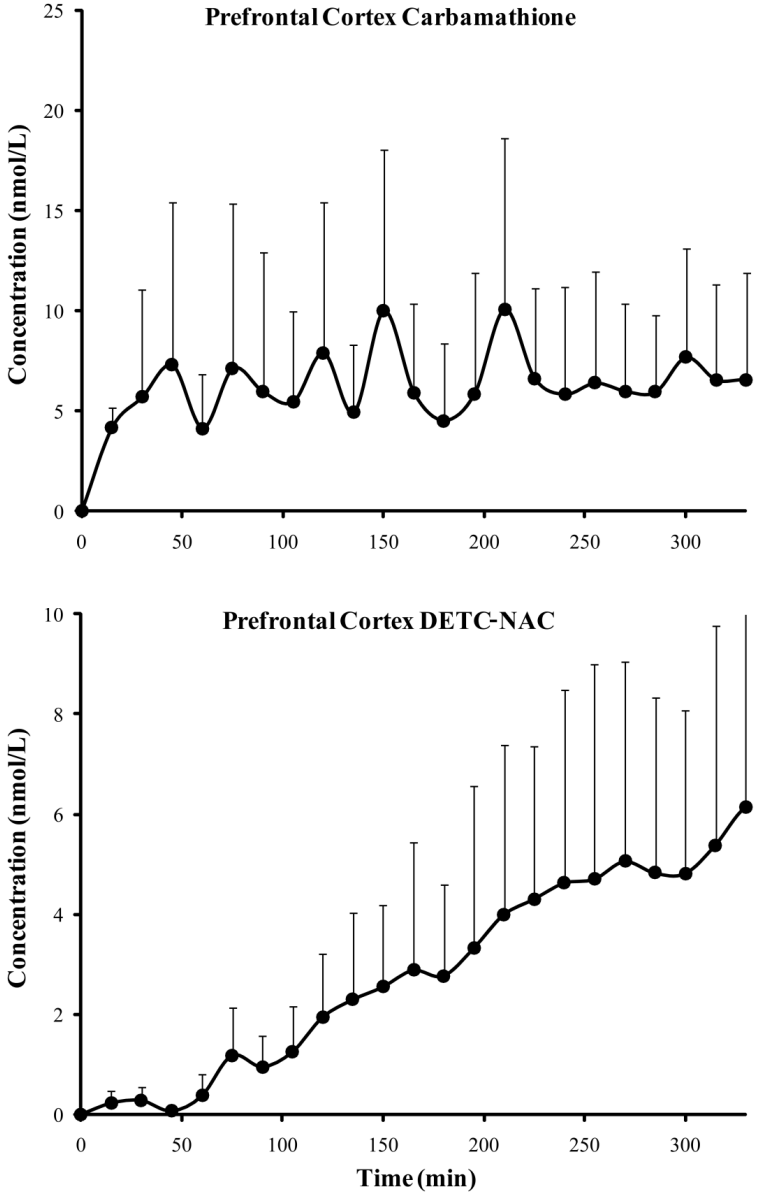

The AUC for carbamathione concentrations in the brain nucleus accumbens, brain prefrontal cortex and plasma after carbamathione administration (200 mg/kg i.v.) were 270 ± 67 μmol/L min, 273 ± 66 μmol/L min and 1854 ± 458 μmol/L min, respectively (see table 3.21). As described in Chapter 4, a 200 mg/kg dose of carbamathione and a 200 mg/kg dose of disulfiram are approximately equimolar (4.3.2.1.1 Administration of Disulfiram). The percent conversion of disulfiram to carbamathione was determined to be less than 2%. This was similar to the value obtained in the study described in Chapter 4 (<1%, 4.3.2.1.1 Administration of Disulfiram).

The concentrations of carbamathione and DETC-NAC in the brain nucleus accumbens and prefrontal cortex had profiles similar to those in the plasma. In the brain nucleus accumbens, carbamathione had a C_{max} of 8.3 ± 4.4 nmol/L at 300 min after disulfiram administration. DETC-NAC had a C_{max} of 3.4 ± 1.5 nmol/L at 300 min after disulfiram administration. In the brain prefrontal cortex, carbamathione had a C_{max} of 10.1 ± 8.5 nmol/L at 210 min after disulfiram administration. DETC-NAC had a C_{max} of 6.1 ± 4.6 nmol/L at 330 min after disulfiram administration. The time profile curves indicated that DETC-NAC was still increasing in concentration at the last collection and had not reached its true C_{max} in the brain. The AUC for DETC-NAC in the brain nucleus accumbens, brain prefrontal cortex and plasma after the administration of disulfiram (200

mg/kg i.p.) were 614 ± 263 nmol/L min, 1.05 ± 0.83 μmol/L min and 17.6 ± 5.9 μmol/L min.

5.4 Discussion

DETC-NAC is a metabolite that is formed after the formation of carbamathione since it is the glutathione side-chain that is modified (see figure 5.1). The results from this study showed that DETC-NAC appeared in the plasma, the brain nucleus accumbens and the brain prefrontal cortex after the administration of disulfiram. The elimination of disulfiram and its numerous metabolites is a very slow process.[2-5] This may explain the slow continuous increase in carbamathione and DETC-NAC in plasma over time. The concentrations of carbamathione and DETC-NAC in the plasma and the brain followed very similar time profiles. However, the concentration of carbamathione in the brain showed more variation than the concentration of DETC-NAC. This may be because carbamathione is the first metabolite formed by the carbamoylation of glutathione and appears to form peripherally before crossing the blood-brain barrier (BBB). Reactive metabolites formed from the biotransformation of drugs are normally detoxified by conjugating with glutathione followed by mercapturic acid metabolism to produce their respective NAC conjugates.[6] Since NAC conjugates are normally excreted, DETC-NAC may be one of the last steps in the metabolism of disulfiram. The

discovery of a NAC metabolite of carbamathione in the brain has many implications for this project. The discovery of DETC-NAC in the brain suggests that the study of other intermediates that may also cross the BBB is warranted. The formation of DETC-NAC and its slow distribution in the brain may help explain the prolonged effects of carbamathione administration on brain neurotransmitters even after carbamathione has been cleared from the brain.

5.5 Conclusions

The work in this chapter showed the application of a UPLC-MS/MS method for the simultaneous detection of carbamathione and a metabolite of carbamathione in rat brain nucleus accumbens, brain prefrontal cortex and plasma dialysate. The analytical method exhibited good linearity, reproducibility, and selectivity. Both carbamathione and the metabolite, DETC-NAC were detected in the brain after the administration of disulfiram. However, this study did not elucidate whether DETC-NAC crossed the BBB or carbamathione was required to cross the BBB to form DETC-NAC. Future studies with DETC-NAC can help illuminate its role, if any, in the effect on brain neurotransmitters observed after both carbamathione and disulfiram administration. Such studies include the investigation of brain neurotransmitters after the administration of DETC-NAC.

5.6 References

1 Paxinos, G. & Watson, C. *The Rat Brain in Stereotaxic Coordinates*. (Academic Press, 1982).

2 Johansson, B. A review of the pharmacokinetics and pharmacodynamics of disulfiram and its metabolites. *Acta Psychiatr Scand Suppl* **369**, 15-26, (1992).

3 Hart, B. W. & Faiman, M. D. Bioactivation of S-methyl N,N-diethylthiolcarbamate to S-methyl N,N-diethylthiolcarbamate sulfoxide. Implications for the role of cytochrome P450. *Biochem Pharmacol* **46**, 2285-2290, (1993).

4 Jin, L., Davis, M. R., Hu, P. & Baillie, T. A. Identification of novel glutathione conjugates of disulfiram and diethyldithiocarbamate in rat bile by liquid chromatography-tandem mass spectrometry. Evidence for metabolic activation of disulfiram in vivo. *Chemical research in toxicology* **7**, 526-533, (1994).

5 Lipsky, J. J., Shen, M. L. & Naylor, S. In vivo inhibition of aldehyde dehydrogenase by disulfiram. *Chemico-biological interactions* **130-132**, 93-102, (2001).

6 Flanagan, R. J. & Meredith, T. J. Use of N-acetylcysteine in clinical toxicology. *Am J Med* **91**, 131S-139S, (1991).

6 CONCLUSIONS AND FUTURE DIRECTIONS

6.1 Summary of Dissertation

6.1.1 CE-LIF Method for GABA, Glu, and Carbamathione in Microdialysis Samples

A capillary electrophoresis (CE-LIF) method was developed for the simultaneous detection of gamma-amino butyric acid (GABA), glutamate (Glu) and carbamathione in microdialysis samples from the brain nucleus accumbens. Microdialysis samples were derivatized with napthalene-2,3-dicarboxyaldehyde (NDA) since it was not fluorescent itself and it reacted rapidly to give stable fluorescent cyanobenzo[*f*]isoindol (CBI) derivatives. The derivatization of the primary amine provided the added advantage of including carbamathione in the analysis of a sample since it is also a primary amine. The limits if detection (LOD) for GABA, Glu and carbamathione were 1.0×10^{-8}, 6.0×10^{-9}, and 1.5×10^{-8} mol/L respectively. These LOD were sufficient for detecting GABA, Glu, and carbamathione in the rat brain. A temporal resolution of 5 min was achieved for this method.

The effect of the intravenous (i.v.) administration of carbamathione (200 mg/kg i.v.) on GABA and Glu levels in the brain nucleus accumbens was evaluated. Administration of carbamathione was correlated to changes in GABA and Glu in

both anesthetized and awake rats. In anesthetized rats, basal GABA levels were significantly reduced and basal Glu levels were significantly increased after the administration of carbamathione. In awake rats, basal GABA levels were significantly reduced whereas basal Glu levels were initially increased and eventually decreased below basal concentrations. The effect of carbamathione on basal Glu levels of the awake rats may be explained by carbamathione being a partial *N*-methyl-*D*-aspartic acid (NMDA) antagonist. The role of carbamathione as a partial NMDA antagonist may be important since NMDA antagonists have been shown to be effective in treating alcohol dependence and blocking cocaine-induced behavior.[1-3]

Ketamine which is also a known NMDA antagonist, was used and may be responsible for the differences observed in Glu levels between anesthetized and awake rats. Several studies with ketamine suggest that ketamine alters the response of NMDA receptors to drug administration. [4-6] The anesthesia also had an impact on the pharmacokinetics (PK) of carbamathione clearance from the brain. The elimination rate constant, K_{elim} was determined to be 0.13 ± 0.01 min^{-1} for anesthetized rats and 0.16 ± 0.02 min^{-1} for awake rats. The slower PK for the anesthetized rats was expected since the anesthesia is known to slow down the basal metabolic rate.

These studies showed that carbamathione administration had an effect of GABA and Glu levels in the nucleus accumbens of the rat brain. Future studies will focus on the addition of dopamine (DA) to the analysis because DA has been shown to be one of the neurotransmitters involved in the pathways associated with addiction.[7,8] Future studies will also focus on adding the determination of carbamathione concentrations in plasma dialysate to the analysis. This would provide additional information on the PK and pharmacodynamics (PD) of carbamathione.

6.1.2 MEKC-LIF Method for GABA, Glu, DA, and Carbamathione in Microdialysis Samples

A micellar electrokinetic chromatography coupled with laser-induced fluorescence (MEKC-LIF) method was developed by modifying an existing method for the simultaneous detection of GABA, Glu, DA, and carbamathione in microdialysis samples from the brain.[9] Similar to the CE-LIF method in Chapter 2, microdialysis samples were derivatized with NDA. The LOD for GABA, Glu, DA and carbamathione were 1.5×10^{-9}, 6.0×10^{-10}, 5.0×10^{-10} and 1.0×10^{-9} mol/L respectively. In addition, a previously developed liquid chromatography-tandem mass spectrometric (LC-MS/MS) method was utilized to determine

carbamathione concentrations in plasma dialysate.[23] The LOD for this method was 2.5 x 10^{-10} mol/L.

These methods were initially used to evaluate the effect of carbamathione administration (200 mg/kg i.v.) on GABA, Glu, and DA levels in the nucleus accumbens and prefrontal cortex of rat brain. A temporal resolution of 5 min was achieved for this method. The half-lives of carbamathione in the plasma, prefrontal cortex and nucleus accumbens were determined to be 4.81 ± 0.97, 4.31 ± 0.59 and 4.19 ± 0.66 min respectively. Thus the sample collection time of 5 min was more than the estimated half-lives of carbamathione. The sample collection time was reduced to 3 min in order to obtain important PK and PD data. However, the values obtained for the elimination constants by 3 min sampling were very close to those obtained by 5 min sampling. This suggested that 5 min sampling was sufficient to obtain the relevant PK and PD data for carbamathione.

Administration of carbamathione was correlated with an initial increase in extracellular Glu concentration and a subsequent decrease after 30 min. This increase and decrease may possible be correlated with the PK of carbamathione in the brain, which suggests that the initial increase may be due to carbamathione acting as a partial NMDA antagonist. Administration of carbamathione was correlated with an increase in DA levels in the brain and this increase was more

pronounced in the nucleus accumbens than in the prefrontal cortex. This was expected since carbamathione also appeared to decrease GABA in the prefrontal cortex, which usually inhibits DA in the nucleus accumbens. Administration of carbamathione was also correlated with a decrease in extracellular GABA levels in the brain with a greater decrease occurring in the prefrontal cortex than in the nucleus accumbens. These changes in GABA, Glu and DA also appeared to be dose-dependent since three doses were evaluated (200, 50, and 20 mg/kg).

These studies demonstrated that carbamathione administration was correlated with changes in brain GABA, Glu, and DA levels. This effect of carbamathione may explain the anti-craving property of disulfiram observed in clinical trials for the treatment of alcohol and cocaine addiction.[10,11] However, the mechanism by which carbamathione administration affects the brain neurotransmitters remains unknown. Future studies will focus on elucidating this mechanism in by selectively inhibiting disulfiram metabolism and investigating whether changes in brain neurotransmitters were observed.

6.1.3 Laboratory-Built MEKC-LIF Method for GABA, Glu, DA, and Carbamathione in Microdialysis Samples

A laboratory-built MEKC-LIF method was developed by modifying an existing method for the simultaneous detection of GABA, Glu, DA, and carbamathione in microdialysis samples from the brain nucleus accumbens.[9] The LOD for GABA, Glu, DA, and carbamathione were 6.0×10^{-9}, 1.0×10^{-8}, 5.0×10^{-9} and 1.0×10^{-8} mol/L respectively. In addition, the LC-MS/MS method described in Chapter 3 was used to determine carbamathione concentrations in plasma dialysate.[23] A temporal resolution of 5 min was achieved since the study described in Chapter 3 determined this resolution to be sufficient.

The goal of this study was to utilize the MEKC-LIF method to determine the changes in rat brain GABA, Glu, and DA levels as related to the intraperitoneal (i.p.) administration of disulfiram (200 mg/kg i.p.) and an inhibitor of disulfiram metabolism (*N*-benzylimidazole [NBI], 20 mg/kg i.p.). These studies demonstrated that carbamathione was detected in the brain after disulfiram administration but was not detected when NBI was administered. Disulfiram also appeared to be correlated with changes in brain neurotransmitters, albeit to a much lesser degree than carbamathione administration (as observed in Chapter 3). When NBI was administered with disulfiram, no statistically significant changes in brain neurotransmitters were observed. However, administration of

carbamathione (200 mg/kg i.p.) in combination with NBI restored the changes observed in brain neurotransmitters. This suggested that NBI did not interfere with the mechanism by which carbamathione administration had an effect on brain neurotransmitters. This was an important study since it demonstrated that the formation of carbamathione was necessary to observe changes in the brain neurotransmitters after both carbamathione and disulfiram administration.

6.1.4 UPLC-MS/MS Method for Carbamathione and a Metabolite of Carbamathione in Microdialysis Samples

Chapter 5 described an ultra-performance liquid chromatography-tandem mass spectrometric (UPLC-MS/MS) method that was originally developed in the Williams, Stobaugh and Faiman laboratories (University of Kansas, Lawrence, KS) to detect carbamathione in plasma samples that were precipitated by perchloric acid. During one of these studies, an *N*-acetyl cysteine (NAC) conjugate of carbamathione (*S*- methyl *N, N*-diethylthiocarbamate-*N*-acetyl cysteine [DETC-NAC]) was discovered in the plasma samples. This UPLC-MS/MS method was used to determine DETC-NAC and carbamathione in microdialysis samples from the plasma, brain nucleus accumbens, and brain prefrontal cortex after the administration of disulfiram (200 mg/kg i.p.). Samples were collected every 15 min for over 5 h.

This study demonstrated that DETC-NAC and carbamathione were detected in the plasma, brain nucleus accumbens and brain prefrontal cortex of awake rats after the administration of disulfiram (200 mg/kg i.p.). This was an exploratory study to determine the existence of a metabolite other than carbamathione in the rat brain after disulfiram administration. This study suggested that there may be other metabolites of disulfiram that either cross the blood-brain barrier (BBB) or are formed in the brain. This study did not demonstrate whether DETC-NAC, carbamathione or both crossed the BBB. This study suggested that the formation of DETC-NAC and its slow distribution in the brain may help explain the prolonged effects of carbamathione administration on brain neurotransmitters even after carbamathione has been cleared from the brain. Future studies will focus on the exploration of other metabolites of disulfiram that may appear in the brain after the administration of disulfiram. Another important study would be the investigation of the effect, if any, of DETC-NAC administration on these brain neurotransmitters.

6.2 Future Directions

The research discussed in this dissertation has many implications for the treatment of alcohol and cocaine addiction. Disulfiram is a drug that has been used for over 60 years in the treatment of alcoholism and has recently been found to be

efficacious in the treatment of cocaine addiction.[11-14] It is important to note that in the cocaine trial, disulfiram efficacy was independent of its effect as an alcohol aversive agent since disulfiram appeared to be more effective when the patients were not alcoholic.[14] These studies and the work in this dissertation suggest that disulfiram has an effect in the brain that is independent of its effect on aldehyde dehydrogenase ($ALDH_2$). The fact that carbamathione, a metabolite of disulfiram produced a change in the brain neurotransmitters suggest that disulfiram may have a centrally mediated effect. Several studies could be conducted to help elucidate the role of carbamathione as a pharmacological agent in alcohol and cocaine studies. The analytical methods developed in this dissertation can be used to analyze the samples generated by such studies.

One important study would be the investigation of the effect of administering cocaine or alcohol followed by carbamathione on the brain neurotransmitters. This study would help elucidate whether carbamathione could change or even reverse the effect of cocaine or alcohol. All the studies in this dissertation involved a single bolus dose of carbamathione or disulfiram. Thus another interesting experiment would be the investigation of the effect of multiple dosing schemes using carbamathione. This study would demonstrate whether the changes in neurotransmitter levels were reversible. This study would also elucidate

whether multiple doses of carbamathione would produce a greater degree of change in the neurotransmitters than a single dose.

Another significant study would involve the study of a behavioral model for alcohol and cocaine addiction. Animal models of drug addiction can provide a means of studying both the behavioral and biological basis of drug addiction. The neurobiological mechanisms involved in the positive reinforcing effects of drugs and the negative reinforcing effects of drug abstinence have been elucidated in several models.[15-18] The effects of pharmacological interventions such as carbamathione administration can be studied using animal models. Studies with such models would also help elucidate the difference in basal neurotransmitters levels between the addicted and normal animal. In addition, information on the effect of pharmacological interventions on these neurotransmitter levels can also be obtained.

In addition to studies into the pharmacology of carbamathione, it would be relevant to explore other metabolites of carbamathione (such as DETC-NAC) and study their effects on important brain neurotransmitters. Metabolite profiling is an important part of the drug discovery and development process. Mass spectrometry is a useful tool in facilitating the identification of previously uncharacterized metabolites, especially when combined with wet chemistry

techniques like nuclear magnetic resonance (NMR) and chemical derivatization.[19-22] As the metabolites are identified, studies into which of the metabolites cross the BBB would also be significant.

6.3 References

1 Karila, L., Gorelick, D., Weinstein, A., Noble, F., Benyamina, A., Coscas, S., Blecha, L., Lowenstein, W., Martinot, J. L., Reynaud, M. & Lepine, J. P. New treatments for cocaine dependence: a focused review. *Int J Neuropsychoph* **11**, 425-438, (2008).

2 Uys, J. D. & LaLumiere, R. T. Glutamate: The New Frontier in Pharmacotherapy for Cocaine Addiction. *Cns Neurol Disord-Dr* **7**, 482-491, (2008).

3 Gass, J. T. & Olive, M. F. Glutamatergic substrates of drug addiction and alcoholism. *Biochemical Pharmacology* **75**, 218-265, (2008).

4 Lorrain, D. S., Baccei, C. S., Bristow, L. J., Anderson, J. J. & Varney, M. A. Effects of ketamine and N-methyl-D-aspartate on glutamate and dopamine release in the rat prefrontal cortex: modulation by a group II selective metabotropic glutamate receptor agonist LY379268. *Neuroscience* **117**, 697-706, (2003).

5 Albrecht, J., Hilgier, W., Zielinska, M., Januszewski, S., Hesselink, M. & Quack, G. Extracellular concentrations of taurine, glutamate, and aspartate in the cerebral cortex of rats at the asymptomatic stage of thioacetamide-induced hepatic failure: modulation by ketamine anesthesia. *Neurochem Res* **25**, 1497-1502, (2000).

6 Razoux, F., Garcia, R. & Lena, I. Ketamine, at a dose that disrupts motor behavior and latent inhibition, enhances prefrontal cortex synaptic efficacy and glutamate release in the nucleus accumbens. *Neuropsychopharmacology* **32**, 719-727, (2007).

7 Di Chiara, G., Bassareo, V., Fenu, S., De Luca, M. A., Spina, L., Cadoni, C., Acquas, E., Carboni, E., Valentini, V. & Lecca, D. Dopamine and drug addiction: the nucleus accumbens shell connection. *Neuropharmacology* **47**, 227-241, (2004).

8 Koob, G. F. & Le Moal, M. Addiction and the brain antireward system. *Annu Rev Psychol* **59**, 29-53, (2008).

9 Siri, N., Lacroix, M., Garrigues, J. C., Poinsot, V. & Couderc, F. HPLC-fluorescence detection and MEKC-LIF detection for the study of amino acids and catecholamines labelled with naphthalene-2,3-dicarboxyaldehyde. *Electrophoresis* **27**, 4446-4455, (2006).

10 Petrakis, I. L., Poling, J., Levinson, C., Nich, C., Carroll, K. & Rounsaville, B. Naltrexone and disulfiram in patients with alcohol dependence and comorbid psychiatric disorders. *Biol Psychiatry* **57**, 1128-1137, (2005).

11 de Sousa, A. & de Sousa, A. An open randomized study comparing disulfiram and acamprosate in the treatment of alcohol dependence. *Alcohol and alcoholism (Oxford, Oxfordshire)* **40**, 545-548, (2005).

12 Boothby, L. A. & Doering, P. L. Acamprosate for the treatment of alcohol dependence. *Clin Ther* **27**, 695-714, (2005).

13 Besson, J., Aeby, F., Kasas, A., Lehert, P. & Potgieter, A. Combined efficacy of acamprosate and disulfiram in the treatment of alcoholism: a controlled study. *Alcohol Clin Exp Res* **22**, 573-579, (1998).

14 Carroll, K. M., Fenton, L. R., Ball, S. A., Nich, C., Frankforter, T. L., Shi, J. & Rounsaville, B. J. Efficacy of disulfiram and cognitive behavior therapy in cocaine-dependent outpatients: a randomized placebo-controlled trial. *Arch Gen Psychiatry* **61**, 264-272, (2004).

15 Kalivas, P. W., Peters, J. & Knackstedt, L. Animal models and brain circuits in drug addiction. *Mol Interv* **6**, 339-344, (2006).

16 Vendruscolo, L. F., Izidio, G. S. & Takahashi, R. N. Drug reinforcement in a rat model of attention deficit/hyperactivity disorder--the Spontaneously Hypertensive Rat (SHR). *Curr Drug Abuse Rev* **2**, 177-183, (2009).

17 Aguilar, M. A., Rodriguez-Arias, M. & Minarro, J. Neurobiological mechanisms of the reinstatement of drug-conditioned place preference. *Brain Res Rev* **59**, 253-277, (2009).

18 Epstein, D. H., Preston, K. L., Stewart, J. & Shaham, Y. Toward a model of drug relapse: an assessment of the validity of the reinstatement procedure. *Psychopharmacology (Berl)* **189**, 1-16, (2006).

19 Liu, D. Q. & Hop, C. E. Strategies for characterization of drug metabolites using liquid chromatography-tandem mass spectrometry in conjunction with chemical derivatization and on-line H/D exchange approaches. *J Pharm Biomed Anal* **37**, 1-18, (2005).

20 Deng, Y., Wu, J. T., Zhang, H. & Olah, T. V. Quantitation of drug metabolites in the absence of pure metabolite standards by high-performance liquid chromatography coupled with a chemiluminescence nitrogen detector and mass spectrometer. *Rapid Commun Mass Spectrom* **18**, 1681-1685, (2004).

21 Tiller, P. R. & Romanyshyn, L. A. Liquid chromatography/tandem mass spectrometric quantification with metabolite screening as a strategy to enhance the early drug discovery process. *Rapid Commun Mass Spectrom* **16**, 1225-1231, (2002).

22 Hop, C. E., Tiller, P. R. & Romanyshyn, L. In vitro metabolite identification using fast gradient high performance liquid chromatography combined with tandem mass spectrometry. *Rapid Commun Mass Spectrom* **16**, 212-219, (2002).

23 Kaul, S., Williams, T. D., Lunte, C. E. & Faiman, M. D. LC-MS/MS determination of carbamathione in microdialysis samples from rat brain and plasma. *J Pharm Biomed Anal* **51**, 186-191, (2010).